Studies on Formation and Repair
of C5–C5'-Linked Dihydrothymine Dimer
as a Radiation-Induced DNA Damage Structure

Takeo Ito

2000

Studies on Formation and Repair
of C5–C5'-Linked Dihydrothymine Dimer
as a Radiation-Induced DNA Damage Structure

Takeo Ito

2000

Contents

General Introduction

Background

DNA is a major target of ionizing radiation and UV-light irradiation that induce many genetoxic effects such as mutagenicity, carcinogenisity and lethality.[1-3] The deleterious effects of ionizing radiation and UV-light have already been studied since the early of this century.[4] By 1950's, cell-killing and mutational action spectra of bacteria were shown to be similar to the absorption spectra of DNA.[5] The investigations on the DNA strand break and the nucleic base modifications induced by high-energy radiation have become increasingly important in relation to the environmental problems on earth since the discovery of ozone hole in 1985.[6]
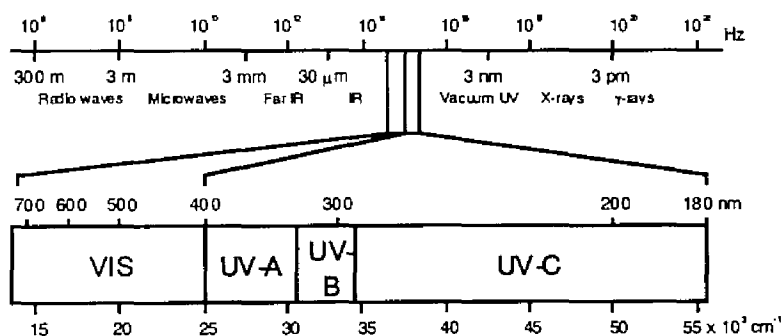
Figure 1. Wavelengths of electromagnetic radiations.

The UV radiation spectrum has been subdivided into three wavelength bands designated UV-A (400–320 nm), UV-B (320–290 nm), and UV-C (290–180 nm). Solar UV radiation consists mainly of UV-A and UV-B, since penetration of the atmospheric ozone layer drops dramatically for wavelengths below 320 nm. Among DNA bases, purine and pyrimidine bases show strong UV absorption, since they have the absorption bands at 260–270 nm and around 200 nm primarily due to (π,π^*) transitions of the heterocyclic structures.[1] While the major mode of nucleic base

1

modification by the UV-light involves photocycloaddition and photohydration of pyrimidine bases, the contribution of the UV-light with high intensity (especially light in the region of vacuum-UV (200–100 nm)) to base damages also involves direct ionization of guanine base with low ionization potential.[7]

DNA damages are induced by both direct and indirect effects of ionizing radiations including X-ray and ^{60}Co γ-ray.[2] The direct effect results from the direct interaction of the radiation energy with DNA to generate radical cations of the bases and dry electrons as in reaction 1. A recent study has shown that an electron-loss center (hole) at a given DNA base radical cation can migrate intramolecularly through a π-stacking of DNA bases, thus arriving at and being trapped most efficiently in a guanine (G) moiety to cause its oxidative damage.[8] On the other hand, since in living cells DNA exists in an environment containing numerous molecules, inorganic ions, and water, the indirect effect becomes more important and induces radiolysis of water to generate the secondary active species such as hydrated electrons (e_{aq}^-), hydroxyl radicals ($^\cdot$OH), etc. It has been estimated that more than 80% of the energy of ionizing radiation deposited in cells results in the water radiolysis by the reactions 2 and 3.

$$DNA \rightarrow DNA^{\cdot+} + e^- \tag{1}$$

$$H_2O \rightarrow {}^\cdot OH + {}^\cdot H + e^- \tag{2}$$

$$nH_2O + e^- \rightarrow e_{aq}^- \tag{3}$$

These species thus formed attack DNA bases and deoxyribose moieties, in which the majority of damages to DNA is thought to be caused by hydroxyl radical ($^\cdot$OH).[2,3,9]

Biological Effects of DNA Base Lesions on Living Things

DNA base damages are induced mainly by UV-light with wavelengths of < 400 nm and ionizing radiation in the electromagnetic spectrum. The major photoproducts in DNA by UV-light are [1] cyclobutane pyrimidine photodimers (Pyr<>Pyr), [2]

pyrimidine(6–4)pyrimidone photoproducts [6–4'-(pyrimidine-2'-one)pyrimidone, Pyr(6–4)Pyo], and [3] pyrimidine photohydrates.[1,10] The cyclobutane pyrimidine photodimers are formed by [2+2] photocycloaddition between C5–C6 double bonds of an adjacent pyrimidine moieties. Among the four isomeric forms, *i.e.*, *cis-syn*, *trans-syn*, *cis-anti*, *trans-anti* occurring in significant yields, the *cis-syn* form is generated predominantly in double stranded B-form DNA. Pyr(6–4)Pyo represents another important class of DNA pyrimidine photoproducts, whose formation likely involves short-lived oxetane or azetidine intermediates. The effect of these lesions on the local and global structures of DNA is an important issue with regard to their ability to form correct base pairs in a replication process. The mutagenesity of these photodimers as incorporated in DNA strands has also been investigated, thus suggesting that the pyrimidine dimer kills cells by blocking replication and transcription of DNA.[11-14] Photoreactivating enzyme, DNA photolyase, absorbs UV-visible light and repairs the photodimers using the excitation energy.[15]
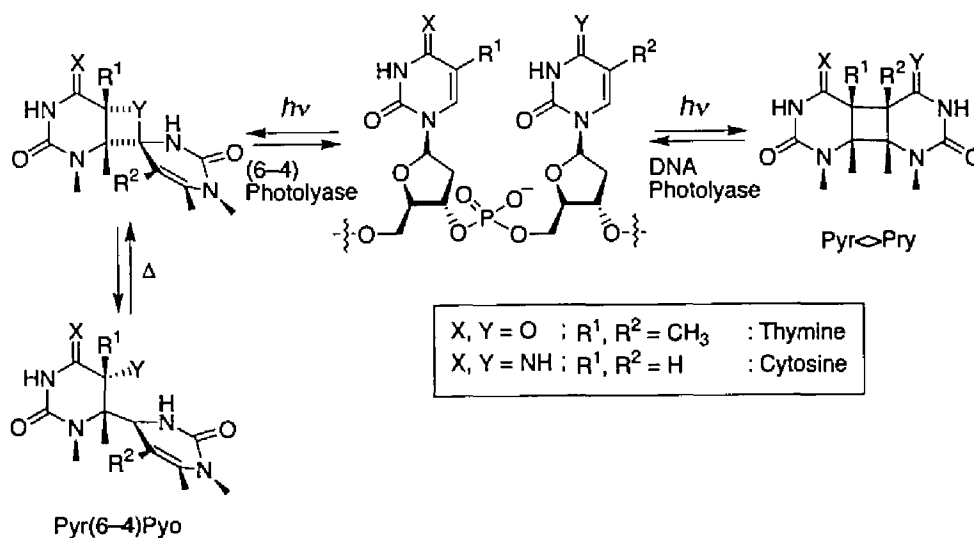

Figure 2. Photoproducts induced at dipyrimidine sites in DNA by UV radiation.

On the other hand, ionizing radiation-induced DNA base damages are often interpreted in terms of indirect attack of the hydroxyl radicals and solvated electrons to the DNA. Hydroxyl radical has the highest reactivity towards the DNA bases, especially the C5–C6 double bonds of the pyrimidine or C8, C4, and C5 positions of the purine.[2,9] 5,6-Dihydroxy-5,6-dihydrothymidine (thymidine glycol) is produced by addition of hydroxyl radical to thymidine base and inhibits the normal replication of DNA.[16] 7,8-Dihydro-8-oxo-2'-deoxyguanosine (8-oxo-Guo) is also a major oxidative damage of DNA produced by either addition of hydroxyl radical at C8 or direct ionization of 2'-deoxyguanosine. This compound has been shown to induce misincorporation of adenine as the supplementary base in the replication process of DNA, and the relationship between the structure and the mutagenesity has been extensively investigated.[17–19]

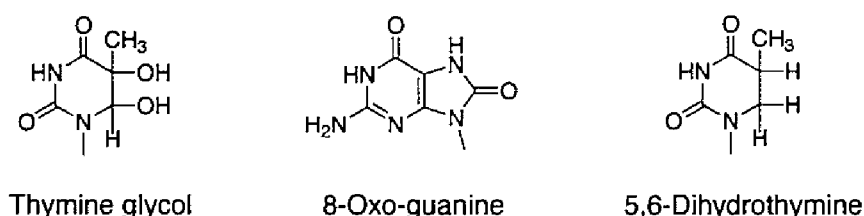Thymine glycol   8-Oxo-guanine   5,6-Dihydrothymine

Figure 3. Radiation-induced base damage structures.

Concerning reductive DNA damages by dry electrons (e$^-$ as in reactions 1 and 2) and/or hydrated electrons e$_{aq}^-$ (reaction 3), cytosine base moiety is a major site of electron-attachment at lower temperatures, as characterized by ESR spectroscopy:[2b,20–23] cytosine radical anion (C$^-$) and thymine radical anion (T$^-$) are thus produced in 64%[23a] (77%)[23b] and 36%[23a] (23%)[23b] yields, respectively. At higher temperatures (ca. 170 K), however, an equilibrium involving mutual electron-transfer process is established between the thymine and cytosine radical anions, from which irreversible protonation
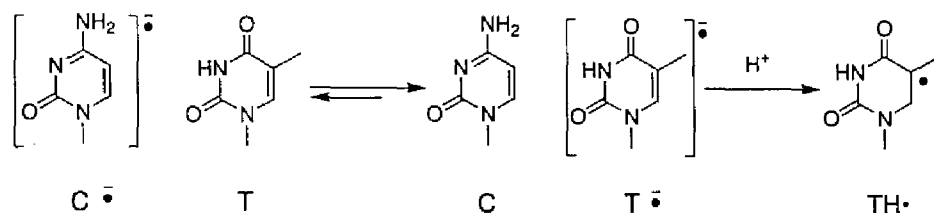
4

Figure 4. Mutual electron transfer process between cytosine and thymine.

at C6 of the thymine radical anion T⁻ takes place to produce a major intermediate of 5,6-dihydrothymin-5-yl radical (TH·).[24] Such a ready mutual electron-transfer process was deduced from pulse radiolytic evidence that thymine, cytosine, and their nucleotides and nucleosides have similar reduction potentials of about -1.1V vs. NHE at pH 8.[24] In comparison with oxidative damages, there has been little evidence for the influence of radiation-induced reductive DNA-base damages on the biological systems. While the electron adduct of thymine affords 5,6-dihydrothymine, a DNA polymerization experiment both *in vitro* and *in vivo* using DNA template containing a 5,6-dihydrothymine structure constitutes no replicative block.[25] Previously, Nishimoto *et al.* identified a novel C5–C5'-linked dihydrothymidine dimer structure that formed in the radiolysis of thymidine aqueous solution under anoxic condition.[26] Such a new class of thymine dimer is structurally similar to the cyclobutane pyrimidine

Thymidine (dThd)   (*R*)-DHdThd: 26 %   C5–C5'-Linked dihydrothymidine dimer
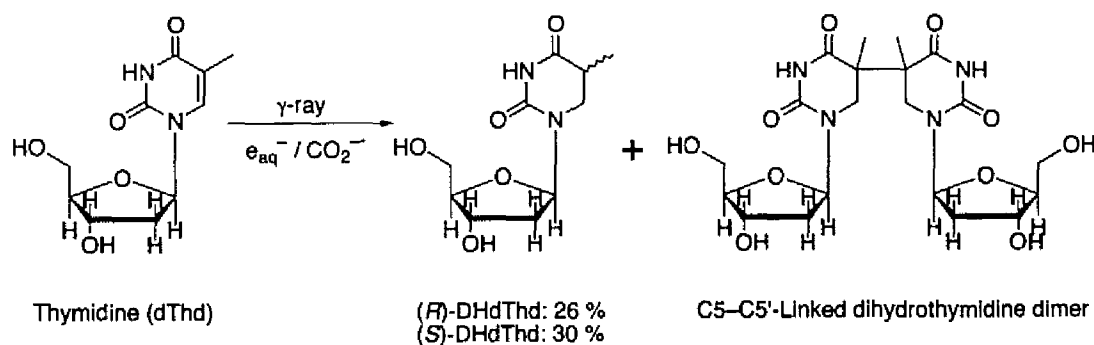   (*S*)-DHdThd: 30 %

Figure 5. Radiation-induced one-electron reduction of thymidine.

photodimers to some extent, and potentially possess biological relevance to the mutagenesity of pyrimidine photodimers.

Enzymatic Repair of DNA Lesions

For defending from toxic lesions, both prokaryotic and eukaryoic cells have evolved DNA repair system. A wide variety of DNA damages such as thymine glycol and cyclobutane photodimers are repaired by excision repair mechanisms.[27] Setlow has shown that a bacteria lacking the normal repair mechanism has a 0.5 death probability when only 10 molecular defects are created per DNA molecule ($\sim 10^7$ nucleotides).[28] DNA glycosylase catalyzes cleavage of the N-glycosidic bond to release the damaged base from the deoxyribose ring. Subsequent action of apurinic-apyrimidinic (AP) endonucleases and 3'- and 5'-phosphodiesterases remove the remaining ribose fragments to add the correct nucleotide by DNA polymerase and DNA ligase (Figure 6).[27] For example, $E.$ $coli.$ endonuclease III ($endo$ III) is a glycosylase specific for removal of oxidative damages of thymine and cytosine.[27a,b]

In contrast, another example of the DNA repair involves a direct chemical reversal of DNA damage. DNA Photolyases contain stoichiometric amounts of two chromophores/cofactors; flavin adenine dinucleotide (FAD) and methenyltetrahydrofolate (MTHF) or 8-hydroxy-5-deazariboflavin.[29] The enzyme binds to Pyr<>Pyr in DNA independent of light, the second chromophore absorbs a 350–450 nm light and transfers the energy to the FADH⁻ cofactor, which in turn transfer an electron to Pyr<>Pyr. The C5–C5' and C6–C6' bonds of cyclobutane ring are split to generate a Pyr and Pyr⁻, and the latter donates an electron back to the flavin cofactor (Figure 7).

The cyclobutane dimers also undergo one-electron oxidation by the photochemically generated excited state quinones[30] and by the radiation chemically produced sulfate radical anions (SO_4^-)[31] to split the C6–C6' and C5–C5' bonds step-wisely. Interestingly, it was demonstrated that photoexcited rhodium oxidants Rh(phi)$_2$DMB³⁺ [Phi, 9,10-phenanthrenequinone diimine; DMB, 4,4'-dimethyl-2,2'-
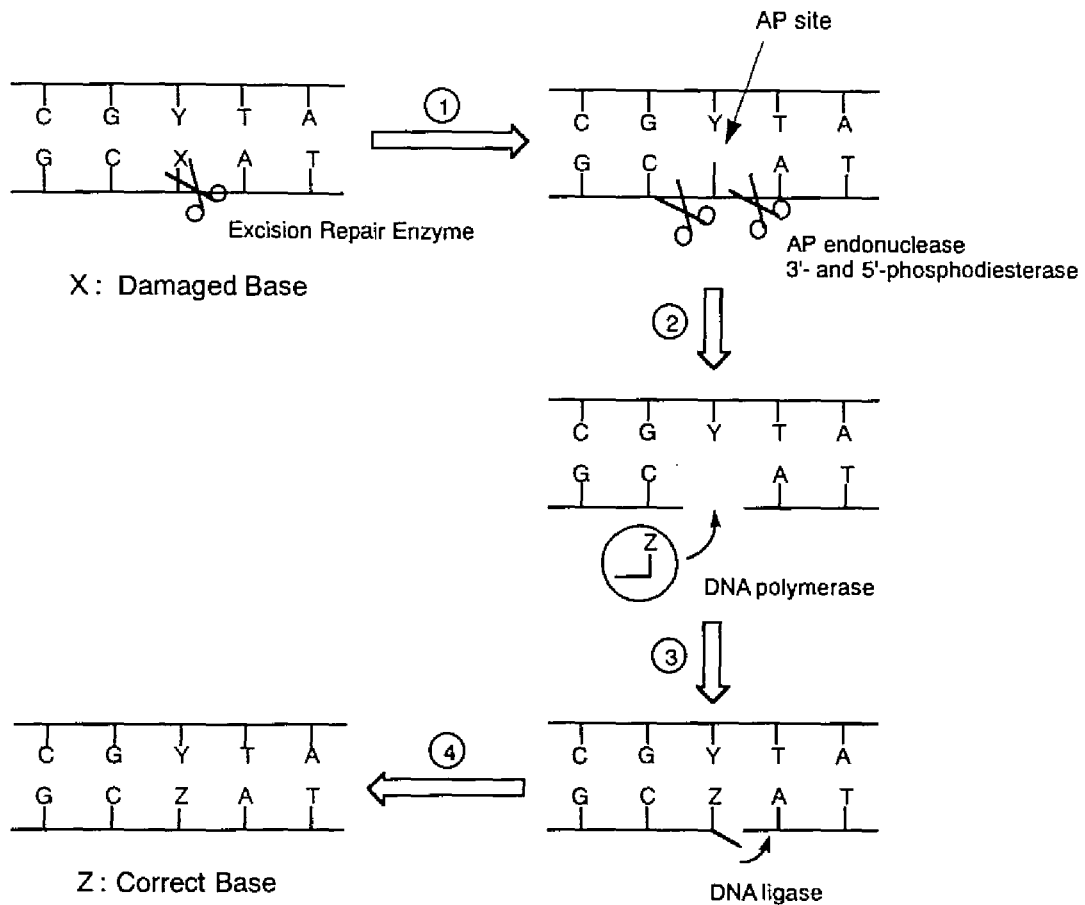
Figure 6. Schematic representation of the base-excision repair (BER) pathway. (1) Base modification in the DNA duplex is recognized and removed by a BER glycosylase to form apurinic-apyrimidinic (AP) site. (2) Either lyase activity intrinsic to the BER glycosyalse or separate AP endonuclease activity at the resulting AP site causes DNA strand cleavage. 3'- And 5'-phosphodiesterase may also be recruited to remove remaining sugar fragments into a one-nucleotide gap with 3'-hydroxy and 5'-phosphate ends. (3) DNA polymerase activity replaces the nucleotide gap with the correct nucleotide. (4) The phosphodiester backbone is sealed by DNA ligase.

7

Figure 7. Schematic presentation of the reaction mechanism of DNA photolyase. (1) Absorption of photon by the second chromophore (in this scheme, MTHF). (2) Energy transfer to FADH⁻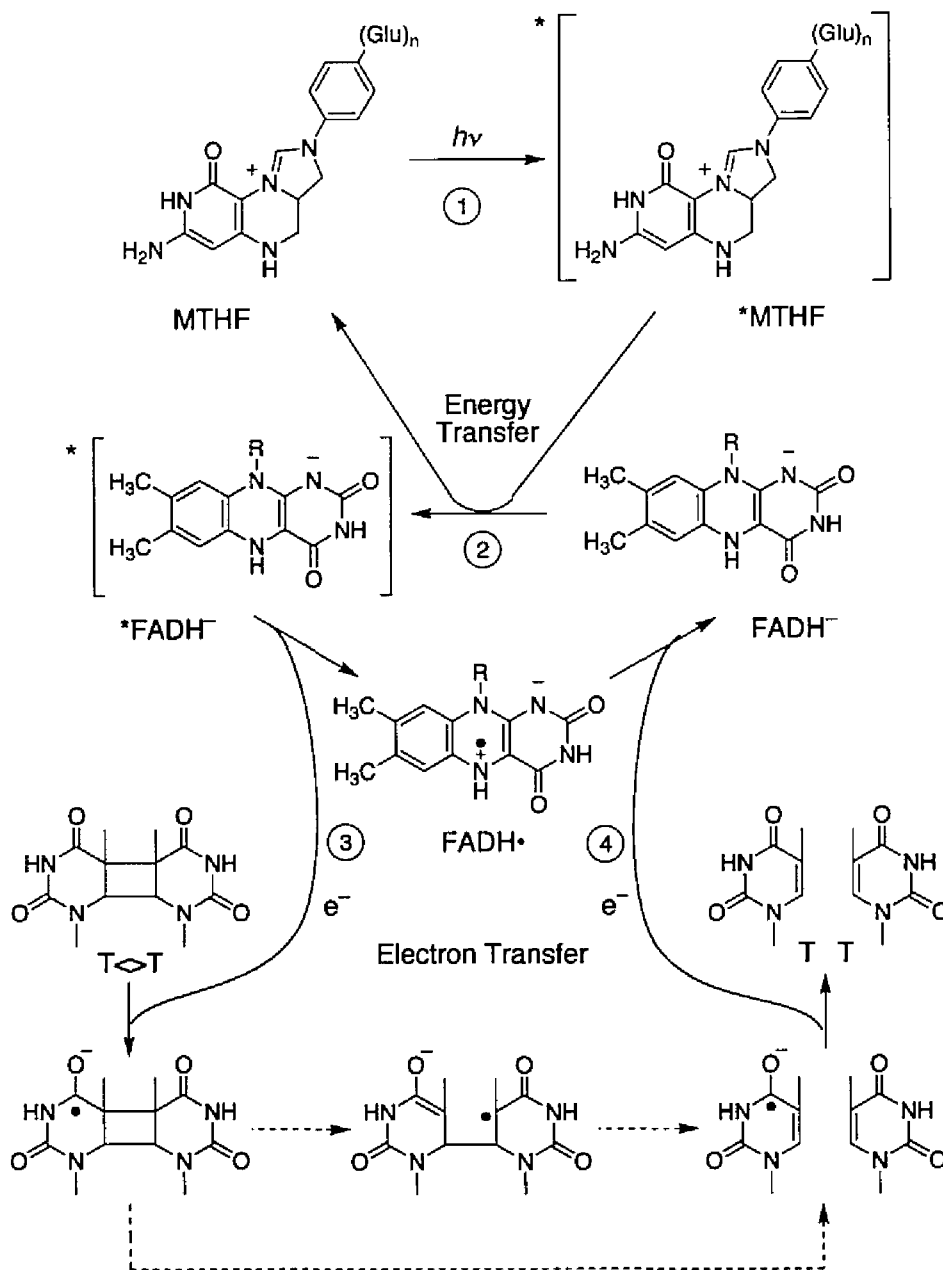. (3) Electron transfer to the dimer and the cycloreversion. (4) Back electron transfer and regeneration of catalytically active flavin, FADH⁻.

bipyridine] tethrated to DNA could promote the splitting of the cyclobutane dimer located at least 26–36 Å away in the DNA base stack via a long-range electron transfer to the rhodium metallointercalator.[32]

Survey of This Thesis

Chapter 1 focuses on the one-electron reducing and nucleophilic addition reactivity of carbon dioxide radical anion (CO_2^-) toward N-substituted thymines derivatives in aqueous solution, leading to the formation of several mono- and di-carboxylic acids including 5-methyl-5,6-dihydroorotic acid (5-methyl-DHO) derivatives. CO_2 radical anion has been suspected as a free radical metabolite, that is generated from CCl_4 by cytochrome P-450-dependent monooxygenase *in vivo* in the perfused rat liver, by means of ESR with a spin-trapping method.[33] Although it was shown that CO_2 radical anion has a dual reactivity with not only one-electron reduction but also radical addition toward the pyrimidine bases,[34] the reaction mechanism has not yet been well understood. The author characterizes the nucleophilic addition mechanism of CO_2 radical anion to the C6 of N-substituted thymines including thymidylyl(3'→5')thymidine to produce 5,6-dihydrothymine-6-carboxylic acids, which competes with one-electron reduction to form 5,6-dihydrothymines and C5–C5'-linked dihydrothymine dimers. In view of the biological function of DHO derivatives that may inhibit dihydroorotate dehydrogenase (DHODase),[35] an analog of 5-methyl-DHO was isolated and the X-ray structural analysis was performed to provide a structural insight into the binding mode of DHO derivatives to DHODase active site.[36]

Chapter 2 describes the structural characteristics of stereoisomeric C5–C5'-linked dihydrothymine dimers and the dimerization mechanism involved in the one-electron reduction of thymine derivatives. Radiolysis of 1-methylthymine and 1,3-dimethylthymine in aqueous solution under anoxic conditions afforded stereoisomeric

C5–C5'-linked dihydrothymine dimers as fractionated to the meso forms of (5R,5'S)- and (5S, 5'R)-bi-5,6-dihydrothymines and racemic compounds of (5R, 5'R)- and (5S, 5'S)-dimers along with 5,6-dihydrothymines. Similar radiolytic reduction of thymidine produced the pseudo-meso compound of (5R,5'S)-, (5S, 5'R)-dimers and two diastereomers of (5R, 5'R)-, and (5S, 5'S)-dimers. X-ray crystallographic analysis of the dimers suggested that the stereoisomeric C5–C5'-linked dihydrothymine dimers may cause some distortion within a DNA duplex if they were incorporated. Based on the results of the pH-dependence of the reactivity, the dimerization mechanism is discussed.

The behavior of the excited state of DNA in solution is of great importance for understanding of photochemistry and photophysics of DNA that are closely related to the conformation of pyrimidine and purine bases in DNA.[37,38] Chapter 3 focuses on the photophysical properties of the C5–C5'-linked dihydrothymine dimers to elucidate their conformational characteristics in solution. It is well recognized that nucleic acid bases aggregate by stacking interaction as to overlap the heteroaromatic rings with each other. Upon excitation of the nucleic acids, the excited molecule (M*) interacts with the ground-state molecule (N) to form exciplex or excimer (M•••N)* [If M and N are the same, the excited complex is termed an excimer.].[39] Dinucleotides and polynucleotides show excimer and exciplex fluorescence emissions from the stacked structures. In addition to the monomer fluorescence (λ_{max} ~340 nm), a long wavelength (λ_{max} ~400 nm) emission with a long lifetime in the range of a few nanosecond has been observed.[40] Among the C5–C5'-linked dimers, meso-dimer of 1-

$$M \quad + \quad h\nu \quad \rightarrow \quad M*$$

$$M* \quad + \quad N \quad \rightarrow \quad (M \bullet\bullet\bullet N)*$$
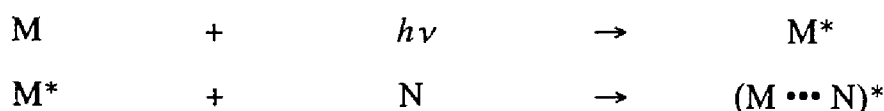
methylthymine showed a characteristic excimer fluorescence emission at λ_{max} = 370 nm, which is attributable to the intramolecular interaction between two dihydropyrimidine rings. Using steady state and time-resolved spectroscopic

methods, the conformational effects of the dimers on the fluorescence characteristics were investigated in both aqueous and non-aqueous solvents.

In Chapter 4 and 5, attempts are made to elucidate oxidative and reductive splitting reactivities of the stereoisomeric C5–C5'-linked dihydrothymine dimers by product analysis and laser flash photolysis. Under oxidative conditions containing several oxidants such as SO_4^-, azide radical ($N_3^.$), and photoexcited anthraquinone sulfonate (AQS*), the C5–C5'-linked dimers undergo one-electron oxidation to produce 5,6-dihydrothymin-5-yl radicals and 5,6-dihydrothymine C5-cations via the corresponding dimer radical cations, followed by deprotonation at C6 to regenerate the monomers. On the other hand, the dimer radical anions produced in the reduction by e_{aq}^- and photoexcited flavin adenine dinucleotide (FADH$^-$*) also generate the monomeric 5-yl radicals as the common intermediates, which are successively reduced into 5,6-dihydrothymines. Interestingly, FADH$^-$*-sensitized splitting reactivity was dependent on the stereoisomeric structures of the dimers, and the meso-dimer of 1-methylthymine gave the corresponding monomer in relatively high yield. Taking into account of the structural characteristics of the C5–C5'-linked dimers, the splitting mechanisms involving either one-electron transfer or two-electron transfer reaction are discussed.

References

(1)   (a) In *Photochemistry and Photobiology of Nucleic Acids*; Wang, S. Y. Ed.; Academic Press: New York, 1976; Vol. I. Chemistry. (b) Cadet, J.; Vigny, P. In *Bioorganic Photochemistry: The Photochemistry of Nucleic Acids*; Morrison, H., Ed.; John Wiley & Sons: New York, 1990; pp 1–272. (c) Bensasson, R. V.; Land, E. J.; Truscott, T. G. In *Excited States and Free Radicals in Biology and Medicine*; Oxford University Press: Oxford, 1993; pp 290–305. (d) Zimbrick, J. D. In *Radiation Damage in DNA: Structure / Function Relationships at Early Times*; Battle Press: Columbus, 1995.

(2)   (a) von Sonntag, C. In *The Chemical Basis of Radiation Biology*; Taylor and Francis: London, 1987. (b) Steenken, S. *Free Rad. Res. Commun.* **1992**, *16*, 349–379. (c) von Sonntag, C.; Schuchmann, H. –P. *Int. J. Radiat. Biol.* **1986**, *49*, 1–34.

(3)   (a) Pogozelski, W. K.; Tullius, T. D. *Chem. Rev.* **1998**, *98*, 1089–1107. (b) Burrows, C. J.; Muller, J. G. *Chem. Rev.* **1998**, *98*, 1109–1151.

(4)   (a) Herri, V. *Compt. Rend.* **1914**, *158*, 1032–1035. (b) Muller, H. J. *Science* **1927**, *66*, 84–87.

(5)   (a) Gates, F. L. *J. Gen. Physiol.* **1930**, *14*, 31–42. (b) Stadler, L. J.; Uber, F. M. *Genetics* **1942**, *27*, 84–118.

(6)   (a) Farman, J. C.; Gardiner, B. G.; Shanklin, J. D. *Nature* **1985**, *315*, 207–210. (b) Wayne, R. P. In *Chemistry of Atmospheres, 2nd eds.*; Clarendon Press: Oxford, 1991. (c) Stolarski, R.; Bojkov, R.; Bishop, L.; Zerefos, C.; Staehelin, J.; Zawodny, J. *Science* **1992**, *256*, 342–349.

(7)   For example, see (a) Orlov. V. M.; Smirnov, A. N.; Varshavsky, Y. M. *Tetrahedron Lett.* **1976**, *48*, 4377–4378. (b) Jovanovic, S. V.; Simic, M. G. *J. Phys. Chem.* **1986**, *90*, 974–978. (c) Sugiyama, H.; Saito, I. *J. Am. Chem. Soc.* **1996**, *118*, 7063–7068.

(8)   (a) Hall, D. B.; Holmlin, R. E.; Barton, J. K. *Nature* **1996**, *382*, 731-735. (b)

Arkin, M. R.; Stemp, E. D. A.; Pulver, S. C.; Barton, J. K. *Chem. Biol.* **1997**, *4*, 389–400. (c) Stemp, E. D. A.; Arkin, M. R.; Barton, J. K. *J. Am. Chem. Soc.* **1997**, *119*, 2921–2925. (d) Dandliker, P. J.; Núñez, M. E.; Barton, J. K. *Biochemistry* **1998**, *37*, 6491–6502. (d) Ropp, P. A.; Thorp, H. H. *Chem. Biol.* **1999**, *6*, 599–605. (e) Núñez, M. E.; Hall, D. B.; Barton, J. K. *Chem. Biol.* **1999**, *6*, 85–97.

(9)   (a) Kuwabara, M. *Radiat. Phys. Chem.* **1991**, *37*, 691–704. (b) Angelov, D.; Berger, M.; Cadet, J.; Getoff, N.; Keskinova, E.; Solar, S. *Radiat. Phys. Chem.* **1991**, *37*, 717–727. (c) Bamatraf, M. M. M.; O'Neill, P.; Rao, B. S. M. *J. Am. Chem. Soc.* **1998**, *120*, 11852–11857.

(10)   (a) Heelis, P. F.; Kim, S. -T.; Okamura, T.; Sancar, A. *J. Photochem. Photobiol. B: Biol.* **1993**, *17*, 219–228. (b) Görner, H. *J. Photochem. Photobiol. B: Biol.* **1994**, *26*, 117–139. (c) Sancar, A. *Biochemistry* **1994**, *33*, 2–9.

(11)   Cleaver, J. E. *Nature* **1968**, *218*, 652–656.

(12)   Singer, B.; Essigmann, J. M. *Carcinogenesis* **1991**, *12*, 949–955.

(13)   Wang, C. -I.; Taylor, J. -S. *Biochemistry* **1992**, *31*, 3671–3681.

(14)   Fix, D.; Bockrath, R. *Mol. Gen. Genet.* **1981**, *182*, 7–11.

(15)   (a) Burdi, D.; Begley, T. P. *J. Am. Chem. Soc.* **1991**, *113*, 7768–7770. (b) Kim, S. -T.; Sancar, A. *Photochem. Photobiol.* **1993**, *57*, 895–904.

(16)   (a) Ide, H.; Kow, Y. W.; Wallace, S. S. *Nucleic Acids Res.* **1985**, *13*, 8035–8052. (b) Clark, J. M.; Beardsley, G. P. *Nucleic Acids Res.* **1986**, *14*, 737–749. (c) Hayes, R. C.; LeClerc, J. E. *Nucleic Acids Res.* **1986**, *14*, 1045–1061.(d) Clark, J. M.; Beardsley, G. P. *Biochemistry* **1987**, *26*, 5398–5403. (e) Hayes, R. C.; Petrullo, L. A.; Huang, H.; Wallece, S. S.; LeClerc, J. E. *J. Mol. Biol.* **1988**, *201*, 239–246. (f) Ide, H.; Wallace, S. S. *Nucleic Acids Res.* **1988**, *16*, 11339–11354.

(17)   Shibutani, S.; Takeshita, M.; Grollman, A. P. *Nature* **1991**, *349*, 431–434.

(18)   (a) Cheng, K. C.; Cahill, D. S.; Kasai, H.; Nishimura, S.; Loeb, L. A. *J. Biol. Chem.* **1992**, *267*, 166–172. (b) Tchou, J.; Grollman, A. P. *Mutat. Res.* **1993**, *299*, 277–287.

(19)   Kouchakdjian, M.; Bodepudi, V.; Shibutani, S.; Eisenberg, M.; Johnson, F.; Grollman, A. P.; Patel, D. J. *Biochemistry* **1991**, *30*, 1403–1412.

(20)   Sevilla, M. D.; D'Arcy, J. B.; Morehouse, K. W.; Englehardt, M. L. *Photochem. Photobiol.* **1979**, *29*, 37–42.

(21)   Sevilla, M. D. Excited States In *Organic Chemistry and Biochemistry*; Pullman, B.; Goldblum, N. Eds.; D. Reidel: Dordrecht, Holland, 1977.

(22)   Sevilla, M. D.; Failor, R.; Clark, C.; Holroyd, R. A.; Pettei, M. *J. Phys. Chem.* **1976**, *80*, 353–358.

(23)   (a) Cullis, P. M.; McClymont, J. D.; Malone, M. E.; Mather, A. N.; Podmore, I. D.; Sweeney, M. C.; Symons, M. C. R. *J. Chem. Soc. Perkin Trans. 2* **1992**, 1695–1702. (b) Sevilla, M. D.; Becker, D.; Yan, M.; Summerfield, S. R. *J. Phys. Chem.* **1991**, *95*, 3409–3415.

(24)   Steenken, S.; Telo, J. P.; Novais, H. M.; Candeias, L. P. *J. Am. Chem. Soc.* **1992**, *114*, 4701–4709.

(25)   Ide, H.; Petrullo, L. A.; Hatahet, Z.; Wallace, S. S. *J. Biol. Chem.* **1991**, *266*, 1469–1477.

(26)   Nishimoto, S.; Ide, H.; Nakamichi, K.; Kagiya, T. *J. Am. Chem. Soc.* **1983**, *105*, 6740–6741.

(27)   For review, see (a) Friedberg, E. C.; Walker, G. C.; Siede, W. In *DNA Repair and Mutagenesis*, ASM Press: Washington, D. C., 1995. (b) David, S. S.; Williams, S. D. *Chem. Rev.* **1998**, *98*, 1221–1261. (c) Lloyd, R. S. *Mutat. Res.* **1998**, *408*, 159–170.

(28)   Setlow, R. B. *Nature* **1978**, *271*, 713–717.

(29)   (a) Kim, S. -T.; Heelis, P. F.; Okamura, T.; Hirata, Y.; Mataga, N.; Sancar, A. *Biochemistry* **1991**, *30*, 11262–11270. (b) Kim, S. -T.; Heelis, P. F.; Sancar,

A. *Biochemistry* **1992**, *31*, 11244–11248.

(30)   (a) Young, T.; Nieman, R.; Rose, S. D. *Photochem. Photobiol.* **1990**, *52*,
661–668. (b) Pouwels, P. J. W.; Hartman, R. F.; Rose, S. D.; Kaptein, R.
Photochem. Photobiol. **1995**, *61*, 563–574.

(31)   Heelis, P. F.; Deeble, D. J.; Kim, S. -T.; Sancar, A. *Int. J. Radiat. Biol.* **1992**,
62, 137–143.

(32)   (a) Dandliker, P. J.; Holmlin, R. E.; Barton, J. K. *Science* **1997**, *275*,
1465–1468.

(33)   (a) Conner, H. D.; Thurman, R. G.; Galizi, M. D.; Mason, R. P. *J. Biol. Chem.*
1986, *261*, 4542–4548. (b) La Cagnin, L. B.; Connor, H. D.; Mason, R. P.;
Thurman, R. G. *Mol. Pharmacol.* **1988**, *33*, 351–357. (c) Reinke, L. A.;
Towner, R. A.; Janzen, E. G. *Toxicol. Appl. Pharmacol.* **1992**, *112*, 17–23.

(34)   (a) Kamal, A.; Garrison, W. M. *Nature* **1965**, *206*, 1315–1317. (b) Neta P.
Radiat. Res. **1972**, *49*, 1–25. (c) Wada, T.; Ide, H.; Nishimoto, S.; Kagiya, T.
Int. J. Radiat. Biol. **1982**, *42*, 215–221.

(35)   (a) Hines, V.; Johnston, M. *Biochemistry* **1989**, *28*, 1227–1234. (b) Jones, M.
E. *Ann. Rev. Biochem.* **1980**, *49*, 253–279 (c) Keys III, L. D.; Johnston, M. *J.
Am. Chem. Soc.* **1985**, *107*, 486–492.

(36)   (a) Defrees, S. A.; Sawick, D. P.; Cunningham, B.; Heinstein, P. F.; Morré, D.
J.; Cassady, J. M. *Biochem. Pharmacol.* **1988**, *37*, 3807–3816. (b)
Mahmoudian, M; Pakiari, A. H.; Khademi, S. *Biochem. Pharmacol.* **1992**, *43*,
283–287.

(37)   Saenger, W. *Principles of Nucleic Acid Structure*; Springer-Verlag: New York,
1984.

(38)   For example, (a) Miller, J. H.; Sobell, H. M. *J. Mol. Biol.* **1967**, *24*, 345–350.
(b) Nakano, N. I.; Igarashi, S. J. *Biochemistry* **1970**, *9*, 577–583. (c) Wu, P.;
Nordlund, T. M. *Biochemistry* **1990**, *29*, 6508–6514. (d) Florián, J.; ˘Sponer,
J.; Warshel, A. *J. Phys. Chem. B* **1999**, *103*, 884–892. (e) ˘Sponer, J.;

Leszczy´nski, J.; Hobza, P. *J. Phys. Chem.* **1996**, *100*, 5590–5596. (f) Hauswirth, W.; Daniels, M. *Photochem. Photobiol.* **1971**, *13*, 157–163. (g) Vigny, P.; Duquesne, M. *Photochem. Photobiol.* **1974**, *20*, 15–25. (h) Becker, R. S.; Kogan, G. *Photochem. Photobiol.* **1980**, *31*, 5–13. (i) Baraldi, I.; Bruni, M. C.; Costi, M. P.; Pecorari, P. *Photochem. Photobiol.* **1990**, *52*, 361–374. (j) Eaton, W.; Lewis, T. P. *J. Phys. Chem.* **1970**, *53*, 2164–2172. (k) Morsy, M. A.; Al-Somali, A. M.; Suwaiyan, A. *J. Phys. Chem. B* **1999**, *103*, 11205–11210.

(39)   Turro, N. J. In *Modern Molecular Photochemistry*; Benjamin/Cummings: Menlo Park, 1987.

(40)   Browne, D. T.; Eisinger, J.; Leonard, N. J. *J. Am. Chem. Soc.* **1968**, *90*, 7302–7323. (b) Leonard, N. J.; Ito, K. *J. Am. Chem. Soc.* **1973**, *95*, 4010–4016.

Chapter 1

One-Electron Reducing and Nucleophilic Addition Reactivity of Carbon Dioxide Radical Anion towards Thymine Derivatives

Abstract: The nucleophilic addition properties of carbon dioxide radical anion $(CO_2^{\cdot-})$ towards N1-substituted thymine derivatives in aqueous solution is studied for comparison with their one-electron reducing reactivity. N_2O-Saturated aqueous solutions of 1-methylthymine, 1,3-dimethylthymine, and thymidylyl(3'→5')thymidine containing excess formate ions were γ-irradiated at 1.0 Gy min^{-1}. Several carboxylated thymines were isolated by preparative HPLC and identified by GC-MS, NMR, and X-ray crystallography. Along with one-electron reduction yielding N-substituted 5,6-dihydrothymines and C5–C5'-linked dihydrothymine dimers, the addition of CO_2 radical anion(s) to the C5–C6 double bond of N-substituted thymines produced several mono- and di-carboxylic acids, among which N-substituted derivatives of 5,6-dihydrothymine-6-carboxylic acid [5-methyldihydroorotic acid (5-methyl-DHO)] were produced in the highest yield. Similar carboxylation by CO_2 radical anions was also observed for thymine dinucleoside monophosphate. The X-ray structure of cis-5,6-dihydro-1-methylthymine-6-carboxylic acid (cis-1,5-dimethyl-DHO) was determined to show a chair conformation in the crystal. The CO_2 radical anion is a nucleophilic radical with rather low reduction potential, thereby possessing a dual reactivity of radical addition preferentially at C6 and one-electron reduction towards thymine-related compounds.

Introduction

Free radicals generated by ionizing radiation, chemical oxidants and several antibiotics give rise to genotoxic damage in biological systems.[1,2] Free-radical chemistry of DNA bases, peptides, and proteins has been studied extensively for a better understanding of the mechanisms by which deleterious free radicals such as hydroxyl radical ($^\cdot$OH), peroxyl radical ($RO_2^\cdot$), nitric oxide radical ($NO^\cdot$) and nitrogen dioxide radical ($NO_2^\cdot$) cause a variety of damage to biomolecules. Among these radical species, the OH radical is recognized as a key oxidizing radical species producing oxidative modification in DNA bases such as 5,6-dihydroxy-5,6-dihydrothymine (thymine glycol) and 7,8-dihydro-8-oxo-2'-deoxyguanosine.[1,2]

Reducing radicals, including alcohol radicals such as 2-hydroxypropan-2-yl radicals ($(CH_3)_2C^\cdot OH$) and carbon dioxide radical anions ($CO_2^{\cdot-}$) generated by radiation have been reported to inactivate biologically active DNA.[3] By means of ESR with a spin-trapping method, the CO_2 radical anion has been identified as a free radical metabolite that is generated from CCl_4 by cytochrome P-450-dependent monooxygenases *in vivo* in the perfused rat liver.[4-6] A good correlation was also observed between the hepatocellular damage and the free radical formation involved in the metabolism of CCl_4.[5] As a typical reactivity, CO_2 radical anion can induce one-electron reduction of thymine derivatives to produce the diastereomers of 5,6-dihydrothymine and C5–C5'-linked 5,6-dihydrothymine dimers.[7,8] Alternatively, CO_2 radical anion induces carboxylation of amino acids[9,10] and pyrimidine bases (for cytosine,[11] orotic acid[12] and thymine[13]) by radical recombination reaction with several carbon-centered radicals of the amino acids or direct addition to the C5–C6 double bonds of the pyrimidines. On the other hand, alcohol radicals show reactivity of nucleophilic addition to C6 and hydrogen abstraction from the C5-methyl group, but not one-electron reduction of thymine derivatives.[14] Such carboxylated products formed by direct reaction of CO_2 radical anion with thymine derivatives have not yet

O
HN
O   N   COOH
    H

Dihydroorotic acid

O
R²-N   CH₃
O   N
    R¹

1a: R¹ = CH₃, R² = H
1b: R¹ = CH₃, R² = CH₃

O
R²-N   CH₃
        COOH
O   N   COOH
    R¹ H

2a

O
R²-N   CH₃
        COOH
O   N   H
    R¹ H

3a

O
R²-N   CH₃
        H
O   N   COOH
    R¹ H

4a,b

O   O
R²-N   CH₃ H₃C   N-R²
        H   H
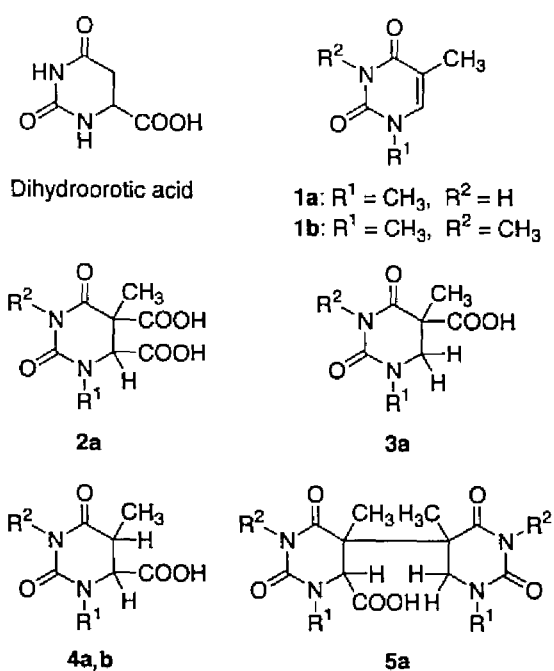O   N   COOH H   N   O
    R¹   R¹

5a

Chart 1. Structures of N-substituted thymines and the carboxylic acid derivatives.

been isolated.

The present paper reports nucleophilic addition of the CO_2 radical anion to the C6 of 1-methylthymine (**1a**) and 1,3-dimethylthymine (**1b**) to produce N-substituted 5,6-dihydrothymine-6-carboxylic acids, which competes with one-electron reduction resulting in the formation of N-substituted 5,6-dihydrothymines and stereoisomeric C5–C5'-linked dihydrothymine dimers (Chart 1). Considerable attention has been focused on the 6-carboxylated pyrimidine structures for understanding of the action mechanism[15] and inhibition mode[16,17] of dihydroorotate dehydrogenase (DHODase), an enzyme of the *de novo* pyrimidine biosynthesis catalyzing the stereoselective oxidation of (S)-5,6-dihydroorotic acid (S-DHO) to orotic acid.[15,18,19] The X-ray structure of a 1,5-dimethyl-DHO derivative was therefore characterised in detail to get structural insight into binding of S-DHO to DHODase active site.

19

Experimental Section

Materials. 1-Methylthymine (**1a**) and thymidylyl(3'→5')thymidine (TpT) were obtained from Sigma Chemical Co. (St. Louis, MO, U.S.A.) and used without further purification. Purified 1,3-dimethylthymine (**1b**) was kindly supplied by Fujii Memorial Research Institute, Otsuka pharmaceutical. Sodium formate (Nacalai Tesque, Kyoto, Japan), thymine (**1c**), NaH_2PO_4 and methanol (HPLC grade, Wako Pure Chemical Industries, Osaka, Japan) were used as received.

HPLC Analysis. Aliquots (10 μl) of the γ-irradiated solutions were analyzed by high-performance liquid chromatography (HPLC), using a Shimadzu 10A HPLC system equipped with a Rheodyne 7725 sample injector. Sample solutions were injected onto a reversed phased column (Wakosil 5C18, ϕ 4.6 mm × 150 mm) containing C18 chemically bonded silica gel (5 μm particle size). The phosphate buffer solutions (10 mM, pH 3.0) containing varying contents (10–25 vol%) of methanol were delivered as the mobile phase at a flow rate of 0.6 ml min^{-1}. The column eluents were monitored by the UV absorbance at 210 nm. For isolation of the products, the irradiated solutions were evaporated to a minimum volume and were subjected to a preparative HPLC using a Tosoh Preparative HPLC system equipped with a Chromatocorder 12 (System Instruments, Tokyo, Japan). The isolation was performed on a reversed phased column (Wakosil 10C18, ϕ 10 mm × 300 mm) containing C18 chemically bonded silica gel (10 μm particle size) and phosphate buffer solution (10 mM, pH 3.0) containing 5–20 vol% methanol was delivered at a flow rate of 3.0 ml min^{-1}. Aqueous fractions that contained the respective products were then collected automatically and evaporated. The resulting residues were lyophilized and subjected to spectroscopic measurements.

NMR and Mass Spectroscopy. ^{1}H and ^{13}C NMR spectra were recorded on a JEOL GSX-270 (270 MHz) Fourier-transform NMR spectrometer. Samples were dissolved in dimethylsulfoxide-d_6 (99.9%; Aldrich). Chemical shifts were expressed in ppm

relative to residual DMSO-d_6 traces ([1]H: 2.49 ppm, [13]C: 39.7 ppm).

High-resolution positive FAB mass spectra (FAB-HRMS) were recorded on a JEOL JMS-SX102A spectrometer, using glycerol matrix. Gas chromatography-mass spectrometry with an electron impact ionization method (GC-EIMS) or a chemical ionization method (GC-CIMS) was performed on a Shimadzu GC-MS QP 1000EX at 70 eV. Helium and 2-methylpropane were used as the carrier gas for the GC-EIMS and the reaction gas for the GC-CIMS, respectively. Prior to the GC-MS analysis, samples were trimethylsilylated in a polytetrafluoroethylene-capped vial with 0.05 ml of N-methyl-N-trimethylsilyltrifluoroacetamide (Pierce) in 0.1 ml of acetonitrile (Pierce) by heating for 30 min at 130 °C. The resulting mixture in solution was separated using a fused silica capillary column (Shimadzu CBP-1-M 25-025, ϕ 0.25 mm × 250 mm).

X-Ray Crystallography. A colorless needle-shaped crystal of (5S, 6S)-5,6-dihydro-1-methylthymine-6-carboxylic acid was grown from aqueous solution (ca. 3 mg ml^{-1}). The crystal was mounted directly on a glass fiber. The measurement was made on a Rigaku AFC7R diffractometer with graphite monochromated Mo-Kα radiation (λ = 0.71609 Å) and a 12-kW rotating anode generator. The diffraction data were collected at room temperature using the ω-2θ scan mode to a maximum 2θ value of 55°. The intensities of three representative reflections were measured after every 150 reflections without applying decay correction. The structure was solved by a direct method using SHELXS 86[20] and expanded using a Fourier technique. The positions of hydrogen atoms were calculated and only isotropic B-values were refined.

General Irradiation and Characterization Procedures. N_2O-Saturated aqueous solutions of 1-methylthymine (**1a**; 5.0 mM) and 1,3-dimethylthymine (**1b**; 5.0 mM) containing sodium formate (1 M) were irradiated with ^{60}Co γ-ray source (1.0 Gy min^{-1}) up to 4.25 kGy at room temperature. The irradiated solutions were evaporated under reduced pressure, and isolated by preparative HPLC. For NMR analysis and X-ray crystallography, the samples were further purified by recrystallization from water.

(5S, 6S)-5,6-Dihydro-1-methylthymine-6-carboxylic acid (4a, cis-1,5-dimethyl-DHO): ^{1}H NMR (399.65 MHz, DMSO-d_6, 25 °C): δ = 1.06 (3H, d, J=6.4Hz, 5-CH$_3$), 2.83 (3H, s, 1-CH$_3$), 3.08 (1H, dq, J=6.4Hz, 5-CH), 4.06 (1H, d, J=6.4Hz, 6-CH), 10.17 (1H, s, 3-NH), 11.33 (br, s, 6-COOH); ^{13}C NMR (100.40 MHz, DMSO-d_6, 25 °C): δ = 10.58, 33.65, 36.83, 61.81, 153.21, 170.85, 171.24 ; GC-CIMS m/z 331 [(M + Si(CH$_3$)$_3$ × 2 + H)$^+$]; GC-EIMS m/z (%) 73 (51), 98 (100), 213 (75), 285 (29), 315 (49); FAB-HRMS (glycerol matrix) calcd for C7H11N2O4 [(M + H)$^+$] 187.0718, found 187.0719; X-ray crystal data C7H10N2O4, monoclinic, P2$_1$/n, colorless, a = 5.189(9) Å, b = 13.087(8) Å, c = 12.494(6) Å, b = 92.13(8)°, V = 847(1) Å^3, Z = 4, R = 0.059, Rw=0.057, GOF=1.46. Crystallographic data excluding structure factors have been deposited with the Cambridge Crystallographic Data Centre as supplementary publication no. CCDC-114556. Copies of the data can be obtained free of charge on application to CCDC, 12 Union Road, Cambridge CB2 1EZ, UK (fax: int. code +(44)1223-336-033; e-mail: deposit@ccdc.cam.ac.uk).

5,6-Dihydro-1,3-dimethylthymine-6-carboxylic acid (4b): ^{1}H NMR (399.65 MHz, DMSO-d_6, 25 °C): δ = 1.11 (3H, d, J=6.8 Hz 5-CH$_3$), 2.89 (3H, s, 1-CH$_3$), 2.98 (3H, s, 3-CH$_3$), 3.17 (1H, dq, J=6.8 Hz, 5-CH), 4.08 (1H, d, J=6.8 Hz, 6-CH), not observed (6-COOH), ^{13}C NMR (100.40 MHz, DMSO-d_6, 25 °C): δ = 11.23, 27.26, 34.83, 36.29, 60.85, 153.53, 170.55, 170.79; GC-CIMS of the trimethylsilyl derivative m/z 273 [(M + Si(CH$_3$)$_3$ + H)$^+$]; GC-EIMS of the trimethylsilyl derivative m/z (%) 73 (41), 98 (68), 155 (100), 213 (14), 257 (4).

5,6-Dihydro-1-methylthymine-5,6-dicarboxylic acid (2a): GC-CIMS of the trimethylsilyl derivative m/z 375 [(M + Si(CH$_3$)$_3$ × 2 + H)$^+$]; GC-EIMS of the trimethylsilyl derivative is shown in Figure 2.
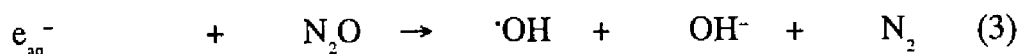
5,6-Dihydro-1-methylthymine-5- or 6-carboxylic acid (3a): GC-CIMS of the trimethylsilyl derivative m/z 331 [(M + Si(CH$_3$)$_3$ × 2 + H)$^+$]; GC-EIMS of the trimethylsilyl derivative m/z (%) 73 (73), 127 (45), 199 (100), 243 (13), 315 (55).

C5–C5'-Linked dihydrothymine dimer 6-carboxylic acid (5a): GC-CIMS of the

trimethylsilyl derivative m/z 543 [(M + Si(CH$_3$)$_3$ × 3 + H)$^+$]; GC-EIMS of the trimethylsilyl derivative is shown in Figure 2.

Results and Discussion

Radiolytic Carboxylation and Characterization of the Products. N$_2$O-Saturated aqueous solutions of thymine derivatives **1a,b** (5.0 mM) containing sodium formate (1.0 M) were γ-irradiated (several doses at 1.0 Gy min^{-1}) to investigate exclusively the reactivity of CO$_2$ radical anion. Radiolysis of a dilute aqueous solution produces oxidizing hydroxyl radicals (·OH) and reducing hydrated electrons (e$_{aq}^-$) along with a small amount of hydrogen atoms (·H). The G-values of these primary water radicals in neutral aqueous solution are $G(e_{aq}^-) = G(\cdot OH) = 2.8 \times 10^{-7}$ mol J^{-1} and $G(\cdot H) = 0.6 \times 10^{-7}$ mol J^{-1}, respectively.[1] In the presence of excess formate ions, OH radicals and H atoms are scavenged by the formate ions and converted into reducing CO$_2$ radical anions as in reactions 1 ($k(\cdot OH) = 3 \times 10^9$ dm^3 mol^{-1} s^{-1}) and 2 ($k(\cdot H) = 3 \times 10^8$ dm^3 mol^{-1} s^{-1}). On the other hand, hydrated electrons are scavenged by N$_2$O and converted to OH radicals (reaction 3, $k = 9.1 \times 10^9$ dm^3 mol^{-1} s^{-1}). Thus, the reaction system involves CO$_2$ radical anions as a primary active species ($G(CO_2^-) = 6.3 \times 10^{-7}$ mol J^{-1}).

HCOO$^-$	+	·OH	→	CO$_2^-$	+	H$_2$O		(1)
HCOO$^-$	+	·H	→	CO$_2^-$	+	H$_2$		(2)
e$_{aq}^-$	+	N$_2$O	→	·OH	+	OH$^-$	+ N$_2$	(3)

Figures 1a and 1b illustrate the representative HPLC profiles of the solutions of **1a** and **1b** after irradiation, as detected at a wavelength of 210 nm. The elution peaks **6a** and **6b** were assigned to 5,6-dihydro-1-methylthymine (50% yield) and 5,6-dihydro-1,3-dimethylthymine (38% yield) by comparing the retention times with those
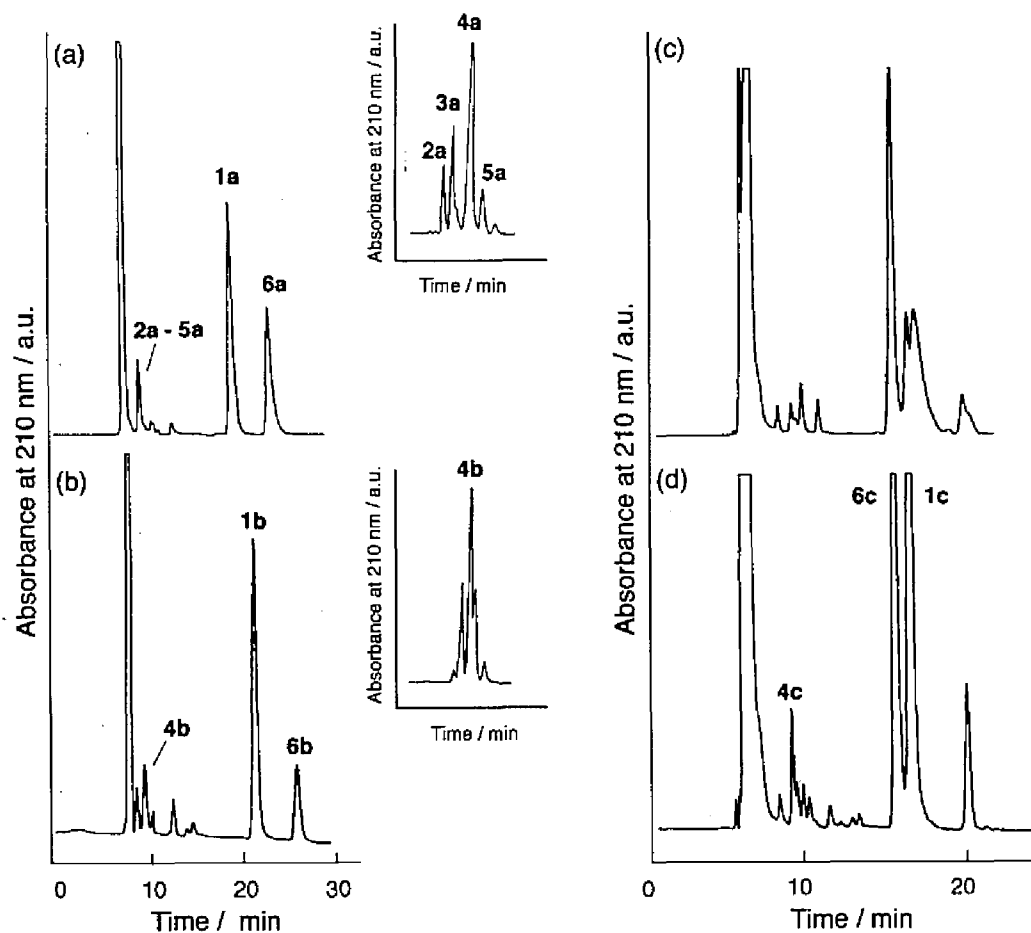
Figure 1. Representative HPLC profiles of aqueous solution of (a) **1a** (1.0 mM) and (b) **1b** (1.0 mM) after γ-irradiation in the presence of sodium formate (200 mM) under N_2O. The analysis was carried out on an ODS-column (φ 4.6 mm × 150 mm) delivered by phosphate buffer solution containing (a) 5 % or (b) 15 % methanol. Insets show the expanded charts of the peak **2a–5a** and **4b**. The HPLC analyses of (c) hydrolysates from products of TpT radiolysis, and (d) products of thymine (**1c**) radiolysis including thymine mono-carboxylic acid (**4c**) and 5,6-dihydrothymine (**6c**) were performed using 5% methanol containing phosphate buffer solutions as eluent.

of the authentic samples, respectively. The other major products of stereoisomeric C5–C5'-linked dihydrothymine dimers were also detected at longer retention times:[8] 7a, meso compound of (5R,5'S)- and (5S,5'R)-bi-5,6-dihydro-1-methylthymine (9% yield); 8a, a racemic compound of (5R,5'R)- and (5S,5'S)-bi-5,6-dihydro-1-methylthymine (9% yield); 7b, meso compound of (5R,5'S)- and (5S,5'R)-bi-5,6-dihydro-1,3-dimethylthymine (8% yield); 8b, a racemic compound of (5R,5'R)- and (5S,5'S)-bi-5,6-dihydro-1-methylthymine (11% yield). These N-substituted derivatives of 5,6-dihydrothymine and C5–C5'-linked dihydrothymine dimer are derived from the related 5,6-dihydrothymin-5-yl radicals as formed via one-electron reduction of thymines followed by protonation at the C6.[7,8]

The elution peaks for the products 2a–5a and 4b derived from 1a and 1b, respectively, were fractionated by preparative HPLC and trimethylsilylated by N-methyl-N-trimethylsilyltrifluoroacetamide for GC-MS analyses. As confirmed by GC-EIMS (Figure 2) or GC-CIMS (see experimental section), these products were mono- and di-carboxylic acids: 2a, 5,6-dihydro-1-methylthymine-5,6-dicarboxylic acid {GC-CI: m/z 375 [(M + Si(CH₃)₃ × 2 + H)⁺]}; 3a and 4a, 5,6-dihydro-1-methylthymine-5- or 6-carboxylic acid {m/z 331 [(M + Si(CH₃)₃ × 2 + H)⁺]}; 5a, 5-(5',6'-dihydro-1'-methylthymin-5'-yl)-5,6-dihydro-1-methylthymine-6-carboxylic acid {m/z 543 [(M + Si(CH₃)₃ × 3 + H)⁺]}. Among the carboxylic acids isolated upon degradation of 1a, the product 4a was further purified by recrystallization from water and subjected to ¹H, ¹³C NMR, a high-resolution fast atom bombardment mass spectrometry (FAB-HR MS), and X-ray crystallography. All data were consistent with a racemic mixture of (5R, 6R)- and (5S, 6S)-5,6-dihydro-1-methylthymine-6-carboxylic acid (cis-1,5-dimethyl DHO, 19% yield). On the other hand, isolation and purification of the minor carboxylic acids 2a, 3a and 5a by preparative HPLC was not successful because of much lower yields. For the lack of comprehensive spectral data at present, the structures of these minor products proposed based on the GC-MS analyses are only tentative. In view of the well characterized structure of 4a, the
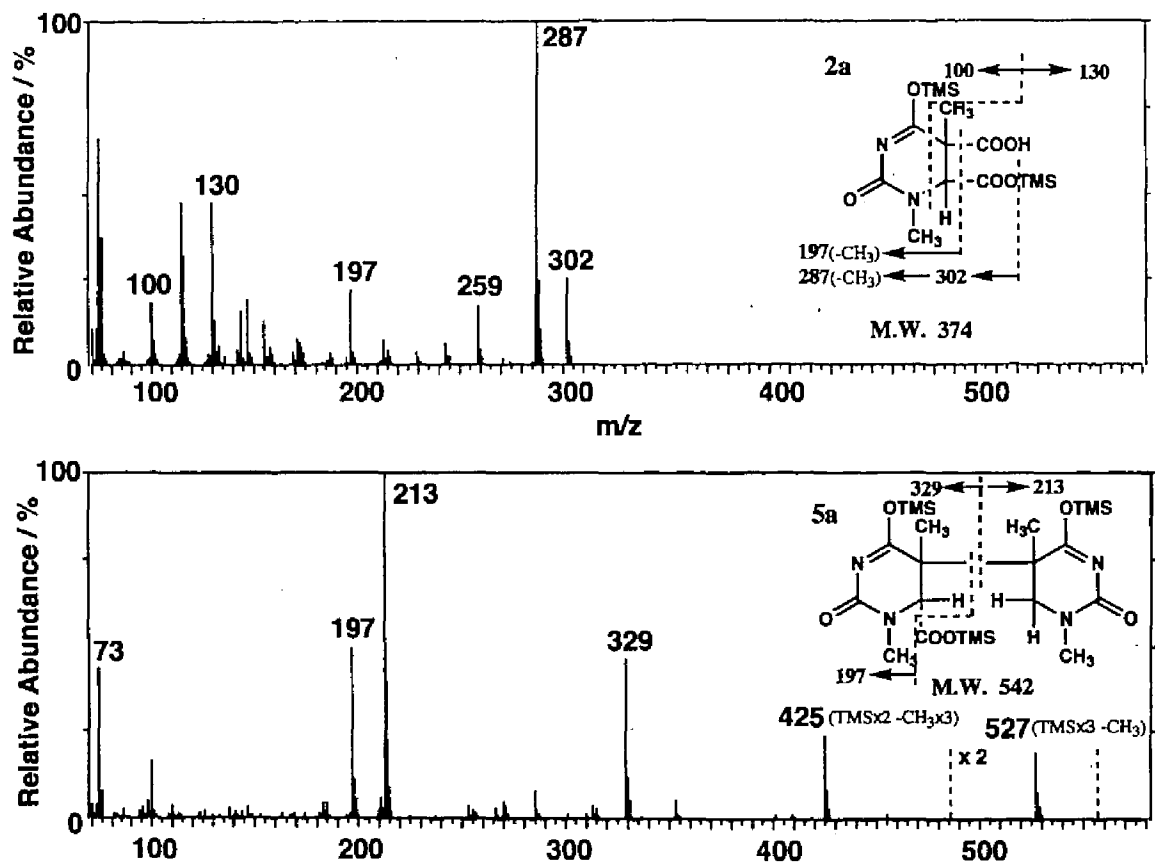
Figure 2. GC-EIMS spectra of trimethylsilylated products of **2a** and **5a** as separated using a fused silica capillary column (see experimental section).

product **3a** seems most likely to be a 5-carboxylated analog rather than a stereoisomer of **4a**, since the GC-EIMS fragmentation pattern of **3a** was different from that of **4a**, while showing an identical trimethylsilylated molecular ion at m/z 331 [(M + $Si(CH_3)_3$ × 2 + H)$^{+}$]. On the other hand, all the spectral data of **4b** were consistent with a racemic mixture of (5*R*,6*R*)- and (5*S*,6*S*)-5,6-dihydro-1,3-dimethylthymine-6-carboxylic acid (15% yield), while the X-ray crystallographic analysis was not successful.

Figures 4 illustrate the three-dimensional structure of **4a** in the crystal, indicating that the methyl and carboxyl groups are oriented in a gauche conformation around the C5–C6 bond [selected torsion angles: $C(5\text{-}CH_3)$–C5–C6–C(6-COOH), 58(1)°; O4–C4–C5–C(5-CH_3), 10(1)°; C(6-COOH)–C6–N1–C(1-CH_3), –82(1)°, and that the pyrimidine ring exhibits a chair conformation. Compared with the pyrimidine ring structures of thymine[21] and its 5,6-saturated derivatives,[22,23] **4a** possesses slightly elongated C5–C6 and N1–C6 bonds which would be a reflection of more loss of the π-electron density by carboxylation. On the other hand, the NMR study in solution indicated that the coupling constants of $J_{5,6}$ = 6.4 Hz observed for **4a** is in close agreement with the previously reported $J_{5,6}$ value (6.6 Hz) for *cis*-5-methyl-DHO.[16] Similarly, the coupling constant of $J_{5,6}$ = 6.8 Hz for **4b** may be consistent with the *cis*-structure, in which the slightly larger $J_{5,6}$ value relative to that of **4a** suggests somewhat less distorted dihydrothymine ring structure of **4b** (Figure 3).
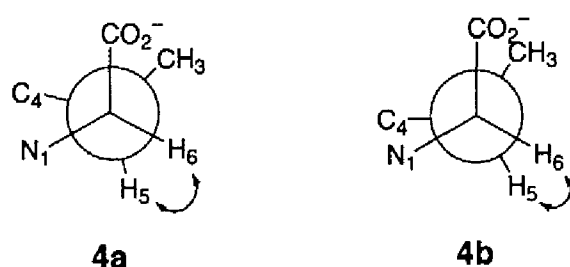

4a   **4b**

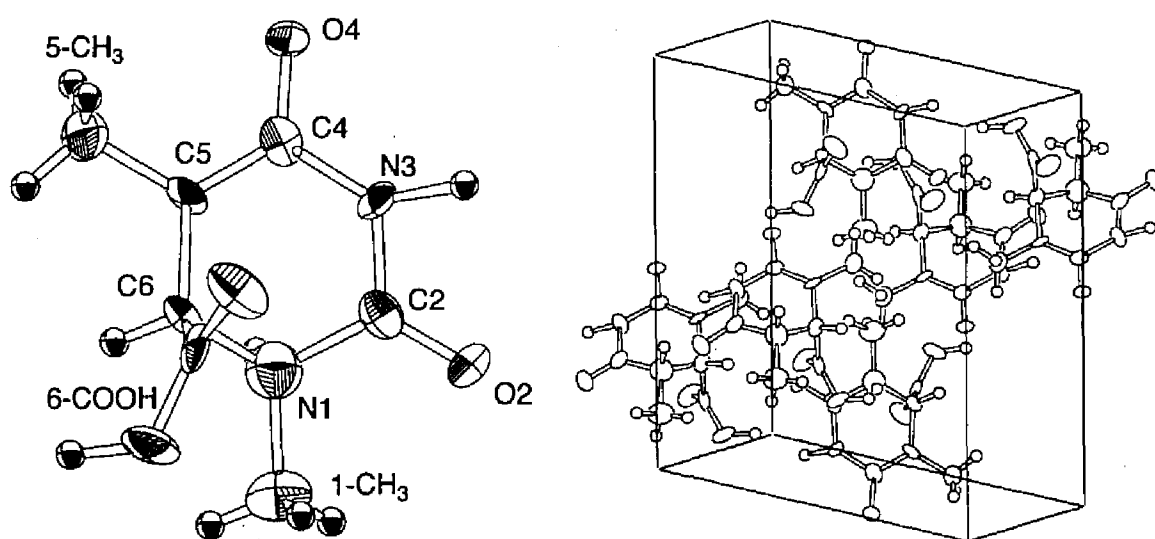**Figure 3.** Projection formulae of **4a,b** for interpreting the characteristic NMR coupling constants.

Figure 4. ORTEP drawing (left) and three-dimensional packing diagram (right) of (5S,6S)-5,6-dihydro-1-methylthymine-6-carboxylic acid (**4a**). The refinement led to a final discrepancy residual factor $R = 5.9$ %, $Rw = 5.7$ %.

Previously, the conformation of the pyrimidine ring in a chair form was assumed for S-DHO to illustrate a mechanism by which the 5-pro-S and 6-hydrogens would be in a trans-diaxial position in the binding of S-DHO to DHODase active site, thereby undergoing energetically favorable dehydrogenation.[16,17] The X-ray structure of cis-1,5-dimethyl-DHO **4a** may demonstrate the validity of a chair-conformation of S-DHO as assumed previously, although characterization of the stereochemistry of trans-1,5-dimethyl-DHO was not successful in the present study.

For evaluating the reactivity of CO_2 radical anion towards DNA bases, N_2O-saturated aqueous solution of the simplest form of oligonucleotide, thymidylyl(3'→5')thymidine (TpT; 1 mM), was γ-irradiated (1.75 kGy) in the presence of sodium formate (200 mM). The irradiated solution was evaporated and the resulting solid was subjected to acid-catalyzed hydrolysis in 80% formic acid (130 °C, 1 hr) into free base components (Figures 1c and d).[24,25] The hydrolysate contained 5-methyl-DHO as indicated in the HPLC analysis by reference to the products, including **4c** derived from the radiolytic carboxylation of thymine (**1c**) (**4c** was assigned to a mono-carboxylic acid by GC-MS analysis; GC-CIMS of the trimethylsilyl derivative m/z 389 [(M+Si(CH$_3$)$_3$ × 3 + H)$^+$]; GC-EIMS: m/z (%) 73 (90), 100 (54), 147 (28), 271 (100), 373 (28)). This suggests that DNA bases, particularly thymine, may undergo carboxylation under conditions of CO_2 radical anion generation, although the rate would be very slow due to electrostatic repulsion between the CO_2 radical anions and the negatively charged DNA [$k = 2.5 \times 10^4$ dm^3 mol^{-1} s^{-1}, as reported by Nabben et al.].[3]

Mechanism of Carboxylation. As the major products in the γ-radiolysis of N_2O-saturated aqueous solution of **1a,b** (1.0 mM) containing sodium formate (200 mM), it was possible to isolate and identify 5,6-dihydrothymines **6a,b**, meso compounds of (5R, 5'S)- and (5S, 5'R)-bi-5,6-dihydrothymines **7a,b**, a racemic compound of (5R, 5'R)- and (5S, 5'S)-bi-5,6-dihydrothymines **8a,b**, and 5,6-dihydrothymine-6-carboxylic

29

acids **4a,b**. Minor carboxylic acids such as 5-carboxylic acid **3a**, 5,6-dicarboxylic acid **2a** and C5–C5'-linked dihydrothymine 6-carboxylic acid **5a** were also detected besides the major **4a** in the γ-radiolysis of **1a**, while they were not quantified in the present study. Table 1 summarizes the G-values of the major products **4a,b** and **6a,b–8a,b** along with those for decomposition of **1a,b**, indicating that the total amount of the major products (4 + 6 + (7 + 8) × 2) accounts for 88% and 72% of the decomposed **1a** and **1b**, respectively.

The products observed in the present study are rationalized by dual reactivity of CO_2 radical anion, one-electron reduction and nucleophilic addition, as shown in Scheme 1. Thymine is known to be one-electron reduced and gives an electron adduct as a primary intermediate not only by hydrated electron at a diffusion-controlled rate ($k(e_{aq}^-) = 1.7 \times 10^{10}$ dm^3 mol^{-1} s^{-1} at pH 6.0)[26] but also by CO_2 radical anion at more than five-order of magnitude slower rate ($k(CO_2^-) = \sim 5 \times 10^4$ dm^3 mol^{-1} s^{-1}).[27] It has also been well established that radical anions of thymine and its related pyrimidine derivatives undergo slow protonation at C6 to form more stable 5,6-dihydrothymin-5-yl radicals irreversibly, while being protonated most readily at O4 into oxygen protonated radicals.[1] As characterised recently in the γ-radiolysis of the Ar-saturated aqueous solution of **1a,b** containing an excess amount of 2-methyl-2-propanol or sodium formate,[8] 5,6-dihydrothymine derivatives **6a,b** and stereoisomeric C5–C5'-linked dihydrothymine dimers **7a,b** and **8a,b** are attributable to the 5,6-dihydrothymin-5-yl radical intermediates ($^\cdot$T-6-H). Thus, upon encounter of two 5-yl radicals $^\cdot$T-6-H disproportionation and radical recombination occur to produce **6a,b** and **7a,b–8a,b**, respectively. In view of the oxidizing property,[8] the 5-yl radicals $^\cdot$T-6-H may undergo more readily one-electron reduction by CO_2 radical anion to give **6a,b** via subsequent protonation. The G-values for decomposition of **1a,b** (2.6 × 10^{-7} mol J^{-1} and 3.4 × 10^{-7} mol J^{-1}, respectively) owing to the reaction with CO_2 radical anions was rather smaller than that of CO_2 radical anions (6.3 × 10^{-7} mol J^{-1}) generated in the reaction systems. This may be partly accounted for by a competitive bimolecular

30

Table 1. G-values for the decomposition of **1a** and **1b** [G(−1a,b)], and for the formation of 6-carboxylic acids [G(**4a,b**)], 5,6-dihydrothymines [G(**6a,b**)], C5–C5'-linked meso-dimers [G(**7a,b**)], and the racemic-dimers [G(**8a,b**)].

	G-values / 10^{-7} mol J^{-1}	
	1-methylthymine (**1a**)	1,3-dimethylthymine (**1b**)
G(−**1a,b**)	2.6	3.4
G(**4a,b**)	0.50	0.52
G(**6a,b**)	1.3	1.3
G(**7a,b**)	0.12	0.13
G(**8a,b**)	0.12	0.19

recombination of CO_2 radical anions into oxalic acids as in reaction 4 (k = 6.5 × 10^8 dm^3 mol^{-1} s^{-1}).[13,28,29]

$$CO_2^- \quad + \quad CO_2^- \quad + \quad 2H^+ \quad \rightarrow \quad (COOH)_2 \quad (4)$$

In accord with the evidence that electron adducts of thymine derivatives are converted to the 5-yl radicals ˙T-6-H but not the 6-yl radicals (˙T-5-H), the 5,6-dihydrothymine-6-carboxylic acids **4a,b** are most likely to be derived from nucleophilic addition of the CO_2 radical anion to **1a,b** at C6 into 6-carboxy-5,6-dihydrothymin-5-yl radicals (˙T-6-CO_2^-) rather than by recombination of CO_2 radical anion with thymine radicals. A previous ESR study has shown that the addition of the CO_2 radical anion to orotic acid takes place preferentially at the electron-deficient C6-position.[12] Similar nucleophilic addition of hydroxymethyl radical, generated by the γ-radiolysis of methanol in N_2O-saturated aqueous solutions, to 1,3-dimethyluracil and 1,3-dimethylthymine at C6 has been reported previously.[14] In contrast with the CO_2

radical anion, the methanol radical does not show a redox reactivity but a typical radical reactivity of addition and hydrogen abstraction. In the present study, it was unable to identify the hydrogen abstraction by CO_2 radical anion which may possibly occur at the 5-methyl group. Support for the formation of oxidizing 5-yl radical ˙T-6-CO_2^- was obtained: addition of reducing N,N,N',N'-tetramethyl-p-phenylenediamine (TMPD; 0.5 mM) to the reaction system of 1a gave rise to a blue-coloration characteristic of TMPD radical cation (TMPD⁺˙) after γ-irradiation, probably due to one-electron reduction of ˙T-6-CO_2^- by TMPD.[30] Such a one-electron reduction of ˙T-6-CO_2^- is consistent with the apparent influence of TMPD addition on the product distribution that the yield of 5,6-dihydrothymine-6-carboxylic acids 4a was dramatically enhanced, while those of 5,6-dihydrothymine-5,6-dicarboxylic acid 2a and C5–C5'-linked 5,6-dihydrothymine-6-carboxylic acid 5a were depressed. The fate of the resulting 6-carboxy-5,6-dihydrothymin-5-yl radicals ˙T-6-CO_2^- may be essentially identical with that of 5,6-dihydrothymin-5-yl radicals ˙T-6-H. The disproportionation with ˙T-6-H or ˙T-6-CO_2^- and the one-electron reduction by CO_2 radical anion produce the 5,6-dihydrothymine-6-carboxylic acids 4a,b. Although C5–C6 unsaturated carboxylic acid, 1-methylthymine-6-carboxylic acid, is possibly produced via deprotonation of C5 cation that is derived from disproportionation of ˙T-6-CO_2^-, such a product could not be observed in the HPLC analysis when detected by UV absorption at 254 nm.

The formation of minor carboxylic acids is accounted for in terms of conventional radical reactions. Radical recombination of CO_2 radical anion with the 5-yl radicals ˙T-6-H or ˙T-6-CO_2^- gives 5,6-dihydrothymine-5-carboxylic acids such as 3a or 5,6-dicarboxylic acids such as 2a. However, the formation of 3a through nucleophilic addition of CO_2 radical anion at the C5 position can not be ruled out. Similarly, a radical recombination between the 5-yl radicals ˙T-6-H and ˙T-6-CO_2^- also occurs to give C5–C5'-linked 5,6-dihydrothymine-6-carboxylic acids such as 5a. The formation of 5a indicates that the lifetimes of both 5-yl radicals ˙T-6-H and ˙T-6-CO_2^-

32

are sufficiently long enough to encounter with each other.

Finally based on the G-values of the major products listed in Table 1, the partition ratio between one-electron reduction and nucleophilic addition of CO_2 radical anion towards N-substituted thymines **1a,b** is approximately estimated as 0.8 : 0.2.

Conclusion

The present study demonstrates the dual reactivity, one-electron reduction and nucleophilic addition in a ratio of 0.8 : 0.2, of the CO_2 radical anion toward 1-methylthymine **1a** and 1,3-dimethylthymine **1b**. One-electron reduction of **1a,b** leads to 5,6-dihydrothymin-5-yl radicals ˙T-6-H, which are key intermediates for the formation of 5,6-dihydrothymines **6a,b** and stereoisomeric C5–C5'-linked dihydrothymine dimers **7a,b** and **8a,b**. Nucleophilic additon of CO_2 radical anion to **1a,b** occurred preferentially at C6 to form 6-carboxy-5,6-dihydrothymin-5-yl radicals ˙T-6-CO_2^- thereby resulting in 5,6-dihydrothymine-6-carboxylic acid **4a,b**. The X-ray crystallography of 5,6-dihydro-1-methylthymine-6-carboxylic acid (1,5-dimethyl-DHO) showed a structural similarity with dihydroorotate that is well known as an intermediate in the *de novo* pyrimidine biosynthesis.
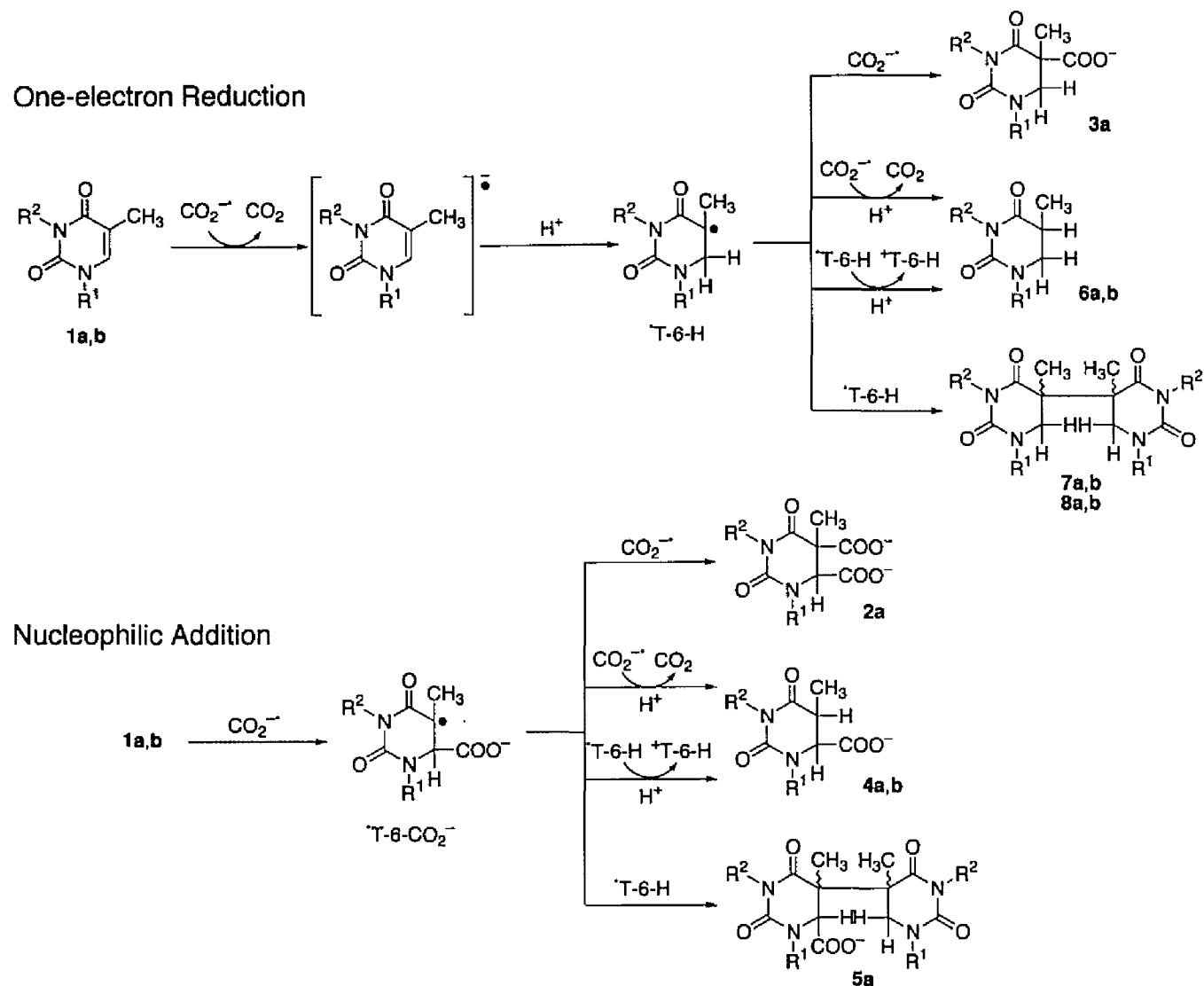
Scheme 1. One-electron reduction and nucleophilic addition mechanisms of thymine derivatives by carbon dioxide radical anion.

References and Notes

(1) von Sonntag, C. In *The Chemical Basis of Radiation Biology*; Taylor & Francis: London, 1987.

(2) Bensasson, R. V.; Land, E. J.; Truscott, T. G. In *Excited States and Free Radicals in Biology and Medicine*; Oxford University Press: Oxford, 1993.

(3) Nabben, F. J.; Van der Stroom, H. A.; Loman, H. *Int. J. Radiat. Biol.* **1983**, *43*, 495–504.

(4) Conner, H. D.; Thurman, R. G.; Galizi, M. D.; Mason, R. P. *J. Biol. Chem.* **1986**, *261*, 4542–4548.

(5) La Cagnin, L. B.; Connor, H. D.; Mason, R. P.; Thurman, R. G. *Mol. Pharmacol.* **1988**, *33*, 351–357.

(6) Reinke, L. A.; Towner, R. A.; Janzen, E. G. *Toxicol. Appl. Pharmacol.* **1992**, *112*, 17–23.

(7) Nishimoto, S.; Ide, H.; Nakamichi, K.; Kagiya, T. *J. Am. Chem. Soc.* **1983**, *105*, 6740–6741.

(8) Ito, T.; Shinohara, H.; Hatta, H.; Nishimoto, S. *J. Org. Chem.* **1999**, *64*, 5100–5108. (Chapter 2)

(9) Scholes, G.; Weiss, J. J.; Wheeler, C. M. *Nature* **1962**, *195*, 802.

(10) Wheelan, P.; Kirsch, W. M.; Koch, T. H. *J. Org. Chem.* **1989**, *54*, 4360–4364.

(11) Kamal, A.; Garrison, W. M. *Nature* **1965**, *206*, 1315–1317.

(12) Neta, P. *Radiat. Res.* **1972**, *49*, 1–25.

(13) Wada, T.; Ide, H.; Nishimoto, S.; Kagiya, T. *Int. J. Radiat. Biol.* **1982**, *42*, 215–221.

(14) Schuchmann, H. –P.; Wagner, R.; von Sonntag, C. *Int. J. Radiat. Biol.* **1986**, *50*, 1051–1068.

(15) Hines, V.; Johnston, M. *Biochemistry* **1989**, *28*, 1227–1234.

(16) Defrees, S. A.; Sawick, D. P.; Cunningham, B.; Heinstein, P. F.; Morré, D. J.; Cassady, J. M. *Biochem. Pharmacol.* **1988**, *37*, 3807–3816.

(17)   Mahmoudian, M.; Pakiari, A. H.; Khademi, S. *Biochem. Pharmacol.* **1992**, *43*, 283–287.

(18)   Jones, M. E. *Ann. Rev. Biochem*. **1980**, *49*, 253–279.

(19)   Keys III, L. D.; Johnston, M. *J. Am. Chem. Soc.* **1985**, *107*, 486–492.

(20)   Sheldrick, G. M. In *Crystallographic Computing 3*; Sheldrick, G. M.; Kruger, C.; Goddard, R. Eds.; Oxford University Press: Oxford, 1985; pp 175–189.

(21)   Geller, M.; Kalinski, A.; Kolos, W.; Kopczy´nska, M. *Biochim. Biophys. Acta* **1972**, *287*, 1–8.

(22)   Hruska, F. E.; Sebastian, R.; Grand, A.; Voituriez, L.; Cadet, J. *Can. J. Chem.* **1987**, *65*, 2618–2623.

(23)   Jolibois, F.; Voituriez, L.; Grand, A.; Cadet, J. *Chem. Res. Toxicol.* **1996**, *9*, 298–305.

(24)   Dizdaroglu, M.; Simic, M. G. *Radiat. Phys. Chem*. **1985**, *26*, 309–316.

(25)   Wagner, J. R.; Blount, B. C.; Weinfeld, M. *Anal. Biochem.* **1996**, *233*, 76–86.

(26)   Buxton, G. V.; Greenstock, C. L.; Helman, W. P.; Ross, A. B. *J. Phys. Chem. Ref. Data* **1988**, *17*, 513–886.

(27)   Neta, P.; Huie, R. *J. Phys. Chem. Ref. Data* **1988**, *17*, 1027–1284.

(28)   Loman, H.; Ebert, M. *Int. J. Radiat. Biol.* **1970**, *18*, 369–379.

(29)   Mulazzani, Q. G.; D'Angelantonio, M.; Venturi, M.; Hoffman, M. Z.; Rodgers, M. A. J. *J. Phys. Chem.* **1986**, *90*, 5347–5352.

(30)   Fujita, S.; Steenken, S. *J. Am. Chem. Soc.* **1981**, *103*, 2540–2545.
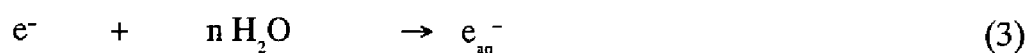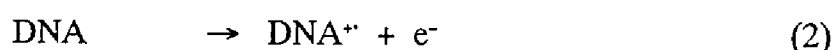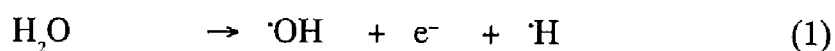
Stereoisomeric C5–C5'-Linked Dihydrothymine Dimers Produced by Radiolytic One-Electron Reduction of Thymine Derivatives in Anoxic Aqueous Solution: Structural Characteristics in Reference to Cyclobutane Photodimers

Abstract : Radiolytic one-electron reduction of 1-methylthymine (**1a**) and 1,3-dimethylthymine (**1b**) in anoxic aqueous solution afforded stereoisomeric C5–C5'-linked dihydrothymine dimers, fractionated into the meso compounds of (5R, 5'S)- and (5S, 5'R)-bi-5,6-dihydrothymines (**3a,b**[*meso*]) and a racemic compound of (5R, 5'R)- and (5S, 5'S)-bi-5,6-dihydrothymines (**3a,b**[*rac*]), along with 5,6-dihydrothymines (**2a,b**). The meso and racemic dimers were produced in almost equivalent yields, possessing structural similarity with *cis-syn*-cyclobutane pyrimidine photodimers that are identified as highly mutagenic and carcinogenic photolesions induced by UV light. Similar radiolytic one-electron reduction of thymidine (**1c**) resulted in the pseudo-meso compound of (5R, 5'S)- and (5S, 5'R)-bi-5,6-dihydrothymidine (**3c[RS]**), and two diastereomers of (5R, 5'R)- and (5S, 5'S)-bi-5,6-dihydrothymidine (**3c[RR]** and **3c[SS]**). X-ray crystal structures indicated that two pyrimidine rings of the stereoisomeric dimers except **3a[rac]** overlap with each other to a considerable extents, as in the *cis-syn*-cyclobutane photodimers. The pyrimidine rings of the dimers were twisted around 5-Me–C5–C5'–5'-Me by 51.1(2)° for **3a[meso]**, −85.4(4)° for **3a[rac]**, −65(1)° for **3b[meso]**, 43(2)° for **3b[rac]**, and 64.9(4)° for **3c[RS]**, respectively. It was predicted that the C5–C5'-linked dihydrothymine dimers may cause some distortion within a DNA duplex if they were incorporated. The pH

dependence of the reactivities was in accord with a mechanism of the C5–C5'-linked dimerization by which electron adducts of 1a–c are irreversibly protonated at C6 and the resulting 5,6-dihydrothymin-5-yl radicals undergo bimolecular coupling.

Introduction

Interaction of ionizing radiation with living cells generates excess free radicals to induce a variety of damages to cellular DNA that are responsible for carcinogenic, mutagenic and lethal effects on the cells.[1] The primary biological effects of ionizing radiation, eventually triggering off the obvious lesions via a sequence of chemical reactions and biological responses on a wide range of time scales, are conventionally classified into two subgroups: the indirect effect and direct effect.[1a] The indirect effect is attributable largely to hydroxyl radicals ($\cdot$OH), hydrated electrons (e_{aq}^-), and hydrogen atoms ($\cdot$H) produced by the radiolysis of excess cellular water (reactions 1 and 3). The direct effect involves absorption of radiation energy by DNA molecule itself to undergo electron ejection into DNA radical cation ($DNA^{+\cdot}$), as is of essential importance upon exposure to high-linear energy transfer (LET) radiation (reaction 2).[2] The concomitant electron ejected from DNA is also hydrated as in reaction 3.

$$H_2O \rightarrow \cdot OH + e^- + \cdot H \qquad (1)$$

$$DNA \rightarrow DNA^{+\cdot} + e^- \qquad (2)$$

$$e^- + n\,H_2O \rightarrow e_{aq}^- \qquad (3)$$

Oxidative DNA damages including various base modifications by OH radicals have been extensively studied to elucidate the detailed mechanism of oxidation.[1] Similar oxidative damages may arise from the DNA radical cations induced by the direct effect of radiations. A recent study has shown that an electron-loss center (hole)
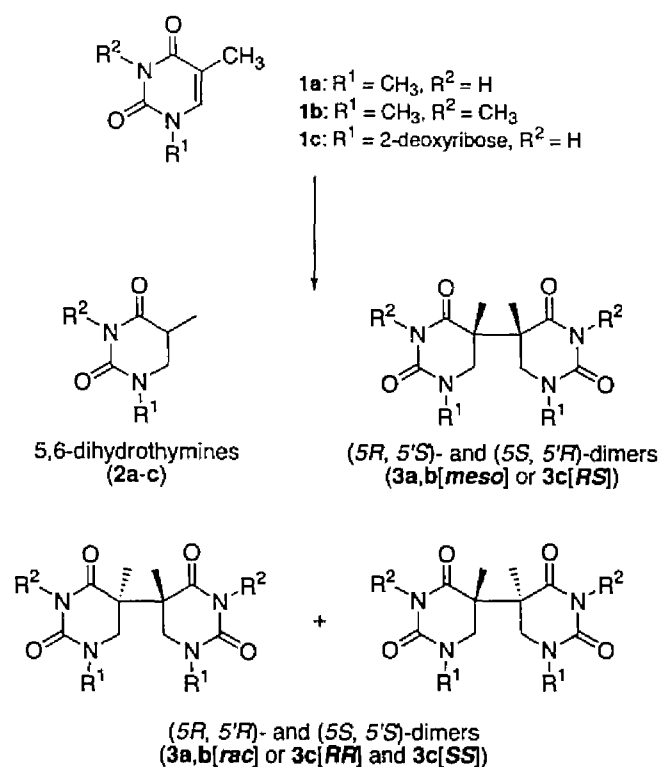
Scheme 1. Radiolytic one-electron reduction of thymine derivatives.

at a given DNA base radical cation can migrate intramolecularly through a π-stacking of DNA bases, thus arriving at and being trapped most efficiently in a guanine (G) moiety to cause its oxidative damage.[3] Under oxic conditions in the presence of oxygen these oxidative damages are significantly enhanced, while a reducing species of hydrated electron (e_{aq}^-) is scavenged by oxygen into less reactive superoxide radical ion (O_2^-).[1a] Several structures of oxidative DNA-base modifications, particularly those of purine modifications, have been identified to account for the biological lesions.[4]

Concerning reductive DNA damages by dry electrons (e^- as in reactions 1 and 2) and/or hydrated electrons e_{aq}^- (reaction 3), the cytosine base moiety is a major site of electron attachment at lower temperatures, as characterized by ESR spectroscopy:[1b,5-9] cytosine radical anion (C^-) and thymine radical anion (T^-) are thus

produced in 64%[9b] (77%)[9c] and 36%[9b] (23%)[9c] yields, respectively. At higher temperatures, however, an equilibrium involving a mutual electron-transfer process is established between the thymine and cytosine radical anions, from which irreversible protonation at C6 of the thymine radical anion T[-] takes place to produce a major intermediate of the 5,6-dihydrothymin-5-yl radical (TH[.]).[10,11] In contrast to oxidative damages, there has been little evidence for the influence of radiation-induced reductive DNA-base damages on biological lesions. Previously, a negative result for the biological effect has been reported that 5,6-dihydrothymine structures incorporated in DNA are responsible for neither a blocking nor a premutagenic lesion,[12] while it is one of the typical damage structures induced by radiolytic reduction of thymine moiety. Although the biological significance of the reductive DNA damages is still obscure, it may be assumed that a reduction mechanism is operative to account for the lethal effect of radiation on hypoxic cells as are involved in solid tumor tissues.[1d]

Previously, Nishimoto *et al.* have reported efficient formation of C5–C5'-linked dihydrothymidine dimer (3c) in the radiolytic one-electron reduction of thymidine (1c) in deoxygenated aqueous solution (Scheme 1), in which 5,6-dihydrothymidin-5-yl radicals (5c) were assumed as the most likely intermediate species (see also Scheme 2).[13] Possible stereoisomers of the C5–C5'-linked dihydrothymidine dimers have not yet been isolated and characterized, while hydrogenated thymidine stereoisomers as the accompanied major products, 5(*S*)-(–)-5,6-dihydrothymidine and 5(*R*)-(+)-5,6-dihydrothymidine, were identified[13] by reference to the reported structures.[14] It seems of interest to compare the conformational characteristics of C5–C5'-linked dihydrothymine dimers with those of cyclobutane pyrimidine photodimers possessing not only C5–C5' but also C6–C6' linkage which are afforded through a formal [2+2] cycloaddition between the C5–C6 double bonds of adjacent pyrimidines upon UV-irradiation of DNA.[14,15] The pyrimidine photodimers have been identified as highly mutagenic and carcinogenic lesions that result in miscoding during the DNA replication due to perturbations of base-pairing interactions and global structural

changes in DNA.[15b] The local and global structures of pyrimidine photodimer-incorporated DNA have been extensively studied by means of computational simulations,[16] NMR spectroscopy,[17] X-ray crystallography,[18] and electrophoresis[19] to get molecular insight into the mechanisms, by which the photodimers induce mutagenicity and in turn interact with a repair enzyme of DNA photolyase.[20] Comparing these structural characterizations with the X-ray crystal structures of DNA-excision repair enzyme and DNA photolyase, it is the most likely that the enzymes may recognize the local structures of the photodimers as well as the whole pattern of small perturbation of the dimer-incorporated DNA.[21]

In light of the biological role of pyrimidine photodimers, the author has a hypothesis that the C5–C5'-linked dihydrothymine dimers could be potentially mutagenic and carcinogenic lesions when formed by chance at a thymine-thymine (TT) tract in DNA upon exposure of hypoxic cells to ionizing radiation. In this study, radiolytic reductions of N1-substituted thymine derivatives such as 1-methylthymine (**1a**), 1,3-dimethylthymine (**1b**) and thymidine (**1c**) (Scheme 1) in deoxygenated aqueous solution have been performed to isolate stereoisomers of C5–C5'-linked dihydrothymine dimers: the meso compounds of (5R, 5'S)- and (5S, 5'R)-bi-5,6-dihydrothymines (**3a,b[*meso*]**), and racemic compounds of (5R, 5'R)- and (5S, 5'S)-bi-5,6-dihydrothymines (**3a,b[*rac*]**) from **1a,b**, and the pseudo-meso compound of (5R, 5'S)- and (5S, 5'R)- bi-5,6-dihydrothymidines (**3c[*RS*]**), and two diastereomers of (5R, 5'R)- and (5S, 5'S)-bi-5,6-dihydrothymidines (**3c[*RR*]**) and (**3c[*SS*]**) from **1c**. The present structural characterization has provided a prediction that the meso form of the C5–C5'-linked dihydrothymine dimeric structure could be formed at a given TT tract in DNA through a small extent of conformational change.

41

Experimental Section

Materials. 1-Methylthymine (Sigma Chemical), thymine (Kohjin) and thymidine (Kohjin) were used as received. Purified 1,3-dimethylthymine was kindly supplied by Fujii Memorial Research Institute, Otsuka Pharmaceutical. Sodium formate and 2-methyl-2-propanol were purchased from Nacalai Tesque and were used without further purification. NaH_2PO_4 and methanol (HPLC grade) were used as received from Wako Pure Chemical Industries.

Radiolytic Reduction of N1-Substituted Thymine Derivatives. Aqueous solutions of N1-substituted thymine derivatives (**1a–c**; 5 mM) containing excess amount (1 M) of sodium formate were prepared with water ion-exchanged using Corning Mega-Pure System MP-190 (>16 MΩ cm). Typically, the pH of the aqueous solutions was adjusted to 7.0 ± 0.1 with phosphate buffer (2 mM). For the experiments on pH-dependence of the radiolytic reduction, aqueous solutions of **1a–c** (1 mM) containing sodium formate (200 mM) or 2-methyl-2-propanol (100 mM) were buffered at pH 3–11 with phosphate buffer (2 mM) and sodium hydroxide. All the solutions were purged with Ar and irradiated in a sealed glass ampule at room temperature with a ^{60}Co γ-ray (dose rate: 0.89 Gy min^{-1}) or an X-ray source (5 Gy min^{-1}) (Rigaku RADIOFLEX-350).

HPLC. Aliquots (10 μL) of the irradiated solutions were analyzed by high-performance liquid chromatography (HPLC), using a Shimadzu 10A HPLC system equipped with a Rheodyne 7725 sample injector. Sample solutions were injected onto a reversed phase-column (Wakosil 5C18, φ 4.6 mm × 150 mm) containing C18 chemically bonded silica gel (5 μm particle size) for analysis of **3a,b**. The C5–C5'-linked dihydrothymidine dimers (**3c**) were analyzed using a reversed phase column of Nacalai Cosmosil 5C18 MS (φ 4.6 mm × 250 mm). The phosphate buffer solutions (10 mM, pH 3.0) containing varying concentrations of methanol (10–25 vol%) were delivered as the mobile phase at a flow rate of 0.6 mL min^{-1}. The column eluents were

monitored by the UV absorbance at 210 nm. For isolation of the products, the irradiated solutions were evaporated to a minimum volume and were subjected to a preparative HPLC, using a Tosoh Preparative HPLC system equipped with a Chromatocorder 12 (System Instruments). The isolation was performed on a reverse-phase column (Wakosil 10C18, ϕ 10 mm × 300 mm) containing C18 chemically bonded silica gel (10 μm particle size) and phosphate buffer solution (10 mM, pH 3.0) containing 5–20 vol% methanol was delivered at a flow rate of 3 mL min^{-1}. After aqueous fractions of the respective products were collected automatically and evaporated, the resulting residues were lyophilized and subjected to spectroscopic measurements.

Spectroscopic Measurements. ^{1}H and ^{13}C NMR spectra were recorded on a JEOL GSX-270 (270 MHz) or EX-400 (400 MHz) Fourier transform NMR spectrometer. The C5–C5'-linked dimers produced from thymidine were measured in D_2O with reference to 3-(trimethylsilyl)propionic-2,2,3,3-d_4 acid (TSP) sodium salt (Aldrich) using EX-400, and those from 1-methylthymine and 1,3-dimethylthymine in dimethyl sulfoxide-d_6 (Nacalai Tesque) were measured using GSX-270. Chemical shifts in DMSO-d_6 were expressed from the residual proton signals of DMSO (δ = 2.49 ppm) for ^{1}H NMR and from the carbon signals (δ = 39.50 ppm) for ^{13}C NMR, respectively. High-resolution positive FAB mass spectra (FAB-HRMS) were recorded on a JEOL JMS-SX102A spectrometer, using glycerol matrix: 5,5'-bi-5,6-dihydro-1-methylthymines calcd for C12H18N4O4 283.141 (M+H)$^+$, found 283.142 (3a[*meso*]) and 283.143 (3a[*rac*]); 5,5'-bi-5,6-dihydro-1,3-dimethylthymines calcd for C14H22N4O4 311.172, found 311.173 (3b[*meso*]) and 311.173 (3b[*rac*]); 5,5'-bi-5,6-dihydrothymidines calcd for C20H30N4O10 487.204, found 487.204 (3c[*RS*]), 487.206, and 487.206 (3c[*RR*] and 3c[*SS*]) .

X-ray Crystallography. The colorless needle-shaped crystals of C5–C5'-linked dihydrothymine dimers were grown from aqueous solutions (~3 mg mL^{-1}). While the dihydrothymidine dimers were coated with 40 vol% collodion-ethanol solution, the

other dihydrothymine dimers were mounted directly on a glass fiber. All measurements were made on a Rigaku AFC7R diffractometer with graphite-monochromated Mo-Kα radiation (λ = 0.71609 Å) and a 12-kW rotating anode generator. The diffraction data were collected at room temperature using the ω-2θ scan mode to a maximum 2θ value of 60.0° for 3a[*meso*] and 3a[*rac*], 55.1° for 3b[*meso*], and 55.0° for 3b[*rac*] and 3c[*RS*]. The intensities of three representative reflections that were measured after every 150 reflections remained constant throughout the data collection, indicating electronic stability of the sample crystals except for 3c[*RS*]. The structures were solved by direct methods (SHELXS 86,[41] SIR 88[42]) and expanded using a Fourier technique. The positions of the hydrogen atoms were calculated. While hydrogen atoms of 3a[*meso*] were refined isotropically, only isotropic B values were refined for hydrogen atoms of the other dimers.

Results and Discussion

Formation and Characterization of C5–C5'-Linked Dihydrothymine Dimers. For investigating reduction reactivity of 1-methylthymine (**1a**), 1,3-dimethylthymine (**1b**), and thymidine (**1c**) exclusively in the radiolysis of aqueous solution, strongly oxidizing OH radicals generated along with reducing species of hydrated electrons and hydrogen atoms from water radiolysis (see reactions 1 and 3) were effectively scavenged by the aid of well-specified scavengers.[1a] The G-values[21] of primary water radicals are known as $G(e_{aq}^-) \approx G(\cdot OH)$ = 2.9 × 10^{-7} mol J^{-1} and $G(\cdot H)$ = 0.6 × 10^{-7} mol J^{-1} in neutral aqueous solution.[1a] In a deoxygenated aqueous solution containing excess amount of [i] 2-methyl-2-propanol ((CH_3)$_3$COH) or [ii] formate ions (HCOO$^-$), OH radicals and hydrogen atoms are scavenged into substantially unreactive 2-methyl-2-propanol radicals (reaction 4: $k(\cdot OH)$ = 5 × 10^8 dm^3 mol^{-1} s^{-1} as a major reaction, $k(\cdot H)$ = 8 × 10^4 dm^3 mol^{-1} s^{-1} as a minor reaction) or converted to a somewhat
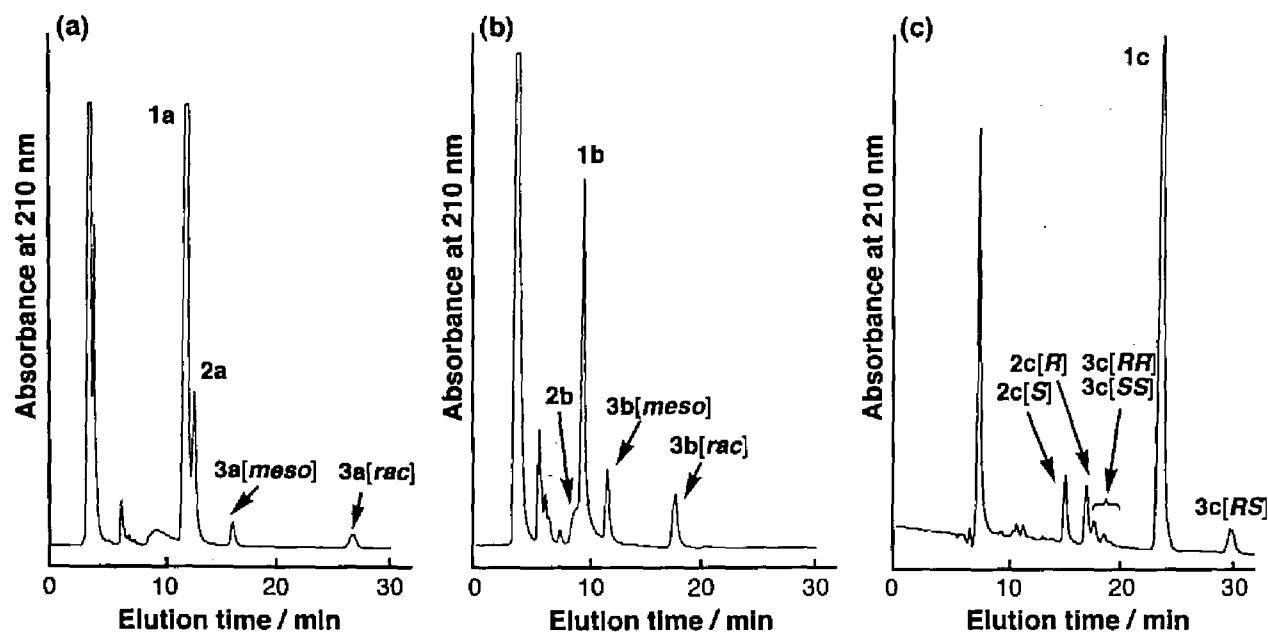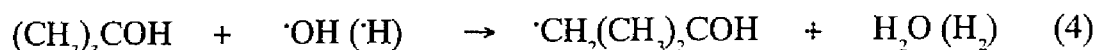
Figure 1. Typical HPLC analyses of phosphate buffer solutions (pH 7.0) of (a) **1a**, (b) **1b**, and (c) **1c** (5 mM) after γ-irradiation (2 kGy) in the presence of sodium formate (200 mM) under Ar, as observed by delivering phosphate buffer solution (pH 3) with (a) 15 %, (b) 25 %, and (c) 10 % of methanol at a flow rate of 0.6 mL min⁻¹. HPLC analysis was performed using (a, b) a Wakosil 5C18 column (φ 4.6 mm × 150 mm) or (c) a Cosmosil 5C18 MS column (φ 4.6 mm × 250 mm).

less reducing species of carbon dioxide radical anions (CO_2^{-}; $G(CO_2^{-}) = 3.5 \times 10^{-7}$ mol J^{-1}) (reaction 5: $k(\cdot OH) = 3 \times 10^9$ dm^3 mol^{-1} s^{-1}, $k(\cdot H) = 3 \times 10^8$ dm^3 mol^{-1} s^{-1}), respectively.[1a] Consequently, the reaction systems involving the restricted radical species for exclusive reduction can be achieved: [i] e_{aq}^{-} (reduction potential at pH 7.0: $E(nH_2O/e_{aq}^{-}) = -2.9$ V vs NHE[22]) + $\cdot$H ($E(H^+/\cdot H) = -2.4$ V[22]) and [ii] $e_{aq}^{-} + CO_2^{-}$ ($E(CO_2/CO_2^{-}) = -1.9$ V[23]).

$$(CH_3)_3COH \; + \; \cdot OH \, (\cdot H) \; \rightarrow \; \cdot CH_2(CH_3)_2COH \; + \; H_2O \, (H_2) \quad (4)$$
$$HCOO^- \; + \; \cdot OH \, (\cdot H) \; \rightarrow \; CO_2^{-} \; + \; H_2O \, (H_2) \quad (5)$$

Figures 1a–c shows representative HPLC chromatograms as monitored by UV absorbance at 210 nm for Ar-purged phosphate buffer solutions (5 mM, pH 7.0) of N1-substituted thymine derivatives 1a–c, respectively, after 2-kGy γ-irradiation in the presence of excess (1 M) sodium formate. Most of the products could not be detected by UV absorption at 254 nm, indicating the efficient formation of C5–C6-saturated thymine structures in the reduction of 1a–c with hydrated electrons and CO_2^{-} as well. The eluents from the respective major peaks were collected by preparative HPLC and fractionation. The fractionated products in aqueous solution containing 10–25 vol% methanol were evaporated at room temperature and submitted to a purity check by analytical HPLC followed by spectroscopic characterization. High resolution positive FAB mass spectrometry (FAB-HRMS) of the isolated HPLC fractions 2a–c (single peak for 2a,b in Figures 1a,b and double peaks for 2c in Figure 1c) and 3a–c (double peaks for 3a,b in Figures 1a,b and triple peaks for 3c in Figure 1c) provided protonated parent ions that are in accord with the molecular formulas of the corresponding 5,6-dihydrothymine derivatives and C5–C5'-linked dihydrothymine dimers, respectively (see the Experimental Section). According to the ^{1}H and ^{13}C NMR spectral data by reference to authentic samples, the products 2a,b were identified as 1-methyl-5,6-dihydrothymine (2a) and 1,3-dimethyl-5,6-dihydrothymine

(2b), respectively. Similar products derived from hydrogenation of 1c were stereoisomeric and identified as 5(S)-(−)-5,6-dihydrothymidine (2c[S]) and 5(R)-(+)-5,6-dihydrothymidine (2c[R]) by comparing the spectral data with those of authentic samples.[13,14] These 5,6-dihydrothymine derivatives are well documented products obtained in the radiolytic reduction of thymine derivatives in aqueous solution. In the separate experiments, the HPLC fractions eluted in shorter retention times (<5 min) in Figures 1a–c were confirmed to contain relatively low yields of C5 and/or C6 carboxylated byproducts resulting from addition of CO_2^- to the C5–C6 double bond of 1a–c.[24,25] As expected, such a carboxylation was excluded in the radiolysis of aqueous solution containing excess 2-methyl-2-propanol instead of sodium formate.

Since the FAB-HRMS data predict that the products 3a–c may be isomeric C5–C5'-linked dihydrothymine dimers, attempts were made to determine their crystal structures by X-ray crystallography. By reference to the crystallographics of 3a,b in Figure 2 (see also Chart 1), we determined that the faster HPLC fractions are the meso compounds of the (5R, 5'S)-bi-5,6-dihydrothymine derivatives (3a,b[meso]), while the slower HPLC fractions are racemic compounds of (5R, 5'R)- and (5S, 5'S)-bi-5,6-dihydrothymine derivatives (3a,b[rac]) (see also Figures 1a,b). In the present study, further separation of the racemic compounds 3a,b[rac] was not performed. In contrast to 3a,b, the crystals of the three HPLC fractions of 3c were unstable and therefore their X-ray crystallographic data were collected by coating with 40 vol% collodion-ethanol solution to identify only 3c[RS]: the X-ray crystallography neither in collodion-coating and in a capillary tube was unsuccessful for the other two products. Figure 3 illustrates the structure and the three-dimensional lattice packing diagram of 3c[RS], indicating that a pair of (5S, 5'R)-bi-5,6-dihydrothymidine and (5R, 5'S)-bi-5,6-dihydrothymidine monohydrates are packed in a unit cell: there is a hydrogen bond between the crystal water and one of the deoxyribose-C(5)-OH group of the dimer. Although crystal structures are unknown, the accompanied two products may be assigned to diastereoisomeric (5R, 5'R)-bi-5,6-dihydrothymidine (3c[RR]) and (5S,
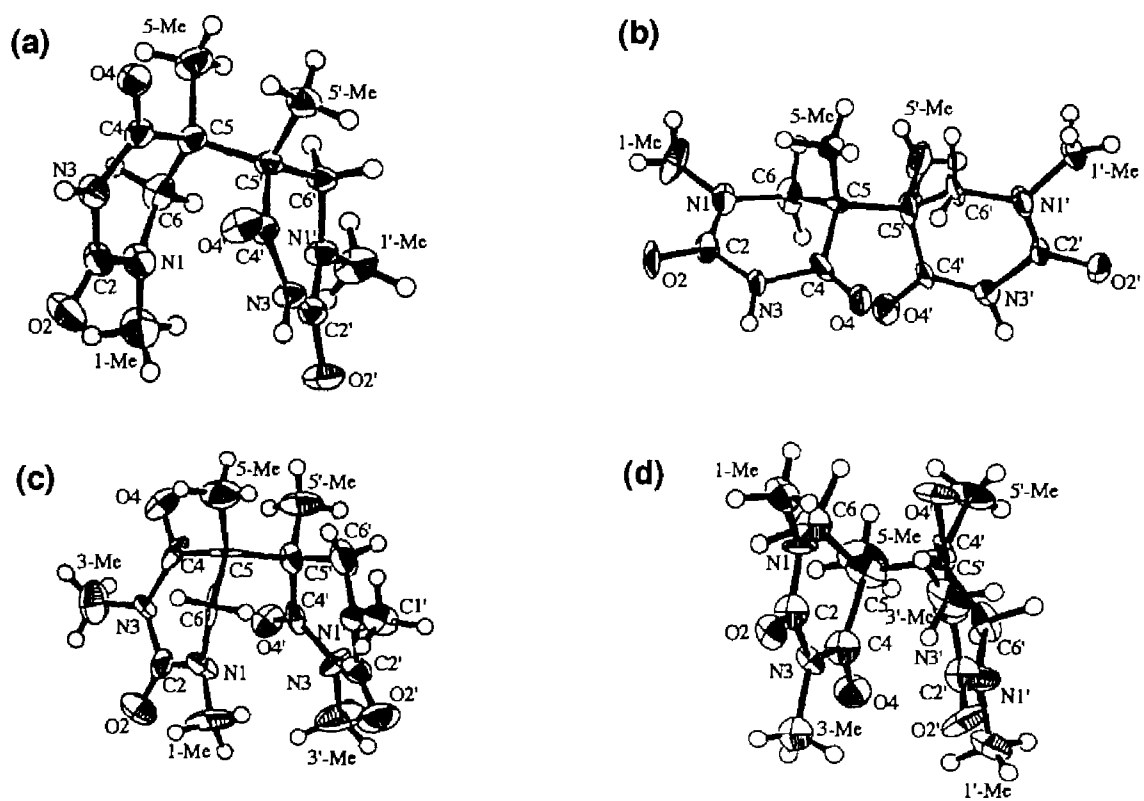
Figure 2. ORTEP Drawings of C5–C5'-linked dihydrothymine dimers: (a) **3a**[*meso*]; (b) **3a**[*rac*]; (c) **3b**[*meso*]; (d) **3b**[*rac*].
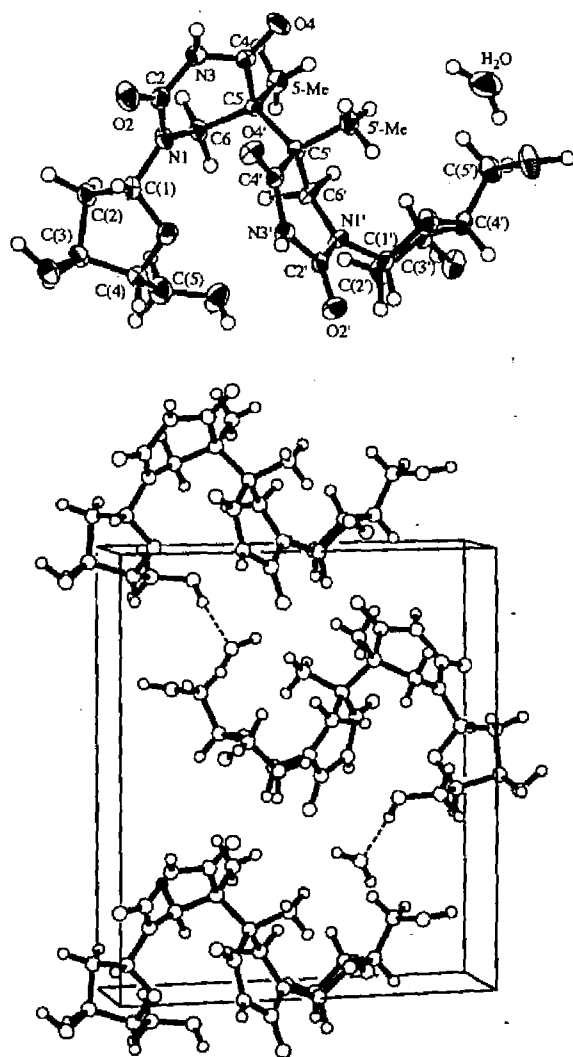
48

Figure 3. ORTEP Drawing and a three-dimensional lattice packing diagram of C5–C5'-linked dihydrothymidine dimer (**3c[RS]**).
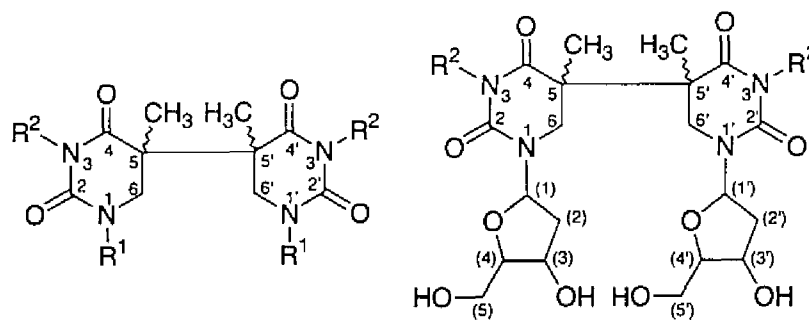
Chart 1

5'S)-bi-5,6-dihydrothymidine (3c[SS]), respectively, in accord with the ^{1}H and ^{13}C NMR data (Table 5). As implicated from Figure 3, the C5–C5'-linked dihydrothymidine dimer bearing hydrophilic deoxyribose moiety favor the crystallization in the form of hydrate, while dehydration of the resulting crystal would cause readily a lattice decomposition. In this context, it is noteworthy that the pseudo-meso compound 3c[RS] is eluted slower than the diastereomers 3c[RR] and 3c[SS] in the HPLC, opposite to the elution speeds of 3a,b[meso] being faster than those of 3a,b[rac] (Figures 1a–c). It is likely that the hydrocarbon component of the 2-deoxyribose moiety is involved in hydrophobic interactions and therefore the accessibility of the furanose ring may play some role in the HPLC behavior of C5–C5'-linked dihydrothymidine dimers.

The X-ray crystallographic data are summarized in Tables 1 and 2. The C5–C5'-linked dihydrothymine dimers 3a–c possess the C5–C5' bond lengths from 1.55 to 1.59 Å. These are comparable to both the C5–C5' and C6–C6' bond lengths of photodimers: 1.58 and 1.60 Å for the cis-syn-1,3-dimethylthymine cyclobutane photodimer,[18b] and 1.548 and 1.596 Å for 1,1'-trimethylenebisthymine cis-syn-photodimer (Thy-[C$_3$]-Thy(cis-syn)).[26] According to the crystal structures shown in Figures 2 and 3, two pyrimidine rings of the C5–C5'-linked dihydrothymine dimers 3a–c overlap with each other, the extent of which was evaluated by the dihedral angles

50

Table 1. Crystal Data and Experimental Details

	3a[*meso*]	3a[*rac*]	3b[*meso*]	3b[*rac*]	3c[*RS*]
a (Å)	8.618(5)	20.645(6)	8.375(4)	13.24(1)	6.000(3)
b (Å)	11.898(4)	6.414(4)	10.602(6)	15.50(1)	14.619(2)
c (Å)	13.020(5)	12.186(4)	17.480(3)	14.73(1)	13.280(2)
β (°)	97.23(5)	121.29(2)	100.79(2)		102.12(2)
V(Å^3)	1324(1)	1378.9(9)	1524(1)	3022(3)	1138.8(6)
Z	4	4	4	8	2
μ(Mo Kα)cm^{-1}	1.08	1.04	1.00	1.01	1.20
Space Group	P2$_1$/c	Cc	P2$_1$/n	Pbcn	P2$_1$
Crystal System	monoclinic	monoclinic	monoclinic	orthorhombic	monoclinic
Residuals[a] (R; R_W)	4.3; 4.9	5.5; 6.6	7.7; 4.9	6.0; 3.7	4.8; 6.0
GOF	1.55	2.17	2.64	1.74	2.58

[a]$R = \Sigma||F_0|-|F_c|| / \Sigma|F_0|$; $R_W = [(\Sigma w(|F_0|-|F_c|)^2 / \Sigma w|F_0|^2)]^{1/2}$.

Table 2. Selected Bond Length, Plain Angles and Torsion Angles of C5–C5'-Linked Dihydrothymine Dimers

	3a[*meso*]	3a[*rac*]	3b[*meso*]	3b[*rac*]	3c[*RS*]
Bond length (Å)					
C5–C5'	1.591(3)	1.568(4)	1.57(2)	1.55(2)	1.583(6)
N1–C2	1.347(3)	1.39(1)	1.36(2)	1.35(2)	1.348(5)
C2–N3	1.364(3)	1.34(1)	1.41(2)	1.41(2)	1.393(6)
N3–C4	1.395(3)	1.410(8)	1.37(2)	1.35(2)	1.379(5)
C4–C5	1.530(3)	1.541(10)	1.56(2)	1.60(2)	1.534(6)
C5–C6	1.530(3)	1.55(1)	1.50(2)	1.53(2)	1.544(5)
C6–N1	1.457(3)	1.455(9)	1.49(2)	1.48(2)	1.459(5)
N1'–C2'	1.339(2)	1.27(1)	1.35(2)	1.35(2)	1.354(5)
C2'–N3'	1.385(2)	1.47(1)	1.40(2)	1.44(2)	1.385(5)
N3'–C4'	1.366(2)	1.348(9)	1.36(2)	1.38(2)	1.372(6)
C4'–C5'	1.528(3)	1.50(1)	1.57(2)	1.56(2)	1.524(6)
C5'–C6'	1.537(3)	1.54(1)	1.51(2)	1.55(2)	1.542(6)
C6'–N1'	1.463(2)	1.457(9)	1.46(2)	1.44(2)	1.467(5)
Plane angle (°) between pyrimidine rings					
	128	160	134	136	113
Torsion angle (°) about					
C5–C5'	51.1(2)	–85.4(4)	–65(1)	43(2)	64.9(4)

between the pyrimidine-containing planes composed of N1, N3, and C5 atoms. The calculation indicates 128° for **3a**[*meso*], 160° or **3a**[*rac*], 134° for **3b**[*meso*], 136° for **3b**[*rac*], and 113° for **3c**[*RS*]. Except for the result for **3a**[*rac*], these dihedral angles are considerably smaller than the corresponding values of 152° (N1–N3–C5 planes) and 153° (C2–C4–C6 planes) for the *cis-syn*-1,3-dimethylthymine cyclobutane photodimer and 178° for Thy-[C₃]-Thy(*cis-syn*). It was also demonstrated that the pyrimidine rings of **3a–c** are not planar where the C6 atoms are out of the planes of the other atoms. Furthermore, the pyrimidine rings of **3a–c** are twisted around the C5–C5' linkage and the torsion angles through 5-Me–C5–C5'–5'-Me vary significantly in the range of 43 to 85°. These values are much greater than 24° for the *cis-syn*-1,3-dimethylthymine photodimer, because the absence of the C6–C6' linkage in the **3a–c** permits more free rotation of pyrimidine rings around the C5–C5' linkage. Nevertheless, it is interesting that two pyrimidine rings of **3a,b**[*meso*] are confronted with each other and thereby cause a stacking of their carbonyl groups as in the *cis-syn*-cyclobutane photodimers. By reference to the twist angle for a successive thymine base pair about the axis of DNA duplex, *e.g.*, 33–39° for the structure of GCGTTTTTCGC,[27] it seems structurally feasible that the meso form of a C5–C5'-linked dihydrothymine dimer structure like **3a**[*meso*] could be produced at a successive thymine base pair by reduction pathway to cause some distortion within a DNA duplex. Similar to *cis-syn*-photodimers, such a meso dimer structure may give rise to insufficient stacking of the pyrimidine rings that will weaken the hydrogen bonds of the 3'- or 5'-dihydrothymine moiety with complementary adenine. In contrast to the meso dimer, the formation of racemic compounds of C5–C5'-linked dihydrothymine dimers such as **3a**[*rac*] from the normal stacking conformation of adjacent thymines in DNA is unlikely, since two pyrimidine rings should be arranged in the almost identical plane without overlapping of their carbonyl groups.

The ¹H and ¹³C NMR data in D_2O or dimethyl sulfoxide-d_6 are consistent with the crystallographic characterizations of C5–C5'-linked dihydrothymine dimers **3a–c**

Table 3. ¹H NMR (DMSO-d_6, 270 MHz) Chemical Shifts (ppm) of C5–C5'-Linked Dihydrothymine Dimers

	3a[*meso*]	3a[*rac*]	3b[*meso*]	3b[*rac*]
5-CH$_3$	1.184 (s)	1.136 (s)	1.167 (s)	1.084 (s)
1-CH$_3$	2.794 (s)	2.875 (s)	2.804 (s)	2.814 (s)
3-CH$_3$	-	-	2.908 (s)	2.892 (s)
3-NH	10.143 (s)	10.100 (s)	-	-
H$_{6A}$, H$_{6'A}$	3.208 (d)	3.003 (d)	3.263 (d)	3.127 (d)
H$_{6A}$, H$_{6'B}$	3.440 (d)	4.143 (d)	3.383 (d)	3.734 (d)
J_{AB} (Hz)	−13.5	−12.2	−13.8	−12.7

Table 4. ¹³C NMR (DMSO-d_6, 67.5 MHz) Chemical Shifts (ppm) of C5–C5'-Linked Dihydrothymine Dimers

	3a[*meso*]	3a[*rac*]	3b[*meso*]	3b[*rac*]
5-CH$_3$	18.781	15.957	19.225	17.338
1-CH$_3$	33.743	34.366	34.818	35.590
3-CH$_3$	-	-	27.814	27.843
C$_5$	44.982	43.822	45.572	44.689
C$_6$	51.932	52.482	50.509	50.442
C$_2$	152.870	151.972	153.471	152.389
C$_4$	173.223	175.295	172.435	173.368

Table 5. ^{1}H and ^{13}C NMR (D_2O, 400 and 100 MHz) Chemical Shifts (ppm) of C5–C5'-Linked Dihydrothymidine Dimers

	3c[*RS*]	3c[*RR*] or 3c[*SS*]
^{1}H NMR		
5-CH$_3$	1.278 (s), 1.305 (s)	1.139 (s), 1.222 (s)
H$_{6A}$, H$_{6'A}$	3.275 (d), 3.323 (d)	3.335 (d), 3.176 (d)
H$_{6B}$, H$_{6'B}$	3.578–3.680a (m)	4.061 (d), 4.090 (d)
J_{6AB}, $J_{6'AB}$ (Hz)	−13.6, −13.2	−12.2, −13.0
deoxyribose		
H$_{(1)}$	6.127 (t), 6.077 (t)	6.174 (t), 6.233 (t)
H$_{(2)}$	1.982–2.189 (m)	1.985–2.221 (m), 6.233 (t)
H$_{(3)}$	4.232–4.280 (m)	4.247–4.282 (m), 4.285–4.310 (m)
H$_{(4)}$	3.764–3.794 (m)	3.778–3.806 (m), 3.797–3.826 (m)
H$_{(5)}$	3.548–3.645a (m)	3.568–3.666 (m), 3.552–3.667 (m)
^{13}C NMR		
5-CH$_3$	20.394, 20.504	17.505, 17.359
C$_6$	46.235, 46.528	47.333, 47.278
C$_2$	156.366, 156.622	155.525, 156.257
C$_4$	178.220, 178.330	179.828, 179.812
C$_5$	47.497, 47.698	46.894, 47.845
deoxyribose		
C$_{(1)}$	86.798, 86.835	86.652, 86.908
C$_{(2)}$	37.860, 38.116	38.006, 38.281
C$_{(3)}$	73.594, 73.631	73.503, 73.448
C$_{(4)}$	87.987, 88.060	88.060, 88.006
C$_{(5)}$	64.139, 64.286	63.993, 64.048

^{a} A part of H$_6$ peaks overlapped with H$_{(5)}$ peaks.

(Tables 3 to 5). Table 3 compares the ^{1}H NMR data between **3a,b[*meso*]** and **3a,b[*rac*]** for better understanding of the conformations in solution. For each dimer, the meso form and the racemic form had similar ^{1}H NMR chemical shifts except for the H6 and H6' resonance. It is thus remarkable that **3a,b[*meso*]** showed downfield shifts in the H6 resonance and in turn upfield shifts in the counterpart H6' resonance; therefore, the H6 and H6' chemical shifts become closer to each other, relative to **3a,b[*rac*]**. Similarly, the H6 and H6' chemical shifts of **3c[*RS*]** were also closer to each other, compared with those of **3c[*RR*]** or **3c[*SS*]**, although both protons showed relatively upfield shifts (Table 5). On the other hand, the ^{13}C NMR chemical shifts showed little difference between the isomers (Tables 4 and 5).

Mechanism of C5-C5'-Linked Dimerization by Radiolytic Reduction. Previously, a brief account for the mechanism by which thymidine undergoes one-electron reduction by hydrated electron or CO_2^- to give C5–C5'-linked dihydrothymidine dimer and 5,6-dihydrothymidines was reported.[13] Thymine is known to undergo one-electron reduction into its radical anion by hydrated electron at a diffusion controlled rate ($k(e_{aq}^-) = 1.7 \times 10^{10}$ dm^3 mol^{-1} s^{-1} at pH 6.0),[28] and similarly by CO_2^- at more than five-order of magnitude slower rate ($k(CO_2^-) = \sim 5 \times 10^4$ dm^3 mol^{-1} s^{-1}).[28] By reference to the reduction potential[23] vs. the normal hydrogen electrode at pH 7.0, CO_2^- ($E(CO_2/CO_2^-) = -1.9$ V) is of less reducing ability than hydrated electron (E (nH_2O/e_{aq}^-)= -2.9 V). Nevertheless, it was confirmed in the previous study[13] that CO_2^- had practically the same one-electron reducing ability as hydrated electron toward **1c**, thus resulting in similar product distribution of **2c[*R*]**, **2c[*S*]**, and **3c** (the stereoisomers were not separated previously).

For the clarity of the mechanism of C5–C5'-linked dimerization, a further attempt was made to investigate the influence of pH on the radiolytic reduction of **1a–c** in anoxic buffer solution. As shown in Figure 4, upon increasing the pH values from 3.0 to 11.0, the *G*-values for both the decomposition of **1a,b** and the formation of
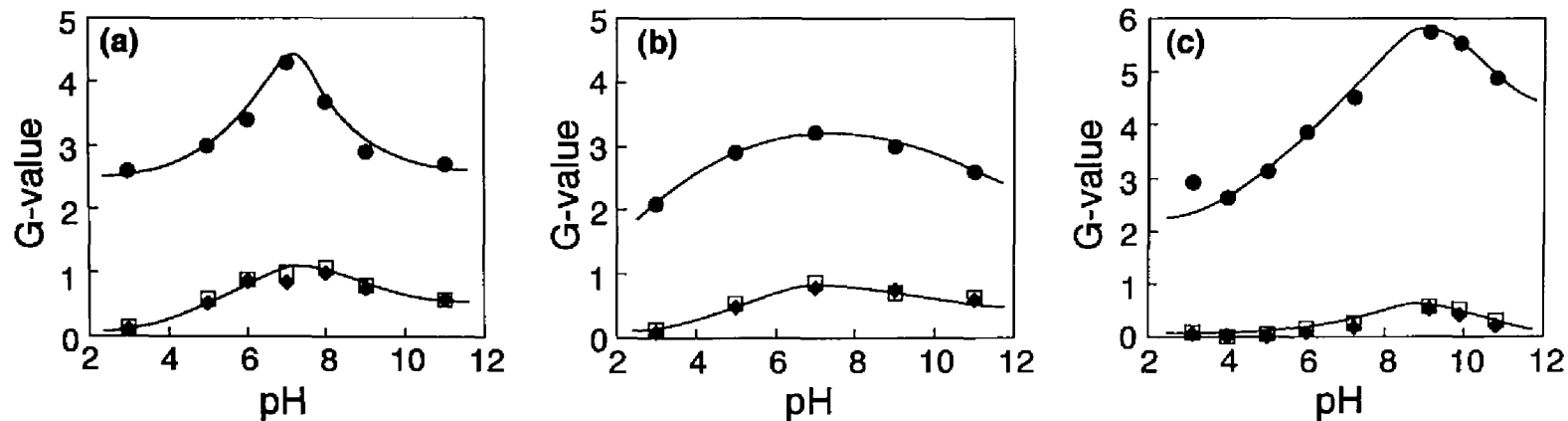
56

Figure 4. pH-Dependent variation of G-values for decomposition of thymine derivatives (●, 1a-c) and formation of C5–C5'-linked dihydrothymine dimers (◆, 3a,b[*meso*] or 3c[*RS*]; □ 3a,b[*rac*] or 3c[*RR*]+3c[*SS*]) in the γ-radiolysis of Ar-purged phosphate buffer solution containing sodium formate (200 mM): C5–C5'-linked dimerization of (a) 1a to 3a, (b) 1b to 3b and (c) 1c to 3c.

C5–C5'-linked dimers 3a,b increased in acidic solution, attained their maxima in neutral solution, and then decreased in basic solution. Similar behavior was also observed for the radiolytic reduction of 1c into 3c, while the pH value resulting in the maximum G-values shifted to somewhat basic region of pH 9.0. In a wide pH range the stereoisomeric C5–C5'-linked dimers as the meso forms and the racemic compounds were produced in almost equivalent yields. The maximum G-values of the respective C5–C5'-linked dimers thus obtained were 3a[$meso$] = 1.07 × 10^{-7} mol J^{-1} (23% selectivity based on the decomposed substrate), and 3a[rac] = 0.97 × 10^{-7} mol J^{-1} (20%), 3b[$meso$] = 1.02 × 10^{-7} mol J^{-1} (30%), 3b[rac] = 0.91 × 10^{-7} mol J^{-1} (27%), for 3c[RS] = 1.22 × 10^{-7} mol J^{-1} (20%) and for 3c[RR] + 3c[SS] = 1.13 × 10^{-7} mol J^{-1} (18%).

In light of previous studies on the reaction of hydrated electrons with pyrimidines,[10] the pH dependence of the C5–C5'-linked dimerization may be rationalized by the reaction pathways given in Scheme 2. The initial and key step involves one-electron reduction of 1a–c by not only hydrated electron but also by CO_2^- to form the corresponding radical anions as the primary intermediates (4a–c) (path 1). It is likely that the electron adducts 4a–c are readily protonated at O4 by water (path 2) to form the reducing radicals (5'a–c) followed by very slow self-termination.[1a] In view of the pKa ≈ 7.2 for the protonated electron adduct of thymine,[10] such protonations of 4a–c will become more significant with decreasing the pH, and inversely deprotonation of 5'a–c (path 2) will be more facilitated with increasing pH value. In competition with the fast protonation at O4 to oxygen-protonated radicals, 4a–c may also undergo another type of protonation at C6 to form 5,6-dihydrothymin-5-yl radicals (5a–c) (path 3) that have oxidizing properties and more stability.[29] This reaction occurs irreversibly to increasing extents as the pH decreases; therefore, both the one-electron reductive decomposition and the C5–C5'-linked dimerization by a radical coupling mechanism of 1a–c (path 4) are enhanced. In basic solution at pH > 10, however, the yields of electron adducts 4a–c should
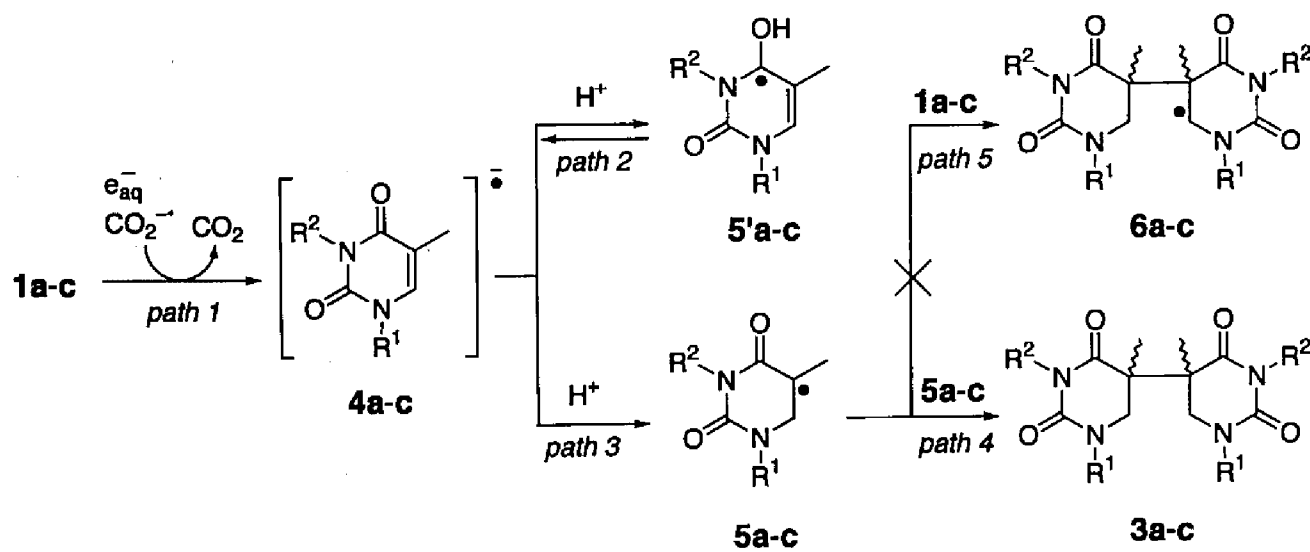
Scheme 2. Mechanism of C5–C5'-linked dimerization of thymine derivatives by radiolytic one-electron reduction.

significantly decrease in correspondence with the pH effect on the yield of primary active species in the water radiolysis: the yield of OH radicals responsible for the formation of CO_2^- in reaction 5 rapidly decreases, while that of hydrated electrons slightly increases, with increasing pH.[30] There is an additional pH effect on the acidic reaction system in the presence of excess formate ions. In accord with the pKa = 3.75 for formic acid, the formate ions involved in the reaction system for conversion of OH radicals to reducing CO_2^- (see reaction 5) are largely protonated in acidic solution at pH < 3.75. Hydrogen abstraction by OH radical from formic acid as in reaction 6 produces a radical species of ·COOH that has a stronger acidity (pKa = 1.4) than the parent formic acid and is dissociative into CO_2^- under the present conditions at pH > 2.0. However, the rate constant of reaction 5 (k(·OH) = 3 × 10^9 dm^3 mol^{-1} s^{-1}) is one-order of magnitude greater than that (k(·OH) = 1 × 10^8 dm^3 mol^{-1} s^{-1}) of reaction 6;[28] therefore, the net efficiency of scavenging OH radicals to reducing CO_2^- being lowered to considerable extent in acidic solution at pH < 3.75.

$$\text{HCOOH} \quad + \quad \text{·OH (·H)} \quad \rightarrow \quad \text{·COOH} \quad + \quad H_2O \ (H_2) \qquad (6)$$
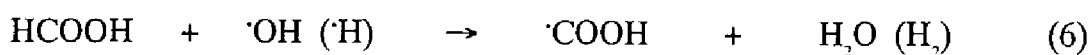
Hydrogen atoms and OH radicals readily add to the C5–C6 double bond of pyrimidines to produce both 5-yl and 6-yl radicals.[1a] We therefore examined a hypothetical radical reactivity whether the C5 radical can add to the C5–C6 double bond of the parent thymine moiety, producing the C5–C5'-linked dimer 6-yl radical (path 5 in Scheme 2), in the representative radiolytic reduction of 1c in phosphate buffer. As shown in Figure 5, while the yields of 3c were almost constant at concentrations of 1c lower than 0.5 mM in formate-containing phosphate buffer (pH 7.0), they were decreased with increasing concentration of 1c. This result may rule out the above hypothesis that the addition reaction of the 5-yl radical 5c to the C5 position of the C5–C6 double bond of 1c will be a notable route to dimeric product 3c, because it should favor the higher concentrations of 1c contrary to the result in Figure

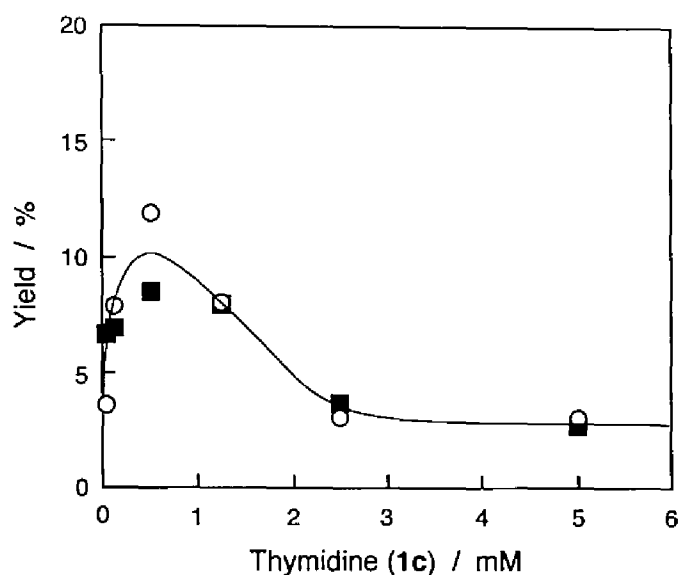**Figure 5.** Influence of the concentration of thymidine (**1c**) on the yields of C5–C5'-linked dihydrothymidine dimers (O, **3c**[*RS*]; ■, **3c**[*RR*]+**3c**[*SS*]) as observed at about 30% decomposition of **1c** in the X-radiolysis of Ar-purged phosphate buffer solution (pH 7.0) containing sodium formate (200 mM).
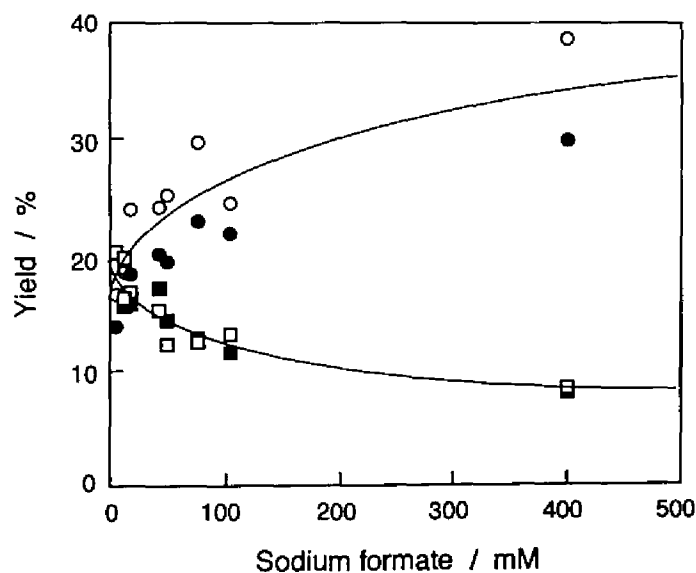

Figure 6. Variation of the yields of dihydrothymidines (●, **2c**[*S*]; O, **2c**[*R*]) and C5–C5'-linked dihydrothymidine dimers (□, **3c**[*RS*]; ■, **3c**[*RR*]+**3c**[*SS*]) in the *γ*-irradiation (150 Gy) of Ar-purged phosphate buffer solutions (pH 7.0) of **1c** (0.1 mM) with increasing concentrations of sodium formate.

5. Figure 5 suggests that contribution of possible hydrogen abstraction of 5c from the deoxyribose moiety of 1c may become more important and thereby inhibit the radical coupling to 3c, upon increasing the concentration of 1c. In the separate experiments using methanol-d_3 as an OH radical scavenger, radiolytic reduction of 1a,b in phosphate buffer also afforded the C5–C5'-linked dimers 3a,b. Assuming a radical addition mechanism by which the dihydrothymine dimer 6-yl radicals (6a,b) will be produced from the reaction of C5 radicals 5a,b with 1a,b and thereafter abstract deuterium atom from CD_3OD (Scheme 3), the dimeric products 3a,b should possess the mono-deuterated structures. The FAB-MS data of 1a and 1b provided the respective parent ions at 283 and 311, demonstrating that the incorporation of deuterium atom into the dimer did not occur. This result is also consistent with the conclusion that the radical coupling mechanism is predominant for the C5–C5'-linked dimerization by radiolytic reduction (path 4).

From the redox properties of the oxygen-protonated and carbon-protonated pyrimidine radicals,[10c] it may be expected that disproportionation of radicals by electron transfer from reducing radicals 5'a–c to oxidizing 5-yl radicals 5a–c (path 6) may occur especially in acidic and neutral solutions to reproduce 5,6-dihydrothymines 2a–c along with regeneration of 1a–c, as shown in Scheme 4. However, this disproportionation would not be an important route to 2a–c, because the 5-yl radical does not readily undergo electron-transfer reactions,[29] thus being rather of neutral radical nature than oxidizing. Such a neutral radical nature of 5a–c accounts for ready bimolecular radical coupling to form C5–C5'-linked dihydrothymine dimers 3a–c as the major products.

It is likely that the 5-yl radicals are a common intermediate for competition between radical coupling into C5–C5'-linked dimer and hydrogen abstraction into 5,6-dihydrothymine. This competition kinetics was confirmed in the radiolytic reduction of 1c (0.1 mM) in Ar-saturated phosphate buffer (pH 7.0) with various concentrations of formate ions as a hydrogen donor. As shown in Figure 6, the yields of 5,6-

dihydrothymidines **2c**[*S*] and **2c**[*R*] increased and inversely those of the C5–C5'-linked dimers **3c** decreased upon increasing the concentration of sodium formate. Another support was that the yields of **2a,b** were 2-fold depressed, *i.e.*, about 60% yield with formate to 30% yield with 2-methyl-2-propanol, when the radiolytic reduction of **1a,b** was performed in Ar-purged phosphate buffer (pH 7.0) containing 2-methyl-2-propanol (100 mM) instead of sodium formate.

6a,b

– CD$_3$OD

•CD$_2$OD

3'a,b

[M+H]$^+$ = 284 (**3'a**)
312 (**3'b**)
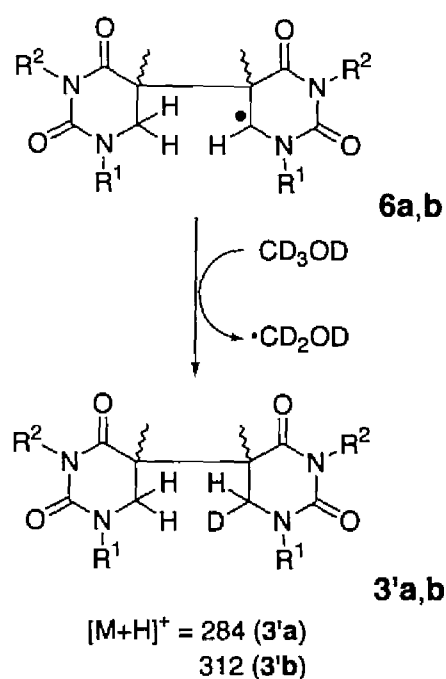
Scheme 3

Biological Implication of C5–C5'-Linked Dihydrothymine Dimers. Radiation biological studies have shown that direct ionization of DNA generates DNA radical cations (holes) and electrons to result in fixation of DNA damages.[1] There have also been several results indicating that DNA is able to transport hole[31] and electron[32–35] through a DNA π-stack.[3] In association with the intra-DNA electron migration, previous ESR studies evaluated the relative abundance of DNA-base radical anions (electron-base adducts) as about 75% for the cytosine site and 25% for the thymine site, respectively.[8] The electron adduct of the thymine site seems to be protonated at

63
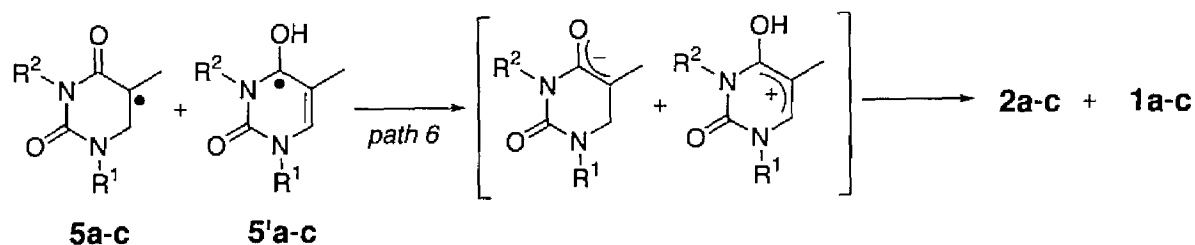
Scheme 4

the C6 to form the 5-yl radical, in accord with the formation of the 5,6-dihydrothymine structure as a major damage fragment in the γ-irradiated aqueous solution of *E. coli* DNA.[36] In the model reactions, the C6-protonation of the electron-thymine adduct occurs more slowly than the corresponding O4-protonation ($k < 2 \times 10^4$ s^{-1})[37] and the N3 protonation ($k = 3.3 \times 10^6$ s^{-1})[38] of the electron-cytosine adduct. Recently, it has also been suggested that the 5,6-dihydrothymin-5-yl radical generated within the DNA duplex may be a precursor to alkaline-labile 2'-deoxyribonolactone generated via radical abstraction of a hydrogen atom at C1' of the adjacent deoxyribose unit.[39]

According to the present mechanistic study in a model reaction system, it may be postulated that the C5–C5'-linked dihydrothymine dimer structure could be produced by coupling of a pair of thymin-5-yl radicals when generated thorough migration of two electrons to a given adjacent thymine-thymine sequence of DNA. Such a hypothetical C5–C5'-linked dimerization in DNA may not occur by sparsely ionizing low LET radiations under usual conditions due to a mechanistic restriction, even though it seems to be structurally feasible. However, the densely ionizing high LET radiations may permit generation of two electrons as the net for migration and reduction to form an adjacent electron-thymine adduct pair. Recently, the effect of high LET O^{7+} heavy ion beam on thymidine in the solid state has been investigated to

64

identify several dimeric structures among the thymidine decomposition products.[40] These dimeric products are possibly attributed to coupling of several types of monomeric radicals that should be more enhanced by densely ionizing high LET radiations to generate nonhomogeneously high concentration of radicals, relative to sparsely ionizing low LET radiations.

Conclusion

Radiolyic reduction of 1-methylthymine **1a**, 1,3-dimethylthymine **1b**, and 2'-deoxythymidine **1c** in aqueous solution afforded stereoisomeric C5–C5'-linked dihydrothymine dimers **3a–c** along with 5,6-dihydrothymine derivatives **2a–c**. X-ray crystallographic analysis of the C5–C5'-linked dimers suggested that the two pyrimidine rings of **3a–c** except **3a**[*rac*] overlap with each other like a "closed-shell" in the crystals. It seems structurally feasible that the "closed-shell"-dimer structure could be produced at a adjacent thymine base moiety by reduction pathway to cause some distortion within a DNA duplex. The pH-responce of the dimerization reactivity demonstrated that the reaction mechanism involves bimolecular coupling of 5,6-dihydrothymin-5-yl radicals that are formed by irreversible protonation of the thymine radical anions at C6.

References and Notes

(1)   (a) von Sonntag, C. In *The Chemical Basis of Radiation Biology*; Taylor and Francis: London, 1987. (b) Steenken, S. *Free Rad. Res. Commun.* **1992**, *16*, 349–379. (c) von Sonntag, C.; Schuchmann, H. –P. *Int. J. Radiat. Biol.* **1986**, *49*, 1–34. (d) Bensasson, R. V.; Land, E. J.; Truscott, T. G. In *Excited States and Free Radicals in Biology and Medicine*; Oxford University Press: Oxford, 1993; pp 290–305.

(2)   (a) Hall, E. J. In *Radiobiology for the Radiologist, 4th ed.*; J. B. Lippincott Company: Philadelphia, 1994. (b) Roots, R.; Chatterjee, A.; Chang, P.; Lommel, L.; Blakely, E. A. *Int. J. Radiat. Biol.* **1985**, *47*, 157–166.

(3)   (a) Hall, D. B.; Holmlin, R. E.; Barton, J. K. *Nature* **1996**, *382*, 731–735. (b) Gasper, S. M.; Schuster, G. B. *J. Am. Chem. Soc.* **1997**, *119*, 12762–12771.

(4)   (a) Shibutani, S.; Takeshita, M.; Grollmann, A. P. *Nature* **1991**, *349*, 431–434. (b) Cheng, K. C.; Cahill, D. S.; Kasai, H.; Nishimura, S.; Loeb, L. A. *J. Biol. Chem.* **1992**, *267*, 166–172. (c) Tchou, J.; Grollman, A. P. *Mutat. Res.* **1993**, *299*, 277–287. (d) Kouchakdjian, M.; Bodepudi, V.; Shibutani, S.; Eisenberg, M.; Johnson, F.; Grollman, A. P.; Patel, D. J. *Biochemistry* **1991**, *30*, 1403–1412.

(5)   Symons, M. C. R. In *The Early Effects of Radiation on DNA*; Fielden, E. M., O'Neill, P., Eds.; Springer: Berlin, 1991; Vol. H54, pp 111–124.

(6)   Sevilla, M. D. In *Excited States in Organic Chemistry and Biochemistry*; Pullman, B., Goldblum, N., Eds.; D. Reidel: Dordrecht, Holland, 1977.

(7)   Sevilla, M. D.; Failor, R.; Clark, C.; Holroyd, R. A.; Pettei, M. *J. Phys. Chem.* **1976**, *80*, 353–358.

(8)   Sevilla, M. D.; Becker, D.; Yan, M.; Summerfield, S. R. *J. Phys. Chem.* **1991**, *95*, 3409–3415.

(9)   (a) Novais, H. M.; Steenken, S. *J. Am. Chem. Soc.* **1986**, *108*, 1–6. (b) Cullis, P. M.; McClymont, J. D.; Malone, M. E.; Mather, A. N.; Podmore, I. D.;

66

Sweeney, M. C.; Symons, M. C. R. *J. Chem. Soc. Perkin Trans. 2* **1992**, 1695–1702. (c) Sevilla, M. D.; Becker, D.; Yan, M.; Summerfield, S. R. *J. Phys. Chem.* **1991**, *95*, 3409–3415.

(10)　(a) Hayon, E. *J. Chem. Phys.* **1969**, *51*, 4881–4899. (b) Theard, L. M.; Peterson, F. C.; Myers, L. S., Jr. *J. Phys. Chem.* **1971**, *75*, 3815–3821. (c) Das, S.; Deeble, D. J.; Schuchmann, M. –N.; von Sonntag, C. *Int. J. Radiat. Biol.* **1984**, *46*, 7–9.

(11)　(a) Steenken, S.; Telo, J. P.; Candeias, L. P. *J. Am. Chem. Soc.* **1992**, *114*, 4701–4709. (b) Deeble, D. J.; Das, S.; von Sonntag, C. *J. Phys. Chem.* **1985**, *89*, 5784–5788.

(12)　Ide, H.; Petrullo, L. A.; Hatahet, Z.; Wallace, S. S. *J. Biol. Chem.* **1991**, *266*, 1469–1477.

(13)　Nishimoto, S.; Ide, H.; Nakamichi, K.; Kagiya, T. *J. Am. Chem. Soc.* **1983**, *105*, 6740–6741.

(14)　Cadet, J.; Balland, A; Berger, M. *Int. J. Radiat. Biol.* **1981**, *39*, 119–133.

(15)　(a) Cadet, J.; Vigny, P. In *Bioorganic Photochemistry: Photochemistry and the Nucleic Acids*; Morrison, H., Ed.; John Wiley & Sons: New York, 1990; pp 1–272. (b) Taylor, J. –S. *Acc. Chem. Res.* **1994**, *27*, 76–82.

(16)　Miaskiewicz, K.; Miller, J.; Cooney, M.; Osman, R. *J. Am. Chem. Soc.* **1996**, *118*, 9156–9163.

(17)　(a) Taylor, J. –S.; Garrett, D. S.; Brockie, I. R.; Svoboda, D. L.; Telser, J. *Biochemistry* **1990**, *29*, 8858–8866. (b) Kan, L. –S.; Voituriez, L.; Cadet, J. *Biochemistry*, **1988**, *27*, 5796–5803. (c) Rycyna, R. E.; Wallace, J. C.; Sharma, M.; Alderfer, J. L. *Biochemistry* **1988**, *27*, 3152–3163.

(18)　(a) Camerman, N.; Camerman, A. *Science* **1968**, *160*, 1451–1452. (b) Camerman, N.; Camerman, A. *J. Am. Chem. Soc.* **1970**, *92*, 2523–2527. (c) Hruska, F. E.; Voituriez, L.; Grand, A.; Cadet, J. *Biopolymers* **1986**, *25*, 1399–1417.

(19)　(a) Wang, C. –I.; Taylor, J. –S. *Proc. Natl. Acad. Sci. U.S.A.* **1991**, *88*,

9072–9076. (b) Wang, C. –I.; Taylor, J. –S. *Chem. Res. Toxicol.* **1993**, *6*, 519–523.

(20) (a) Park, H. –W.; Kim, S. –T.; Sancar, A.; Deisenhofer, J. *Science* **1995**, *268*, 1866–1872. (b) Vassylyev, D. G.; Kashiwagi, T.; Mikami, Y.; Ariyoshi, M.; Iwai, S.; Ohtsuka, E.; Morikawa, K. *Cell* **1995**, *83*, 773–782.

(21) The number of molecules produced or changed per 1 J of radiation energy absorbed by the reaction system.

(22) Swallow, A. J. In *Radiation Chemistry. An Introduction*; Longman: London, 1973.

(23) Schwarz, H. A.; Creutz, C.; Sutin, N. *Inorg. Chem.* **1985**, *24*, 433–439.

(24) Various carboxylated monomeric and dimeric thymine derivatives were separated by HPLC when phosphate buffer solutions (10 mM, pH 3.0) contained higher contents of methanol (10–25 vol%). The structural characterization by X-ray crystallography of 5,6-dihydrothymine-6-carboxylic acid as a major product among them was performed to get insight into the inhibitory effect on dihydroorotate dehydrogenage (Chapter 1).

(25) Wada, T.; Ide, H.; Nishimoto, S.; Kagiya, T. *Int. J. Radiat. Biol.* **1982**, *42*, 215–221.

(26) Leonard, N. J.; Golankiewicz, K.; McCredie, R. S.; Johnson, S. M.; Paul, I. C. *J. Am. Chem. Soc.* **1969**, *91*, 5855–5862.

(27) Nelson, H. C. M.; Finch, J. T.; Luisi, B. F.; Klug, A. *Nature* **1987**, *330*, 221–226.

(28) Buxton, G. V.; Greenstock, C. L.; Helman, W. P.; Ross, A. B. *J. Phys. Chem. Ref. Data* **1988**, *17*, 513–886.

(29) Whillans, D. W.; Johns, H. E. *J. Phys. Chem.* **1972**, *76*, 489–493.

(30) Spinks, J. W.; Woods, R. J. In *Introduction to Radiation Chemistry, 3rd ed.*; John Wiley & Sons: New York, 1990.

(31) (a) Saito, I.; Takayama, M.; Sugiyama, H.; Nakatani, K.; Tsuchida, A.; Yamamoto, M. *J. Am. Chem. Soc.* **1995**, *117*, 6406–6407. (b) Sugiyama, H.;

Saito, I. *J. Am. Chem. Soc.* **1996**, *118*, 7063–7068. (c) Breslin, D. T.; Schuster, G. B. *J. Am. Chem. Soc.* **1996**, *118*, 2311–2319.

(32)   Dandliker, P. J.; Holmlin, R. E.; Barton, J. K. *Science* **1997**, *275*, 1465–1468.

(33)   (a) Murphy, C. J.; Arkin, M. R.; Jenkins, Y.; Ghatlia, N. D.; Bossmann, S. H.; Turro, N. J.; Barton, J. K. *Science* **1993**, *262*, 1025–1029. (b) Arkin, M. R.; Stemp, E. D. A.; Holmlin, R. E.; Barton, J. K.; Hörmann, A.; Olson, E. J. C; Barbara, P. F. *Science* **1996**, *273*, 475–480. (c) Holmlin, R. E.; Dandliker, P. J.; Barton, J. K. *Angew. Chem., Int. Ed. Engl.* **1997**, *36*, 2714–2730. (d) Olson, E. J. C.; Hu, D.; Hörmann, A.; Barbara, P. F. *J. Phys. Chem. B* **1997**, *101*, 299–303.

(34)   Murphy, C. J.; Arkin, M. R.; Ghatlia, N. D.; Bossmann, S.; Turro, N. J.; Barton, J. K. *Proc. Natl. Acad. Sci. U.S.A.* **1994**, *91*, 5315–5319.

(35)   Netzel, T. L. *J. Chem. Educ.* **1997**, *74*, 646–651.

(36)   Téoule, R.; Bonicel, A.; Bert, C.; Fouque, B. *J. Am. Chem. Soc.* **1978**, *100*, 6749–6750.

(37)   Shragge, P. C.; Hunt, J. W. *Radiat. Res.* **1974**, *60*, 233–249.

(38)   Hissung, A.; von Sonntag, C. *Int. J. Radiat. Biol.* **1979**, *35*, 449–458.

(39)   (a) Barvian, M. R.; Greenberg, M. M. *J. Org. Chem.* **1995**, *60*, 1916–1917. (b) Barvian, M. R.; Greenberg, M. M. *J. Am. Chem. Soc.* **1995**, *117*, 8291–8292. (c) Greenberg, M. M.; Barvian, M. R.; Cook, G. P.; Goodman, B. K.; Matray, T. J.; Tronche, C.; Venkatesan, H. *J. Am. Chem. Soc.* **1997**, *119*, 1828–1839. (d) Kotera, M.; Bourdat, A. -G.; Defrancq, E.; Lhomme, J. *J. Am. Chem. Soc.* **1998**, *120*, 11810–11811.

(40)   Gromova, M.; Balanzat, E.; Gervais, B.; Nardin, R.; Cadet, J. *Int. J. Radiat. Biol.* **1998**, *74*, 81–97.

(41)   Sheldrick, G. M. In *Crystallographic Computing 3*; Sheldrick, G. M., Kruger, C., Goddard, R., Eds.; Oxford University Press: Oxford, 1985; pp 175–189.

(42)   Burla, M. C.; Camalli, M.; Cascarano, G.; Giacovazzo, C.; Polidori, G.; Spagna, R.; Viterbo, D. *J. Appl. Crystallogr.* **1989**, *22*, 289–303.

Chapter 3

Conformational Effects on Photophysical Characteristics of C5–C5'-Linked Dihydrothymine Dimers in Solution

Abstract: Photophysical characteristics of N-substituted C5–C5'-linked dihydrothymine dimers (1a,b[*meso*], meso compounds of $(5R,5'S)$-bi-5,6-dihydrothymines; 1a,b[*rac*], racemic compounds of $(5R,5'R)$-bi-5,6-dihydrothymines and $(5S,5'S)$-bi-5,6-dihydrothymines) in protic/aprotic solvents with varying polarity have been investigated by UV-absorption, and steady-state and time-resolved fluorescence spectroscopies. Among the C5–C5'-linked dimers, $(5R,5'S)$-bi-5,6-dihydro-1-methylthymine (1a[*meso*]) showed a weak UV-absorption at 270–350 nm and fluorescence emission at 300–550 nm with the quantum yield (Φ_F) of ~0.1 in phosphate buffer (pH < 10) at 293 K. Racemic compound of 5,6-dihydro-1-methylthymine dimer (1a[*rac*]), and meso and racemic compounds of 5,6-dihydro-1,3-dimethylthymine dimers (1b[*meso*] and 1b[*rac*]) in phosphate buffer were non-fluorescent under similar conditions. The conformation-dependent fluorescence spectrum and the long fluorescence lifetime of 1a[*meso*] ($\tau_F^{ave} = 1.76$ ns) as well as the UV-absorption spectrum were interpreted in terms of the formation of an excimer that favors a "closed-shell" conformation both in the ground state and the excited singlet state. In basic solutions at pH > pKa = 11.7, the fluorescence quantum yield of 1a[*meso*] decreased due to a dominated "open – shell" conformation which may be formed by electric repulsion between the deprotonated pyrimidine chromophores of 1a[*meso*] in a dianion form.

Introduction

Hydrogen-bonding and stacking interactions among pyrimidine and purine bases that are essential in constructing DNA double strands have been extensively studied by means of UV-absorption, fluorescence and phosphorescence emissions, NMR, and IR spectroscopies, as well as X-ray crystallography and theoretical calculation.[1-14] To get structural insight into the photochemical reactivity of DNA base constituents, considerable efforts have been made to characterize the photophysical properties of various pyrimidine and purine derivatives in terms of inter- and intramolecular interactions. The most typical and biologically relevant photochemical reactions of DNA involve the formation of cycrobutane photodimer between adjacent thymine moieties and the photoreactivating repair of this toxic lesion by DNA photolyase.[1,15-17] However, a definite correlation between the intramolecular interaction and the photophysical properties of the adjacent thymines have not yet been fully obtained, because the UV-absorption and fluorescence characteristics of thymine and its dinucleotide analogs are complicated due to the presence of tautomers (2,4-diketo, keto-enol, and dienol forms), closely lying π,π^* and n,π^* transition states, and quite low fluorescence quantum yield ($\Phi_F \sim 1 \times 10^{-4}$) at ambient temperature.[5,9-14,18,19]

In Chapter 2, the author discussed the formation of C5–C5'-linked dihydrothymine dimers (1a,b, 5,5'-bi-5,6-dihydro-1-methylthymine derivatives) in the radiolysis of thymine derivatives in aqueous solution under anoxic conditions.[20,21] Interestingly, the C5–C5'-linked dihydrothymine dimers have structural similarity with cyclobutane thymine dimers as one of the major UV-induced toxic lesions of DNA.[1,20-22] The X-ray crystal structures revealed that the dihydropyrimidine rings of (5R,5'S)-bi-5,6-dihydro-1-methylthymine (1a[meso], meso compound) are stacked up in a "closed-shell" conformation, while those of (5R,5'S)- and (5S,5'R)-bi-5,6-dihydro-1-methylthymines (1a[rac], racemic compound) show no such a stacking interaction

71

to form an "open — shell" conformation. As for the photoreactivity, the dihydrothymine dimers 1a,b undergo an electron transfer from photoexcited reduced form of flavin (*FADH⁻). Consequently, the C5–C5' bonds split to regenerate monomeric thymines along with 5,6-dihydrothymines by a conformation-dependent mechanism, by which the "open — shell" dimers would favor a successive two-electron reduction by *FADH⁻ and the "closed-shell" dimers are not two-electron reduced due to an electrostatic repulsion between the pyrimidine rings.[23] On the other hand, 5,6-dihydrothymine structures that are also produced along with the dimeric products 1a,b is a well-documented DNA base lesion as induced by radiolysis of DNA, and the biological relevance has been a subject of considerable investigations.[24,25] However, photophysical characteristics of the dihydrothymines have attracted less attention, relative to those of mono- and poly-nucleic acid bases.[1,19,26]

In this study, the author has measured UV-absorption and fluorescence spectra of C5–C5'-linked dihydrothymine dimers 1a,b, by reference to 5,6-dihydro-1-methylthymine as a monomer constituent and its dinucleotide model compound, for understanding of the properties of intramolecular interaction between two dihydrothymine chromophores. Particular attention has been paid to the intramolecular excimer formation between dihydrothymine chromophores of 1a[*meso*] that was strongly affected by the preferential "closed-shell" conformations both in the ground and excited states.

Experimental Section

Chemicals. 1-Methylthymine (Sigma Chemical) and, thymine (Wako Pure Chemical) were used as received. Stereoisomeric C5–C5'-linked 5,6-dihydrothymine dimers and 5,6-dihydro-1-methylthymine (2) were synthesized and purified following the
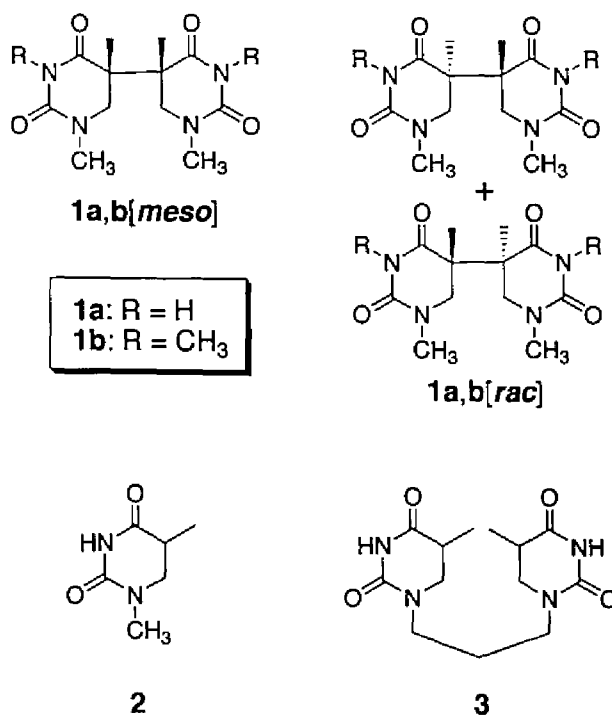
Chart 1. Structures of dihydrothymine derivatives.

methods reported previously.[20] Purity of the dimers was checked by HPLC. KCl, KBr and KI were recrystallized from water before use. Tetrahydrofuran (THF) and 1,4-dioxane of spectroscopic grades (Wako) were used without further purification. The water employed was prepared using a Corning Mega-Pure System MP-190 (>16 MΩ cm).

Synthesis. **1,3-Dimethylthymine**: Following the method of Wulff and Fraenkel,[27] thymine (10 g) in 1 M NaOH (150 mL) was treated with 15 mL of dimethyl sulfonate (caution, highly toxic) and stirred for 30 min at room temperature. The resulting mixture was refluxed for 90 min and then cooled to a room temperature. The solution was extracted three times with 50-mL portions of benzene. The extract was dried over MgSO$_4$ and evaporated to dryness in vacuum, leaving a white solid. The solid was recrystallized from water, yielding 3.41 g of the product with the NMR spectra identical to those reported previously.[27]

1,1'-Trimethylenebis(thymine):[19,28] Bis(trimethylsilyl)thymine was synthesized as previously reported.[29] A 3.6 g portion of bis(trimethylsilyl)thymine was dissolved in 26 mL of dry 1,3-dibromopropane. The solution was refluxed for 2 hr under anhydrous conditions and then poured into 100 mL of water. The mixture was extracted with three 100-mL portions of chloroform. The chloroform extract was dried over $MgSO_4$ and evaporated in vacuum, leaving a pale yellow solid. The solid of 1-(3-bromopropyl)thymine was recrystallized from 2-propanol to yield 1.37 g (62 %). 1-(3-Bromopropyl)thymine (1.24 g) in bis(trimethylsilyl)thymine (4.1 g) was refluxed at 110 °C for 3 hr under anhydrous conditions with stirring. Unreacted bis(trimethylsilyl)thymine was evaporated in vacuum and the residue was washed with three 30-mL portions of chloroform-ethanol (1:1). The resulting precipitate was recrystallized from water, yielding 0.69 g of 1,1'-trimethylenebis(thymine) (32 %).

1,1'-Trimethylenebis(5,6-dihydrothymine) (3): Ar-Saturated aqueous solution of 1,1'-trimethylenebis(thymine) (0.144 g) containing sodium formate (6.81 g) was irradiated up to 5.35 kGy at room temperature with a ⁶⁰Co γ-ray source (dose rate: 0.55 Gy min⁻¹). 1,1'-Trimethylenbis(5,6-dihydrothymine) was isolated from the major products by preparative HPLC (Tosoh Preparative HPLC system) equipped with a reversed phase column (Wakosil 10C18, φ 10 mm × 300 mm): ¹H NMR (400 MHz, D_2O, 25 °C), δ (ppm/TSP-d_4) 1.089 (6H, d, J = 6.83 Hz), 1.789 (2H, q, J = 7.08), 2.715-2.772 (2H, m), 3.309 and 3.346 (2H, ABX, $J_{5,6}$ = 5.87, 9.29, $J_{6A,6B}$ = 5.86), 3.329 (4H, t, J = 7.08); ¹³C NMR (100 MHz, D_2O, 25 °C), δ (ppm/TSP-d_4) 12.442, 25.354, 34.772, 43.953, 47.848, 152.931, 173.340; HR-FAB MS calcd for C13H21N4O4 [(M+H)⁺] m/z = 297.1563, found 297.1568.

Absorption and Emission Measurements. Typically, steady-state UV absorption spectra of 1a,b[meso] and 1a,b[rac] (0.1 mM) in phosphate buffer (10 mM, pH 7.0) were measured with a Shimadzu MPS-2000 spectrophotometer (path length: 1.0 cm). Basic aqueous solutions of 1a,b[meso] and 1a,b[rac] (0.1 mM) were prepared by addition of NaOH (0.1 M) to solutions of Na_2HPO_4, by which the final concentration

became 25 mM of phosphate buffer. Ion strength of the buffer solutions was adjusted to 0.15 by addition of 1M KCl.[30,31]

Fluorescence spectra were recorded on a Hitachi F-2000 fluorescence spectrophotometer. The fluorescence quantum yields (Φ_F) were evaluated from the area of fluorescence spectra and the absorbance at 312 nm, by reference to 0.01 mM quinine sulfate in 0.5 M H_2SO_4 (Φ_F = 0.546). All the sample solutions were purged with Ar before UV-absorption and fluorescence emission measurements. Fluorescence lifetimes were measured by a time-resolving equipment described before.[32]

Calculations. All semi-empirical calculations were performed using the MOPAC algorithm (AM1 and INDO/1 levels) in the CAChe software package (version 3.9, Oxford Molecular Group) on Apple Power Macintosh. Ground-state geometries were optimized by the AM1 prior to the calculation of excited-state properties by the INDO/1. A Conductor-like Screening Model (COSMO), which makes a good approximation especially for solvents with high polarity, was used for modeling of solvent effect.

Results

UV-Absorption Characteristics. Figure 1 shows UV-absorption spectra of 1a,b[meso] and 1a,b[rac] (0.1 mM) in phosphate buffer (10 mM) at pH 7.0 at room temperature. Relative to the racemic isomer 1a[rac], the meso isomer 1a[meso] exhibited hypochromism with reduced intensity of absorption shoulder at 220 nm. Instead, 1a[meso] exhibited hyperchromic effect and a weak absorption in the longer wavelength region tailing up at 350 nm that was not observed for 1a[rac]. These absorption spectral characteristics were independent of the varying concentrations of 1a[meso] (0.006–0.1 mM). In contrast to 1a, 1b[meso] and 1b[rac] resulted in

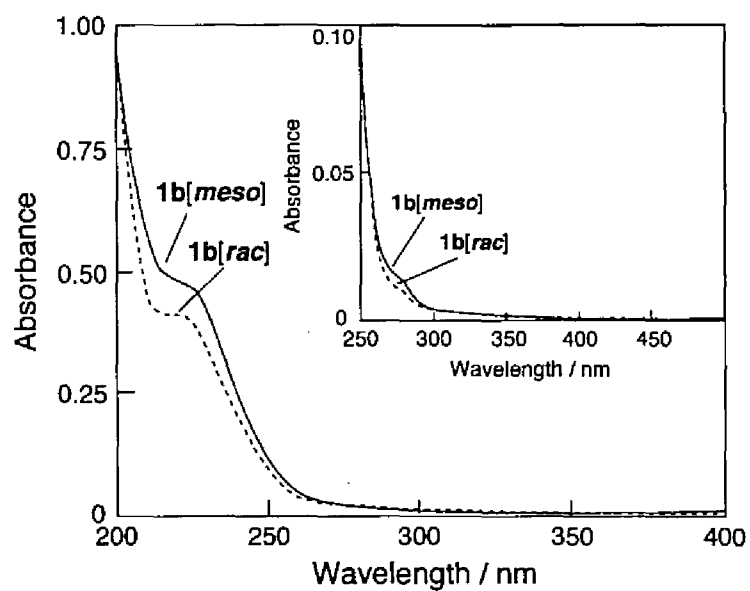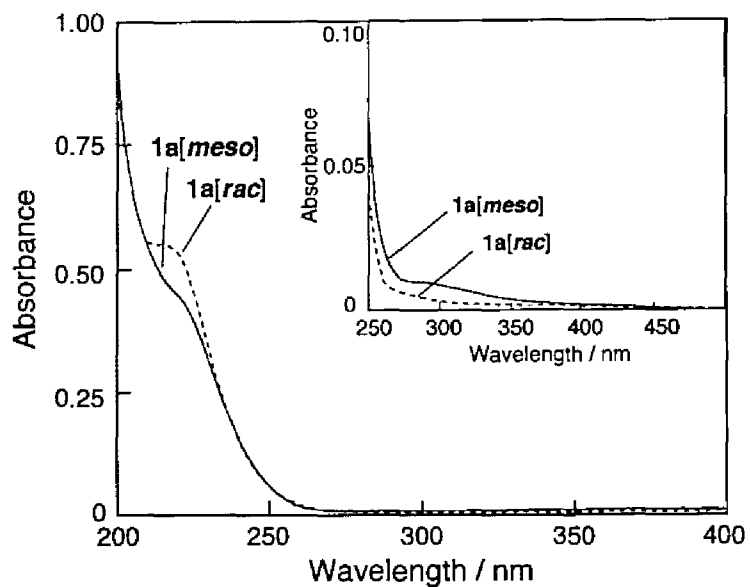**Figure 1.** UV-Absorption spectra of (a) **1a[*meso*]** and **1a[*rac*]** (0.1 mM) and (b) **1b[*meso*]** and **1b[*rac*]** (0.1 mM) in phosphate buffer (pH 7.0) at 293 K. Insets show the expanded charts in the wavelength range of 250–500 nm.
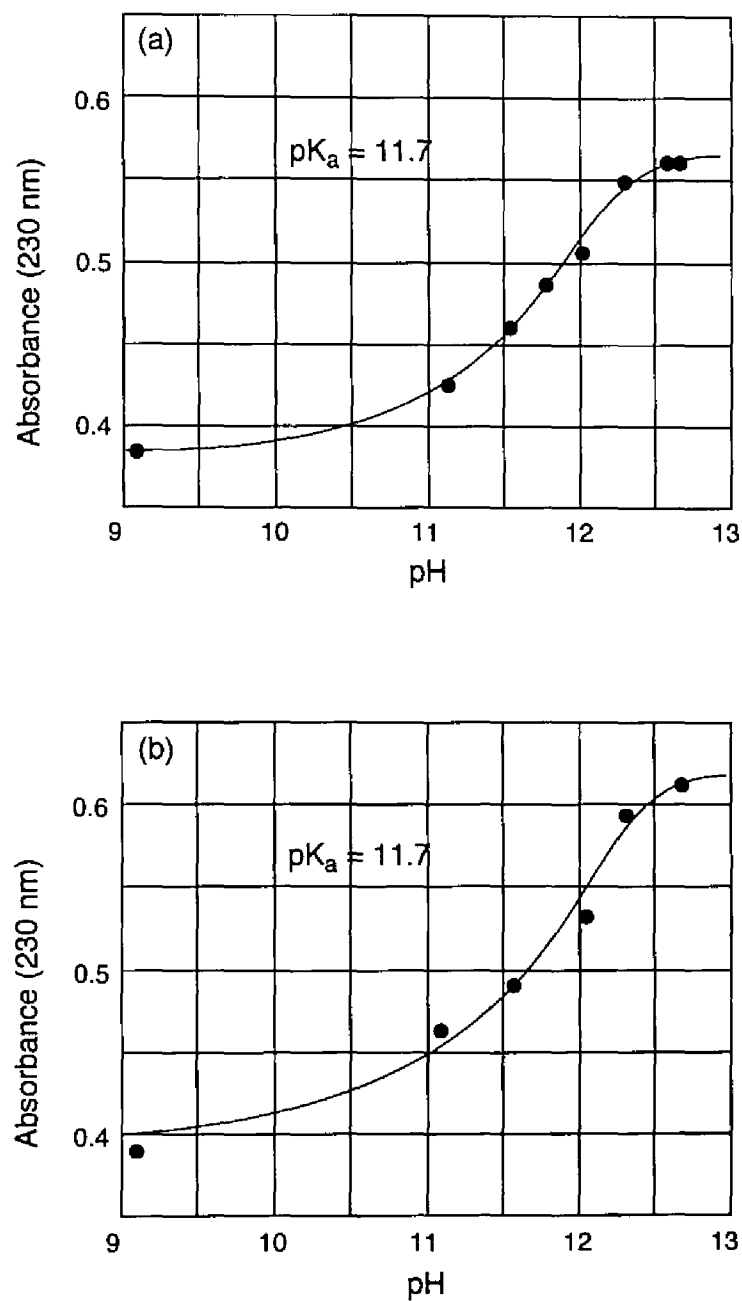
Figure 2. Titration curves monitored by the UV absorbance at 230 nm of
(a) **1a**[*meso*] and (b) **1a**[*rac*] in phosphate buffer at 293 K. Final ion
strength was adjusted to 0.15 by addition of KCl. The half-equivalence
points gave pKa (**1a**[*meso*]) = 11.7 and pKa (**1a**[*rac*]) = 11.7, respectively.

substantially similar absorption spectra in the wavelength range of 200–350 nm, while there were some differences in the molar extinction coefficient.

The UV-absorption spectra of 1a[*meso*] in tetrahydrofuran (THF)-H$_2$O and dioxane-H$_2$O mixed solvents with various proportions were strongly affected by the polarity and the aprotic/protic nature of solvents. As the content of non-aqueous component, THF or dioxane, increased and thereby a less polar and aprotic environment became more important, both the hypochromism observed at 220 nm and the hyperchromism at around 300 nm were reduced to more extent (data not shown). In accord with the solvent effect on the UV-absorption spectra, the hypochromism characteristic of 1a[*meso*] is attributable to a hydrophobic stacking interaction between the dihydropyrimidine chromophores. This is also supported by the previous NMR structural analysis that 1a[*meso*], but not all the other dimers, prefers a "closed-shell" conformation even in solution.[23]

The pKa values for the C5–C5'-linked 1-methylthymine dimers 1a in the ground state were determined from pH-response of the absorbance at 230 nm (Figure 2). From the titration curves for 1a (0.1 mM) in phosphate buffer (25 mM) with ion strength of 0.15 at 293 K, identical pKa values of 11.7 corresponding to N3-deprotonation of dihydrothymine chromophore were obtained for 1a[*meso*] and 1a[*rac*], respectively. Similar pKa values of 11.4 and 11.6 have been reported for 5,6-dihydrouracil and 5,6-dihydrothymine, respectively, as determined by the acid-base titration and UV-absorption spectroscopic methods.[31]

Emission Characteristics. Figure 3 shows fluorescence spectra of the meso dimer 1a[*meso*] in aqueous solution (pH 7.0 and 11.0) at room temperature, as observed upon excitation at 312 nm. The broad and red-shifted emission spectra with the maximum at λ_{max} = 370 nm (ΔE = 323 kJ mol^{-1}) which showed no vibrational fine structure were observed in the wide concentration range of 0.006–0.1 mM. The intensity of the fluorescence increased, but the spectral profile was not altered with
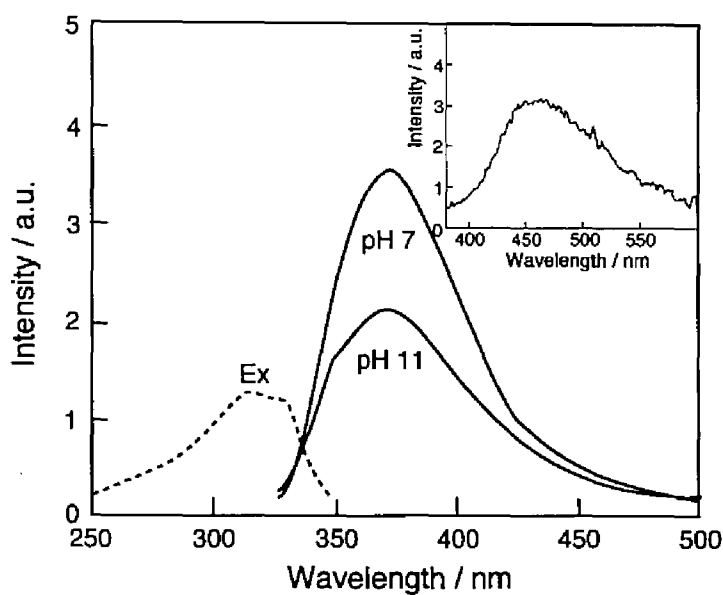
Figure 3. Fluorescence spectra (solid line) of **1a**[*meso*] (0.1 mM) in phosphate buffer (pH 7.0 and 11.0) at 293 K upon excitation at λ_{ex} = 312 nm, and the excitation spectrum (dotted line) upon monitoring fluorescence emission at λ_F = 370 nm. All the other dimers (**1a**[*rac*], **1b**[*meso*], and **1b**[*rac*]) were non-fluorescent under similar conditions. Inset shows phosphorescence spectrum of **1a**[*meso*] (0.5 mM) in phosphate buffer (pH 7.0) observed at 77 K upon excitation at 300 nm.

increasing concentrations of 1a[*meso*]. In contrast to 1a[*meso*], neither dilute nor concentrated aqueous solutions of the other dimers 1a[*rac*], 1b[*meso*] and 1b[*rac*] showed such a fluorescence emission under similar conditions. The excitation spectrum corresponding to the fluorescence emission of 1a[*meso*] at 370 nm is also shown in Figure 3, which was not totally identical to the absorption spectrum of 1a[*meso*] but seemed relevant to the red-shifted absorption tail. In accord with this spectral correlation, the non-fluorescent compounds 1a[*rac*], 1b[*meso*] and 1b[*rac*] showed no such a red-shifted absorption band.

Furthermore, the fluorescence spectra (λ_{ex} = 270 nm) of a reference compound of 5,6-dihydro-1-methylthymine 2 corresponding to a monomer constituent of 1a[*meso*] in aqueous solution were also measured (Figure 4). In the dilute aqueous solution of 2 (0.2 mM) a monomer fluorescence was observed with a maximum wavelength at λ_{max} = 340 nm. The intensity of the monomer fluorescence decreased to evolve a new broad emission band in the longer wavelength range (λ_{max} = 370 nm), when the concentration of 2 was increased up to 4.0 mM. For further investigation, 1,1'-trimethylenebis(5,6-dihydrothymine) (3), in which dihydropyrimidine bases are linked by a trimethylene chain at N1 and N1', was synthesized and the fluorescence spectra were measured in the concentration range of 0.006–0.1 mM. As shown in Figure 4, 3 exhibited a broad fluorescence without change of the spectral profile in the wavelength range of 300–500 nm (λ_{max} = 370 nm), which was substantially similar to the behavior of 1a[*meso*]. On the basis of these observations, the broad emission of 1a[*meso*] is considered to be characteristic of an excimer originated from a "closed-shell" conformation in which both dihydropyrimidine chromophores are intramolecularly stacked to get some stabilization energy in the excited state (see also Figure 9). It should be noted that this transient is not excimer in a strict definition, since the 5,6-dihydrothymine chromophores of 1a[*meso*] may be of a partial stacking interaction in their ground states, as implicated by the characteristic absorption spectrum. Thus, it is most likely that the excimer is formed by direct excitation of the
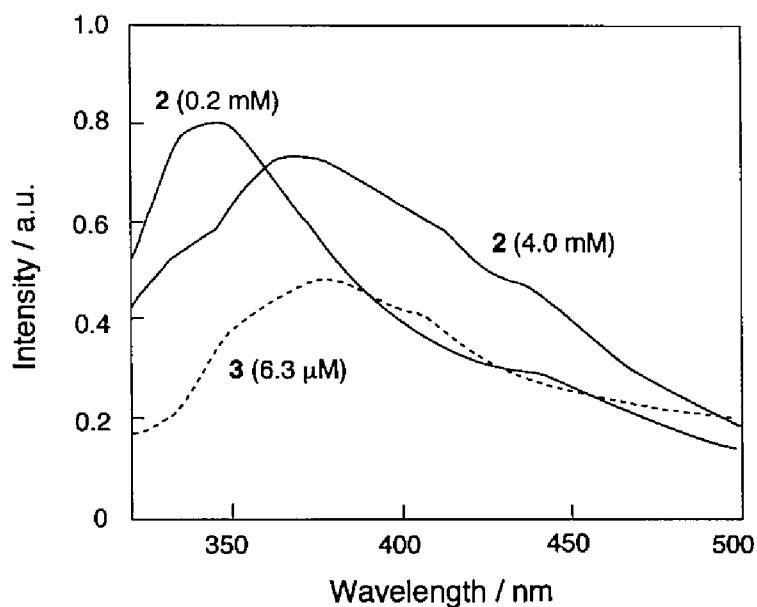
Figure 4. Fluorescence spectra of **2** (0.2 and 4.0 mM) and **3** (6.3 μM) in phosphate buffer at 293 K upon excitation at λ_{ex} = 270 nm.
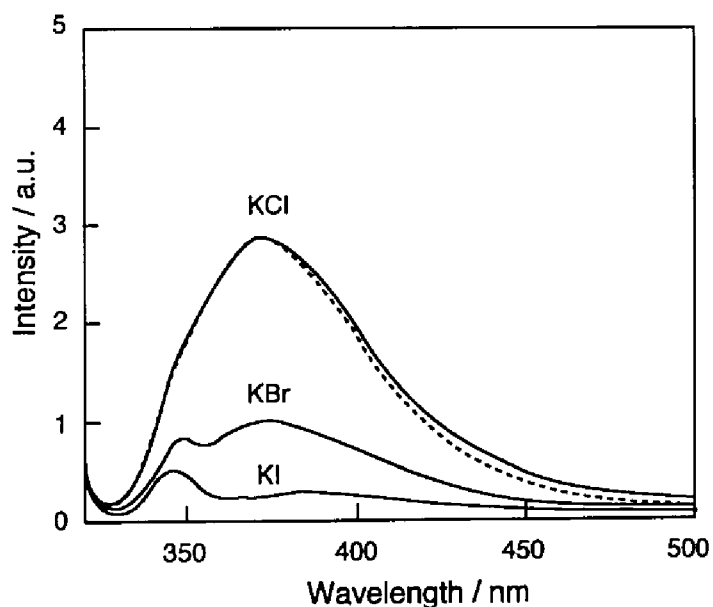

Figure 5. External heavy-atom effect on the fluorescence emission of **1a**[*meso*] (0.1 mM) in aqueous solution at 293K. Samples were excited at 312 nm in the absence (dotted line) and in the presence (solid lines) of KCl, KBr or KI (200 mM).

81

ground-state 1a[*meso*] in a similar "closed-shell" conformation, thereby attaining a proximate stacking distance in the excited state. In contrast to the meso isomer 1a[*meso*], the racemic isomer 1a[*rac*] which would favor predominantly an "open – shell" conformation in the ground state provided no evidence for the formation of such a stacked conformation even in the excited state.

The fluorescence spectra of 1a[*meso*] (0.1 mM) were measured in aqueous solution in the presence of 200 mM halide ions (KCl, KBr, KI) upon excitation at 312 nm. As shown in Figure 5, the fluorescence emission was quenched by Br⁻ and I⁻, but not by Cl⁻, indicating an external heavy-atom effect on the fluorescence of 1a[*meso*]. Similar to Cl⁻, the dissolved amount of oxygen could not quench the fluorescence (data not shown). These behavior suggest that the fluorescence emission originates from a singlet excimer with a relatively short lifetime.

For further characterization, emission spectrum of 1a[*meso*] in aqueous solution was also determined at lower temperature of near 77 K with excitation at 300 nm. As is evident from Figure 3, a delayed emission spectrum (λ_{max} = 460 nm, ΔE = 260 kJ mol⁻¹) was observed concomitant with the fluorescence spectrum at λ_{max} = 370 nm. This emission at λ_{max} = 460 nm is in good accordance with the phosphorescence emissions of thymine in 2-methyltetrahydrofuran with λ_{max} = 460 nm,[11] or thymine and its dinucleotide in H_2O-ethyleneglycol (1:1) glass with λ_{max} = 440 nm.[19] Thus, in contrast to the fluorescence spectra, phosphorescence emission of 1a[*meso*] may be attributed to dihydropyrimidine chromophore in the excited triplet state, but not to a triplet excimer.

In a similar manner as the UV-absorption, the excimer fluorescence emission of 1a[*meso*] in THF-H_2O and dioxane-H_2O mixed solvents with various proportions were affected by the polarity and the aprotic/protic nature of solvents. Although apparent intensity of the excimer fluorescence decreased due to the reduced hydrophobic stacking interaction between dihydropyrimidine chromophores in the ground state, the fluorescence quantum yield (Φ_F) was significantly enhanced upon

Table 1. Fluorescence Quantum Yields[a] of **1a**[*meso*] (0.1 mM) in Aqueous Solution with Varying Fractions of THF or 1,4-Dioxane at 298 K.

solvent	fraction of non-aqueous solvent	Φ_F
H$_2$O		0.11
THF / H$_2$O	25 vol%	0.12
	50 %	0.24
	75 %	0.20
Dioxane / H$_2$O	25 %	0.12
	50 %	0.20
	75 %	0.35

[a] Evaluated by reference to 0.01 mM quinine sulfate in 0.5 M H$_2$SO$_4$ (Φ_F = 0.546).

increasing the content of non-aqueous component, THF or dioxane, in the binary mixed solvent (Table 1). This phenomenon may be closely associated with the evidence that non-fluorescent dihydropyrimidine chromophores of **1a**[*meso*] favor a hydrophobic stacking interaction in the ground state in aqueous solution, thereby forming fluorescent excimer in the excited state. It is thus plausible that the excimer state of **1a**[*meso*] becomes more intensely fluorescent as a result of solvation by less polar aprotic molecules such as THF or dioxane, despite reduced fraction of the "closed-shell" conformation.

The pKa value for **1a**[*meso*] in the fluorescent excimer state (pKa*) was determined by a titration method with monitoring the fluorescence emission at λ_{max} = 370 nm. Figure 6 shows variation of the fluorescence quantum yields of **1a**[*meso*] in phosphate buffer as a function of pH. The quantum yields were almost constant (Φ_F ~ 0.1) at pH values below 10, but decreasing dramatically in the pH region between 11 and 12. The pKa* value thus obtained was close to the ground-state pKa value (11.7), suggesting that the fluorescence lifetime of **1a**[*meso*] in the intramolecular excimer
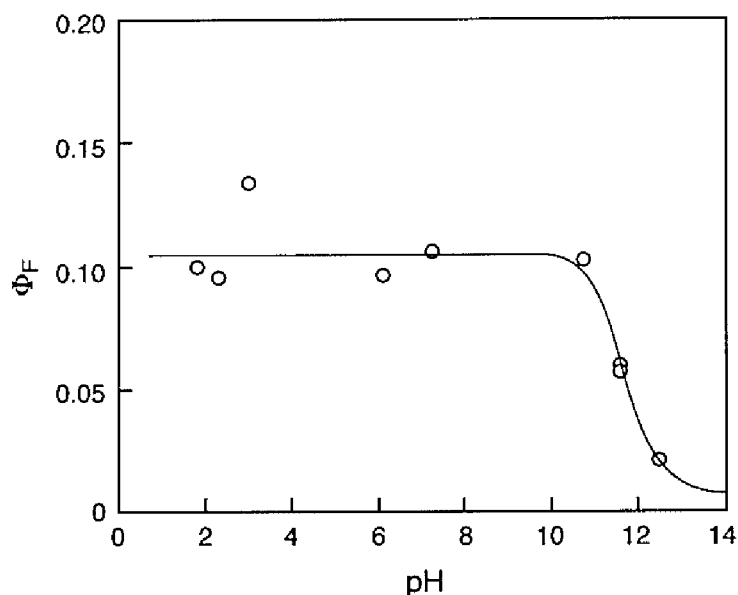
Figure 6. Titration curve monitored by the fluorescence quantum yield (Φ_F) of **1a**[*meso*] in phosphate buffer at 293 K. The half-equivalent point gave pKa* (**1a**[*meso*]) = ~11.5.

state is too short to establish the acid-base equilibrium in the excited singlet state. In accord with these behavior, the dimers probably undergo deprotonation almost exclusively in the ground state to form the dimer dianions at pH values above the pKa = 11.7. Such a deprotonation would cause conformational change from the "closed-shell" to "open – shell" structures because of electrostatic repulsion and increased solvation by water of the negatively charged dihydrothymine rings. In spite of the "opened-shell" conformation, the N3-deprotonated dihydrothymine chromophore may be of a keto–enol (lactim) tautomer and thereby shows UV-absorption at longer wavelengths to give weaker fluorescence emission. Therefore, the reduction of fluorescence quantum yield at pH > pKa* ≈ pKa may be attributed to direct excitation of the ground-state dimer dianions, but not to deprotonation of the excimer-state dimers in the "closed-shell" conformation.

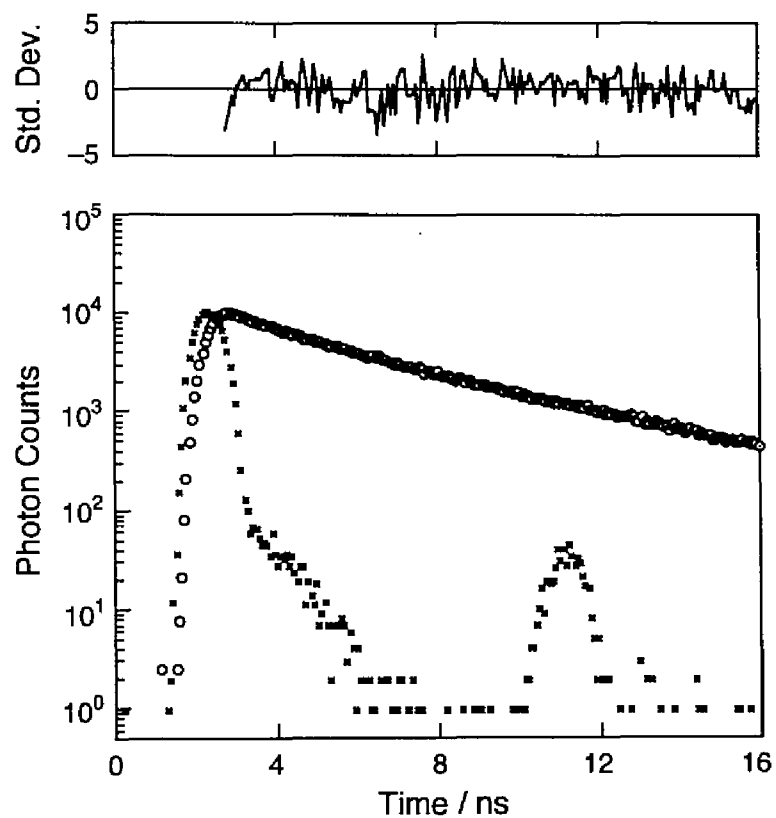**Fluorescence Lifetime.** The fluorescence emission from pulsed laser-excited

84

Figure 7. A typical fluorescence decay trace of **1a**[*meso*] ($\lambda_F = 370$ nm) in phosphate buffer at pH 3.0 along with instrumental response profile. The double-exponentially-fitted decay profile (solid line) and its standard deviation (upper panel) were derived in the range of 3–16 ns.
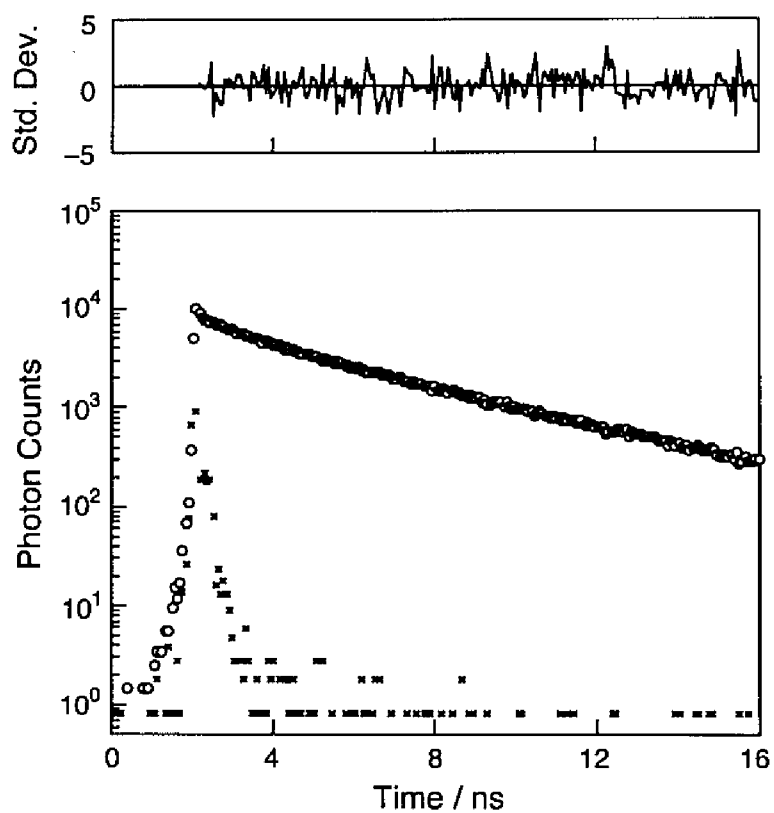
Figure 8. A typical fluorescence decay trace of **1a**[*meso*] ($\lambda_F = 370$ nm) in phosphate buffer at pH 11 along with instrumental response profile. The triple-exponentially-fitted decay profile (solid line) and its standard deviation (upper panel) were derived in the range of 3–16 ns.

Table 2. Fluorescence Lifetimes of 1a[*meso*] (0.1 mM) in Phosphate Buffer (10 mM, pH 3–11) at 293 K.[a]

pH	λ_{em}	α_1	τ_1 / ns	α_2	τ_2 / ns	α_3	τ_3 / ns
3	350	0.045	5.13	0.059	1.19		
	370	0.060	4.73	0.041	1.47		
	400	0.058	4.68	0.039	1.47		
	450	0.051	5.06	0.047	1.23		
7	370	0.58	4.39	0.25	1.01		
11	370	0.43	4.61	0.24	1.35	0.40	0.10

[a] The emission decays were fitted globally to double- or triple-exponential expression: $I(t, \lambda)$ = $\alpha_1(\lambda) \exp(-t/\tau_1) + \alpha_2(\lambda) \exp(-t/\tau_2)$ (+ $\alpha_3(\lambda) \exp(-t/\tau_3)$) where the lifetimes ($\tau_n$) were linked and the preexponential factors (α_n) varied freely.

1a[*meso*] (0.1 mM, pH 3, 7, and 11) excited by pulsed laser at 350–450 nm at room temperature decayed in a non-single exponential manner, as shown in Figures 7 and 8. A double-exponential approximation provided the best fit to the transient fluorescence emission observed at a representative wavelength of 370 nm in acidic (pH 3) and neutral (pH 7) solutions, thus resulting in the corresponding lifetimes as listed in Table 2. The decay parameters were independent of the wavelength of fluorescence emission in the range of 370–420 nm, indicating that neither monomer emission nor fluorescence of impurities contributes to the observed transient emission. On the other hand, triple-exponential decay of the fluorescence emission of 1a[*meso*] was observed when excited at pH 11 in aqueous solution (Figure 8). In this pH region, the dimer may be partially deprotonated into the dimer dianion in the ground state prior to excitation, therefore the additional short-lived component (τ_3 = 0.10 ns) being ascribed to the dianion in the "open – shell" conformation that results in decreased quantum yield in basic solution.

Theoretical calculations. In order to assign the electronic absorption band, semi-empirical calculations by the AM1 and INDO/1 methods was performed for the C5–C5'-linked dimers in polar solution. The AM1 calculation for **1a**[*meso*] revealed that the highest occupied molecular orbital (HOMO) and the HOMO–1 are delocalized on n-orbitals over two dihydropyrimidine chromophores, and that the lowest unoccupied molecular orbital (LUMO) and the LUMO+1 are localized on antibonding π^* orbitals of either dihydropyrimidine chromophore. The levels of HOMO and HOMO–1 and those of LUMO and LUMO+1 are nearly degenerated with splitting by about 0.15 eV, respectively. Furthermore, the excited singlet states (S_n) were found to be created through $(n,\pi*)$ transients from the HOMO n-orbital to the unoccupied π^* orbitals. The transition energies from the ground state (S_0) to the three excited singlet states (S_1-S_3) were calculated as $E(S_1) - E(S_0) = 29197$ cm^{-1}, $E(S_2) - E(S_0) = 29387$ cm^{-1}, and $E(S_3) - E(S_0) = 32246$ cm^{-1} with oscillator strengths of 1.0~1.3 × 10^{-3}, respectively. These energy gaps are in good agreement with the UV-absorption spectroscopic data shown in Figure 1. Unfortunately, the satisfactory data for the optimized geometries in the ground and excited singlet states failed to be obtained by the present semi-empirical level of calculations because of the flexibility of dihydropyrimidine rings.

Discussion

The X-ray crystallography of the C5–C5'-linked dimers **1a,b** has shown that the dihydropyrimidine rings of the dimers, except **1a**[*rac*], overlap intramolecularly to some extent with dihedral angles of 5-Me–C5–C5'–5'-Me being 43–65°. In contrast to such "closed-shell" conformations, the X-ray crystal structure of **1a**[*rac*] was of an "open − shell" conformation with respect to the dihydropyrimidine rings. More striking is that only **1a**[*meso*] favors the "closed-shell" conformation even in solution,

as confirmed by the NMR structural analysis.[23]

In this study, the author has shown the photophysical characteristics of dihydropyrimidine chromophore in the C5–C5'-linked dihydrothymine dimers at room temperature, comparing with those of several 5,6-dihydrothymine derivatives. The structure-dependent fluorescence emission (λ_{max} = 370 nm) of **1a[*meso*]** with relatively high quantum yield (Φ_F ~0.1) was red-shifted by 30 nm by reference of the monomer fluorescence of 5,6-dihydro-1-methylthymine **2**, and was characteristic of an excimer that is different from monomer fluorescence emissions of the diketo (lactam) and keto–enol (lactim) tautomers of thymine.[14]

Comparing with the dihydrothymine dinucleotide analogue **3** with a flexible trimethylene chain, the distance between the two dihydrothymine rings of the C5–C5'-linked dimers in the "closed-shell" conformation are closer to attain a stacking interaction in the ground state. In view of the structure-dependent emission spectrum, the fluorescence of **1a[*meso*]** could be observed only when the dihydrothymine chromophores are excited with retaining the "closed-shell" conformation. According to the structural characteristics, the meso dimers are predicted to have higher rotational energy around the C5–C5' bond in solution than the racemic dimers. As the molecular rigidity becomes greater, the radiationless internal conversion process may be suppressed to increase the fluorescence quantum yield. It is thus suggested that **1a[*meso*]** in a "closed-shell" conformation is more fluorescent than the racemic isomers **1a[*rac*]** in an "open – shell" conformation in which non-fluorescent deactivation process is predominant due to the effective internal conversion by the free rotation through the C5–C5' bonds. The solvent effect on the UV-absorption spectra that the hypochromism was more reduced with increasing contents of less polar solvents in aqueous solution is accounted for by the increased fraction of "open – shell" conformations. In view of the enhanced fluorescence quantum yield of **1a[*meso*]** with increased fraction of THF or dioxane, the hydrogen-bonding interaction between the dihydrothymine ring and water may change the stability of
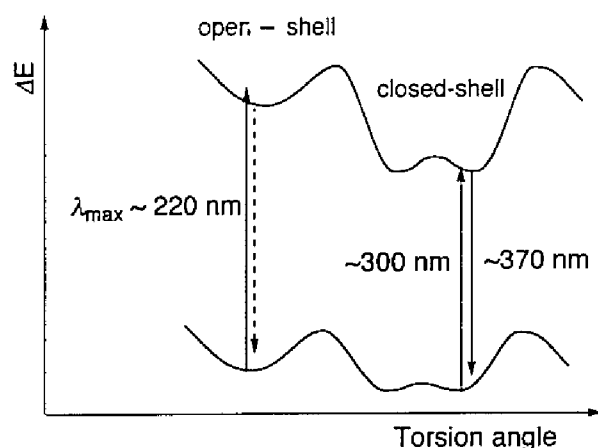
Figure 9. Proposed potential energy surfaces for the ground and lowest excited singlet state of **1a**[*meso*] as a function of the torsion angle through the C5–C5' bond.

$^{1}(n,\pi^{*})$ transition as discussed below.

The previous time-resolved emission analyses of oligo- and poly-nucleotides has shown that an excimer formation enhances the fluorescence lifetimes occurring in the ns range.[33,34] This is in good accordance with our result for **1a**[*meso*] that the excimer fluorescence emission is observable with an average lifetime $\tau_F^{ave} = 1.76$ ns. The two fluorescence-decay components of **1a**[*meso*] with different lifetimes that were observed in aqueous solution at room temperature (Table 2) could be interpreted in terms of a rapid dynamic equilibrium between a fluorescent excimer state with favorable orientation of dihydrothymine chromophores and a less fluorescent excimer state with unfavorable orientation, both of which are in the "closed-shell" conformation (Figure 9). In view of the excitation spectra corresponding to the excimer fluorescence of **1a**[*meso*] in Figure 3, a possible route to intramolecular excimer formation via excited-state dihydrothymine chromophore in the "open – shell" conformation may be ruled out. This is not the case for the dihydrothymine dinucleotide analog **3** with a flexible trimethylene chain.

On the other hand, it has been suggested that methylation of purine and

pyrimidine bases enhances intermolecular interaction.[35-37] In a recent study, methyl-substitution of pyrimidine rings was found to enhance the pyrimidine–pyrimidine interaction, as demonstrated by comparing the ^{1}H NMR signals of 1,1'-(α,ω-alkanediyl)bisthymine and 1,1'-(α,ω-alkanediyl)bisuracil.[36] The C5–C5'-linked 1,3-dimethylthymine dimers **1b** is however non-fluorescent despite the dimethylthymine rings being in "closed-shell" conformation in the crystals.[20] As characterized by the previous NMR analysis in solution, the absence of the fluorescence emission from **1b**[*meso*] and **1b**[*rac*] may be attributed to a preference for "open – shell" conformation in aqueous solution due to the steric hindrance of methyl groups at N3 and N3', in contrast to a "closed-shell" conformation in the crystal.

As shown above, the theoretical calculation of the C5–C5'-linked dimer structures indicated that the UV-absorption band at longer wavelength is assigned to an ^{1}(n,π^*) transition. The dihydrothymine chromophores of the C5–C5'-linked dimers do not involve a strong ^{1}(π,π^*) transition band at around 260 nm because of the loss of C5–C6-double bond. Consequently, the weak carbonyl ^{1}(n,π^*) transition band might become explicitly observable. However, considering the lower fluorescence quantum yield in more protic and polar solvents, the energy level of the lowest forbidden ^{1}(n,π^*) state may be localized above the carbonyl ^{1}(π,π^*) state in aqueous solution. Similar solvent effect on the fluorescence emission has been observed in a solution of thymine monomer, suggesting that such an energy-state inversion would be induced by protic solvents which destabilizes the ^{1}(n,π^*) state but stabilizes the ^{1}(π,π^*) state.[11,12]

Conclusion

The present study demonstrated the first example of excimer fluorescence emission from the dihydrothymine chromophores of the C5–C5'-linked dimer **1a**[*meso*] with the quantum yield of Φ_F ~0.1 in the wavelength range of

300–550 nm. The UV-absorption spectrum and the long fluorescence lifetime with $\tau_F^{ave} = 1.76$ ns suggested that two dihydrothymine chromophores of **1a**[*meso*] favor a "closed-shell" conformation both in the ground state and the excited singlet state. A semi-empirical calculation predicted that a rather forbidden $^1(n,\pi^*)$ transition of **1a**[*meso*] in the "closed-shell" conformation may be responsible for the excimer fluorescence.

References and Notes

(1)   Cadet, J.; Vigny, P. In *Bioorganic Photochemistry: Photochemistry and the Nucleic Acids*; Morrison, H., Ed.; John Wiley & Sons: New York, 1990; pp 1–272.

(2)   Saenger, W. *Principles of Nucleic Acid Structure*; Springer-Verlag: New York, 1984.

(3)   Miller, J. H.; Sobell, H. M. *J. Mol. Biol.* **1967**, *24*, 345–350.

(4)   Solie, T. N.; Schellman, J. A. *J. Mol. Biol.* **1968**, *33*, 61–77.

(5)   Nakano, N. I.; Igarashi, S. J. *Biochemistry* **1970**, *9*, 577–583.

(6)   Wu, P.; Nordlund, T. M. *Biochemistry* **1990**, *29*, 6508–6514.

(7)   Florián, J.; ˇSponer, J.; Warshel, A. *J. Phys. Chem. B* **1999**, *103*, 884–892.

(8)   ˇSponer, J.; Leszczy´nski, J.; Hobza, P. *J. Phys. Chem.* **1996**, *100*, 5590–5596.

(9)   Hauswirth, W.; Daniels, M. *Photochem. Photobiol.* **1971**, *13*, 157–163.

(10)   Vigny, P.; Duquesne, M. *Photochem. Photobiol.* **1974**, *20*, 15–25.

(11)   Becker, R. S.; Kogan, G. *Photochem. Photobiol.* **1980**, *31*, 5–13.

(12)   Baraldi, I.; Bruni, M. C.; Costi, M. P.; Pecorari, P. *Photochem. Photobiol.* **1990**, *52*, 361–374.

(13)   Eaton, W.; Lewis, T. P. *J. Phys. Chem.* **1970**, *53*, 2164–2172.

(14)   Morsy, M. A.; Al-Somali, A. M.; Suwaiyan, A. *J. Phys. Chem. B* **1999**, *103*, 11205–11210.

(15)   Lisewski, R.; Wierzchowski, K. L. *Chem. Comm.* **1969**, 348–349.

(16)   Kleopfer, R.; Morrison, H. *J. Am. Chem. Soc.* **1972**, *94*, 255–264.

(17)   Otten, J. G.; Yeh, C. S.; Byrn, S.; Morrison, H. *J. Am. Chem. Soc.* **1977**, *99*, 6353–6359.

(18)   Reuther, A.; Nikogosyan, D. N.; Laubereau, A. *J. Phys. Chem.* **1996**, *100*, 5570–5577.

(19)   Browne, D. T.; Eisinge, J.; Leonard, N. J. *J. Am. Chem. Soc.* **1968**, *90*, 7302–7323.

(20) Ito, T.; Shinohara, H.; Hatta, H.; Nishimoto, S. *J. Org. Chem.* **1999**, *64*, 5100–5108. (Chapter 2)

(21) Nishimoto, S.; Ide, H.; Nakamichi, K.; Kagiya, T. *J. Am. Chem. Soc.* **1983**, *105*, 6740–6741.

(22) Taylor, J. -S. *Acc. Chem. Res.* **1994**, *27*, 76–82.

(23) Ito, T,; Shinohara, H.; Hatta, H.; Fujita, S.; Nishimoto, S. *J. Phys. Chem.*, *in press*. (Chapter 5)

(24) von Sonntag, C. *The Chemical Basis of Radiation Biology*; Taylor and Francis: London, 1987.

(25) Ide, H.; Petrullo, L. A.; Hatahet, Z.; Wallace, S. S. *J. Biol. Chem.* **1991**, *266*, 1469–1477.

(26) Leonard, N. J.; Ito, K. *J. Am. Chem. Soc.* **1973**, *95*, 4010–4016.

(27) Wulff, D. L.; Fraenkel, G. *Biochim. Biophys. Acta.* **1961**, *51*, 332–339.

(28) Ka´zmierczak, F.; Langer, J.; Golankiewicz, K. *Roczniki Chem. Ann. Soc. Chim. Pol.* **1972**, *47*, 1943–1948.

(29) Nishimura, T.; Iwai, I. *Chem. Pharm. Bull.* **1964**, *12*, 352–356.

(30) Bates, R. G.; Bower, V. E. *Anal. Chem.* **1956**, *28*, 1322–1324.

(31) Butler, T. C.; Johnson, D.; Dudley, K. H. *J. Heterocycl. Chem.* **1982**, *19*, 657–658.

(32) Ito, S.; Oki, S.; Hayashi, T.; Yamamoto, M. *Thin Solid Films* **1994**, *244*, 1073–1077.

(33) Ballini, J. P.; Daniels, M.; Vigny, P. *J. Lumin.* **1982**, *27*, 389–400.

(34) Ballini, J. P.; Vigny, P.; Daniels, M. *Biophys. Chem.* **1983**, *18*, 61–65.

(35) Helmkamp, G. K.; Kondo, N. S. *Biochim. Biophys. Acta* **1968**, *157*, 242–257.

(36) Itahara, T. *Bull. Chem. Soc. Jpn.* **1997**, *70*, 2239–2247.

(37) Shugar, D.; Szer, W. *J. Mol. Biol.* **1962**, *5*, 580–582.

Chapter 4

Radiation-Induced and Photosensitized Splitting of C5–C5'-Linked Dihydrothymine Dimers: Product and Laser Flash Photolysis Studies on Oxidative Splitting Mechanism

Abstract : Radiation-induced and photosensitized one-electron oxidation of stereoisomeric C5–C5'-linked dihydrothymine dimers (**1a,b**[*meso*]: meso compound of (*5R*, *5'S*)-bi-5,6-dihydrothymine; **1a,b**[*rac*]: racemic compound of (*5R*, *5'R*)- and (*5S*, *5'S*)-bi-5,6-dihydrothymines), which are the major products yielded by radiolytic reduction of 1-methylthymine (**2a**) and 1,3-dimethylthymine (**2b**) in aqueous solution, was studied to compare with the photoreactivating repair mechanism of cyclobutane pyrimidine photodimers. Reacting with sulfate radical anion (SO_4^-), azide radical ($N_3^{\cdot}$), or photoexcited anthraquinone-2-sulfonate (AQS) as oxidants, the C5–C5'-linked dihydrothymine dimers **1a,b** split to regenerate the corresponding thymine monomers **2a,b** along with 5,6-dihydrothymines (**3a,b**) in a pH dependent manner. The transient absorption spectra of 5,6-dihydrothymin-5-yl radicals (**6a,b**) were observed in the nanosecond laser flash photolysis of **1a,b** in phosphate buffer under conditions of SO_4^- generation. Both the product study and the laser flash photolysis study indicated an oxidative splitting mechanism by which one-electron oxidation of the C5–C5'-linked dimers **1a,b** produces the radical cation intermediates (**4a,b**) which undergo facile fragmentation into 5,6-dihydrothymin-5-yl radicals **6a,b** and C5-cations (**5a,b**), followed by deprotonation at C6 of **5a,b** to regenerate the monomers **2a,b**.

Introduction

It has been established that DNA is a vital target of genetoxic agents such as a variety of chemical oxidants, ionizing radiation, UV-light, and certain antibiotics, that cause chemical modification in DNA.[1] For certain structures of the DNA toxic lesions a number of repair enzymes in the cells have been identified and characterized with respect to their structures and biological functions. Most typically, excision-repair enzymes recognize and excise damaged bases or oligo-sequences containing damaged base sites of DNA and then replace them with normal DNA bases by the aid of DNA polymerase.[2] There are also a different class of direct in situ repair-enzymes that regenerate normal bases without excising the damaged bases or the DNA backbone. For example, DNA photolyase (Mr = 55000-65000) absorbs UV-visible light and thereby catalyzes a redox splitting of the cyclobutane pyrimidine photodimers, which are well-known to be highly mutagenic and carcinogenic lesions induced by UV-exposure.[3,4] This enzyme utilizes a deprotonated reduced chromophore (FADH$^-$) of flavin adenine dinucleotide and an antenna chromophore of methenyltetrahydrofolate (MTHF) or 8-hydroxy-5-deazaflavin (8-HDF). Thus, in the binding of DNA photolyase to DNA as a light-independent reaction, the cofactor MTHF or 8-HDF absorbs visible light and transfers energy to form the electronically excited state of FADH$^-$ (FADH^{-*}), which in turn transfers an electron to the cyclobutane pyrimidine photodimer. Concerted splitting at the C5–C5' and C6–C6' bonds of the resulting photodimer radical anion and successive electron transfer back to the flavin reproduce the monomeric pyrimidines.[4a] As demonstrated by photochemical and radiation chemical studies, the splitting reaction of photodimers could also occur by a one-electron oxidation mechanism involving appropriate oxidants such as sulfate radical anion (SO$_4^-$), OH radical (˙OH),[5] and photoexcited anthraquinone-2-sulfonate (AQS*).[6] The oxidative splitting mechanism is thought to be distinct from the one-

electron reduction mechanism,[4,7,8] by which the photodimer radical cation undergoes facile splitting at the C6–C6' bond in the initial step and successively at the C5–C5' bond. Such a mechanistic difference in the splitting of photodimers has been accounted for by recent computational studies based on the semiempirical AM1, and *ab initio* HF and MP2 methods.[9]

In the course of our study on the DNA base damage structures induced by radiolytic reduction, the author has isolated and identified a novel C5–C5'-linked dihydrothymine dimers, the meso compound of (5R, 5'S)-bi-5,6-dihydrothymine (1a,b[*meso*]) and the racemic compound of (5R, 5'R)- and (5S, 5'S)-bi-5,6-dihydrothymines (1a,b[*rac*]).[10,11] Interestingly, the three-dimensional structures of these C5–C5'-linked dimers as characterized by X-ray crystallography are similar to the cyclobutane thymine photodimers possessing both of the C5–C5'- and C6–C6'-bonds. This implied that the C5–C5'-linked dihydrothymine dimers may cause some distortion within a DNA duplex if they were incorporated and could be substrates for DNA photolyase. Chapters 4 and 5 focuse on the splitting of the C5–C5'-linked dihydrothymine dimers into thymine monomers to get structural insight into a redox mechanism, compared with the well-characterized fragmentation reactivity of the C5–C5' and C6–C6' bonds of pyrimidine photodimers. This chapter reports radiation-induced and photosensitized one-electron oxidation of the stereoisomeric C5–C5'-linked dimers of 1-methylthymine (1a[*meso*], 1a[*rac*]) and 1,3-dimethylthymine (1b[*meso*], 1b[*rac*]) by several oxidizing species such as sulfate radical anion SO_4^{-}, azide radical ($N_3^{.}$), and photoexcited anthraquinone-2-sulfonate AQS*. Along with the product study, a laser flash photolysis study was also performed to observe the transient intermediates involved in the oxidative splitting of C5–C5'-linked dihydrothymine dimers under conditions of photochemical SO_4^{-} generation.
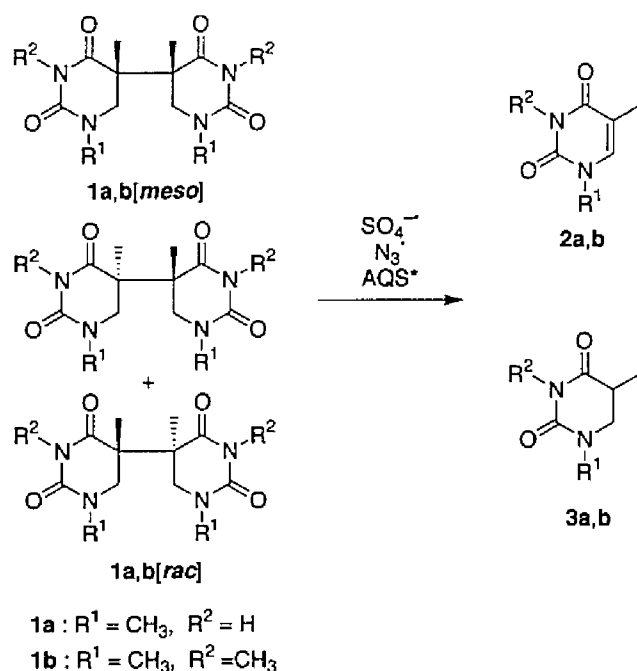
Chart 1. One-electron oxidative splitting of C5–C5'-linked dihydrothymine dimers.

Experimental Section

Materials. 1-Methylthymine (**2a**) (Sigma Chemical) was used as received. Purified 1,3-dimethylthymine (**2b**) was kindly supplied by Fujii Memorial Research Institute, Otsuka pharmaceutical. Anthraquinone-2-sulfonate (AQS), potassium peroxodisulfate ($K_2S_2O_8$), potassium bromide (KBr), sodium azide (NaN_3), and 2-methyl-2-propanol were purchased from Nacalai Tesque and were used without further purification. Reagents for high-performance liquid chromatography (HPLC) including solvents, sodium dihydrogenphosphate (NaH_2PO_4), and methanol (HPLC grade) were used as received from Wako Pure Chemical Industries. C5–C5'-linked dihydrothymine dimers (**1a,b**) of 1-methylthymine and 1,3-dimethylthymine were synthesized and purified by

following the methods reported previously.[10,11]

Radiolytic Oxidation. Aqueous solutions of C5–C5'-linked dihydrothymine dimers (**1a,b**: 0.58 mM) containing [1] 2-methyl-2-propanol (50 mM) and $K_2S_2O_8$ (5.0 mM), [2] KBr (100 mM), or [3] NaN_3 (50 mM) were prepared with water ion-exchanged by Corning Mega-Pure System MP-190 (> 16 MΩ cm). The aqueous solutions were buffered at pH 4, 7, and 10 with phosphate buffer (2 mM) and sodium hydroxide, and then purged with [1] Ar or [2, 3] N_2O before γ-irradiation. Steady-state γ-irradiation was performed in a sealed ampule at room temperature with a ^{60}Co γ-ray source (dose rate: 0.79–0.70 Gy min^{-1}). The γ-irradiated sample solutions, which were stable at room temperature in the dark, were subjected to HPLC analysis as described below.

Photosensitized Oxidation. Typically, solutions of **1a,b** (1 mM) in phosphate buffer (5.0 mM) containing AQS (0.4 mM) were adjusted to pH 4, 7, and 10, and then purged with Ar before photoirradiation. The solutions in sealed Pyrex glass tubes (λ_{ex} > 280 nm) were photoirradiated under magnetic stirring (1000 rpm) at 24 °C with a high-pressure Hg arc (450 W, Eiko-sha 400).

HPLC Analysis. HPLC analyses were performed with Shimadzu 3A and 10A HPLC systems equipped with Rheodyne 7725 sample injector. Aliquots (10 μL) of irradiated sample solutions were injected onto a 5 μm C18 reversed-phase column (Wakosil 5C18, ϕ 4.6 mm × 150 mm, Wako). The phosphate buffer solutions (10 mM, pH 3.0) containing various concentrations of methanol (15–25 vol %) were delivered as the mobile phase. The column eluents were monitored by the UV absorbance at 210 nm.
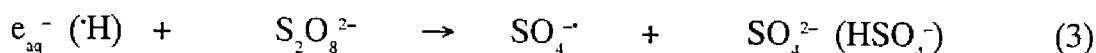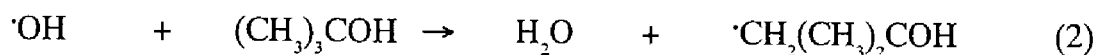
Nanosecond Laser Flash Photolysis. The laser flash photolysis experiments were carried out with a Unisoku TSP-601 flash spectrometer. A Continuum Surelite-I Nd:YAG (Q-switched) laser with the fourth harmonic at 266 nm (ca. 50 mJ per 6 ns pulse) was employed for the flash photoirradiation. The probe beam from a Hamamatsu 150-W xenon short arc (CA 263) was guided with an optical fiber scope to be arranged in an orientation perpendicular to the exciting laser beam. The probe beam was monitored with a Hamamatsu R2949 photomultiplier tube through a

Hamamatsu S3701-512Q MOS linear image sensor (512 photodiodes). Timing of the exciting pulsed laser, the probe beam, and the detection system was achieved through a Tektronix model TDS 320 double channel oscilloscope that was interfaced to an NEC PC-9801 computer. Solutions of 1a[*meso*] and 1a[*rac*] (1.0 mM) at pH 4, 7, and 10 in phosphate buffer (5.0 mM) containing $K_2S_2O_8$ (50 mM) were deaerated by Ar bubbling prior to the laser flash photolysis experiments.

Results and Discussion

Splitting of C5–C5'-Linked Dihydrothymine Dimers by Oxidizing Radicals Generated in the Radiolysis.

The oxidizing sulfate radical anion ($SO_4^{-\cdot}$), as generated from the reaction of peroxodisulfate ion ($S_2O_8^{2-}$) with hydrated electron (e_{aq}^-) in the aqueous radiolysis system, has been conveniently utilized for investigating the one-electron oxidation reactivity of pyrimidines and purines.[12] This radiation chemical method was employed in the present study to get mechanistic insight into one-electron oxidative splitting of C5–C5'-linked dihydrothymine dimers (1a,b[*meso*] and 1a,b[*rac*]). Thus, Ar-saturated solutions of 1a,b[*meso*] and 1a,b[*rac*] (0.5 mM) in phosphate buffer containing 2-methyl-2-propanol (50 mM) and $K_2S_2O_8$ (5.0 mM) were γ-irradiated up to 800 Gy. In the radiolysis of aqueous solution, strongly oxidizing hydroxyl radicals ($\cdot$OH) and reducing species of e_{aq}^- are generated along with smaller amount of reducing hydrogen atoms ($\cdot$H) (reaction 1). The G-values[13] of such primary water radicals are known as $G(e_{aq}^-)$ = $G(\cdot OH)$ = 2.8 × 10^{-7} mol J^{-1} and $G(\cdot H)$ = 0.6 × 10^{-7} mol J^{-1} in neutral aqueous solution. Under the present conditions, OH radicals are scavenged by 2-methyl-2-propanol into substantially unreactive 2-methyl-2-propanol radicals ($\cdot CH_2(CH_3)_2COH$) as in reaction 2 ($k(\cdot OH + (CH_3)_3COH)$ = 6 × 10^8 dm^3 mol^{-1} s^{-1}).[1a,14] On the other hand, hydrated electrons e_{aq}^- are scavenged by $S_2O_8^{2-}$ to produce oxidant SO_4 radical anions ($E^o(S_2O_8^{2-} / SO_4^{2-}$ = 2.4 V vs. NHE)[15] as in reaction 3 ($k(e_{aq}^-$

$$H_2O \quad \rightarrow \quad \cdot OH \quad + \quad \cdot H \quad + \quad e_{aq}^- \qquad (1)$$

$$\cdot OH \quad + \quad (CH_3)_3COH \quad \rightarrow \quad H_2O \quad + \quad \cdot CH_2(CH_3)_2COH \qquad (2)$$

$$e_{aq}^- \ (\cdot H) \quad + \quad S_2O_8^{2-} \quad \rightarrow \quad SO_4^{-} \quad + \quad SO_4^{2-} \ (HSO_4^-) \qquad (3)$$

As analyzed by HPLC, **1a,b**[*meso*] and **1a,b**[*rac*] were oxidized by the radiation chemically generated SO_4 radical anions and their C5–C5' bonds split to produce the corresponding thymine monomers (**2a,b**) and 5,6-dihydrothymine derivatives (**3a,b**) (Chart 1), which were accompanied by isomerization from meso-dimers **1a,b**[*meso*] to racemic-dimers **1a,b**[*rac*] or *vice versa*. Figure 1 shows radiation dose responses of the dimer decomposition and the product formation in phosphate buffer at pH 7, the initial slopes of which gave the respective G-values as listed in Table 1. The fairly high yields of **2a,b** are in accord with a prediction that the C5–C5'-linked dimers **1a,b**, as afforded by one-electron reductive dimerization of thymine monomers **2a,b**,[11] may undergo the reverse splitting by a one-electron oxidation mechanism.

Table 1 indicates that the G-value of dimer decomposition ($G(-1)$) exceeds that of SO_4 radical anion ($G(SO_4^-) < 3.2 \times 10^{-7}$ mol J^{-1} depending on pH) to some extent. This suggests that some radical intermediates involved in the oxidation of **1a,b** by SO_4 radical anions are able to decompose **1a,b**. In view of the previous result that the β-oxoalkyl compounds such as 6-hydroxy-5,6-dihydrothymin-5-yl radicals possess oxidizing properties,[17] one-electron oxidation by such oxidizing 5-yl radicals may account for the excess G-values of dimer decomposition. Indeed the oxidative splitting of **1a,b** at the C5–C5' bond may generate 5,6-dihydrothymin-5-yl radicals (**6a,b**), as supported by the occurrence of isomerization (see Scheme 1).

The SO_4^--induced splitting of **1a,b** to produce **2a,b** and **3a,b** were dependent on pH of the aqueous solution. A trend is seen in Table 1 that the restoration of **1a,b**
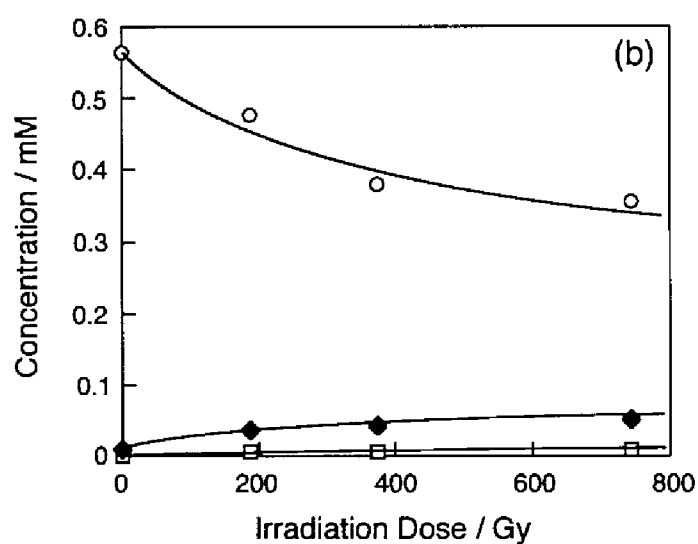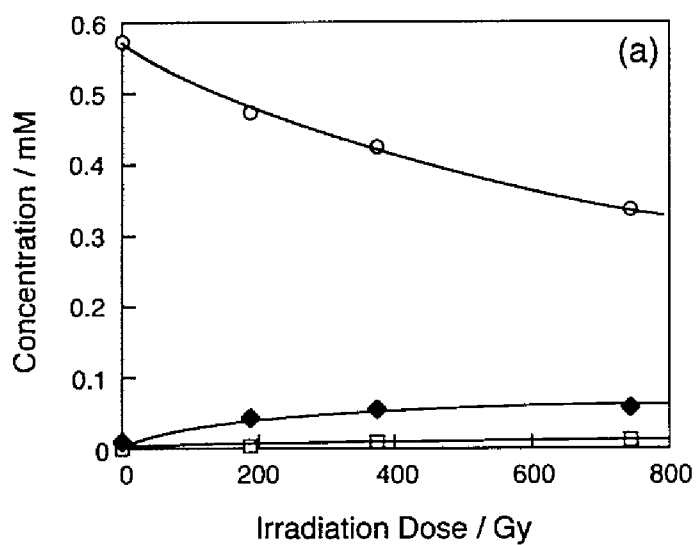
Figure 1. Oxidative splitting of (a) **1a**[*meso*] and (b) **1a**[*rac*] (0.58 mM) in the γ-radiolysis of Ar-purged phosphate buffer solution containing $K_2S_2O_8$ (5.0 mM) and 2-methyl-2-propanol (50 mM): (O) decomposition of **1a**[*meso*] or **1a**[*rac*]; (♦) formation of **2a**; (□) isomerization of **1a**.

to **2a,b** becomes more efficient upon increasing the pH value: the yields of **2a,b** in basic solution at pH 10 are about 1.5-times greater than those in acidic solution at pH 4. On the other hand, there was substantially no influence of stereoisomerism on the splitting reactivity at each pH. Table 1 also suggests that 1,3-dimethyl-5,6-dihydrothymine dimers **1b**[*meso*] and **1b**[*rac*] are oxidized by SO_4 radical anions somewhat more readily than 1-methyl-5,6-dihydrothymine dimers **1a**[*meso*] and **1a**[*rac*]. It is likely that the inductive electron-donating 3-methyl group may facilitate one-electron oxidation of **1b** relative to **1a**. As a different aspect in this context, a methyl substitution results in a more negative reduction potential of 5,6-dihydropyrimidines.[18]

Less oxidizing Br_2 radical anions (Br_2^-; E^0 (Br_2^- / 2Br$^-$) = 1.7 V vs. NHE)[15] were also generated by γ-radiolysis of N_2O-saturated phosphate buffer solution containing excess amount of KBr (100 mM) to examine the oxidative splitting reactivity of the C5–C5'-linked dihydrothymine dimers. Under the present conditions of radiolysis, more than 98% of hydrated electrons are converted into OH radicals by N_2O (reaction 4; $k(e_{aq}^- + N_2O)$ = 9.1 × 10^9 dm^3 mol^{-1} s^{-1}).[14] The OH radicals are in turn scavenged by Br$^-$ ions to produce oxidizing Br_2 radical anions (reactions 5 and 6).[1]

$$e_{aq}^- \ + \ N_2O \ \rightarrow \ N_2 \ + \ \cdot OH \ + \ OH^- \quad (4)$$

$$Br^- \ + \ \cdot OH \ \rightarrow \ Br\cdot \ + \ OH^- \quad (5)$$

$$Br\cdot \ + \ Br^- \ \rightarrow \ Br_2^- \quad (6)$$

In contrast to the reactivity toward SO_4 radical anions, neither **1a**[*meso*] nor **1a**[*rac*] (0.5 mM) was decomposed by Br_2 radical anions thus generated in phosphate buffer at pH 7. Such an ineffective oxidizing reactivity of Br_2 radical anions has been observed for the reactions with cyclobutane pyrimidine photodimers.[5] Even for electron-rich thymine bearing a C5–C6 double bond, Br_2 radical anions showed practically negligible reactivity ($k(Br_2^- + \text{thymine}) < 10^7$ dm^3 mol^{-1} s^{-1}).[19]

Table 1. Oxidative Splitting of 1a,b (0.58 mM) in Phosphate Buffer Solutions by Radiation Chemically Generated Oxidizing Radicals $SO_4^{-\cdot}$ or $N_3^{\cdot}$

Substrate	pH	G-value × 10⁷ / mol J⁻¹			
		−1	2	3	isomerization
Sulfate radical anion (SO₄⁻)					
1a[*meso*]	4	4.1	2.1 (49%)ᵃ	2.6 (62%)	0.08 (2%)
	7	3.6	2.3 (43%)	1.6 (42%)	0.31 (9%)
	10	3.7	2.8 (74%)	0.75 (20%)	0.31 (8%)
1a[*rac*]	4	3.2	1.6 (48%)	0.83 (26%)	0.21 (6%)
	7	3.3	2.2 (68%)	0.77 (23%)	0.34 (10%)
	10	2.9	2.3 (77%)	0.99 (34%)	0.23 (8%)
1b[*meso*]	4	5.2	3.0 (58%)	0.52 (10%)	0.33 (6%)
	7	4.3	3.3 (78%)	0.57 (13%)	0.50 (12%)
	10	4.0	3.4 (85%)	0.55 (14%)	0.38 (10%)
1b[*rac*]	4	4.4	2.8 (65%)	0.66 (15%)	0.27 (6%)
	7	3.6	3.1 (86%)	0.65 (18%)	0.31 (9%)
	10	3.4	3.2 (92%)	0.65 (19%)	1.3 (40%)
Azide radical (N₃·)					
1a[*meso*]	4	0.23	0.18 (77%)	0.10 (45%)	-
	7	0.16	0.17(107%)	0.11 (73%)	-
	10	0.33	0.37(113%)	0.15 (44%)	-

ᵃSelectivity based on G-values for the decomposition of 1a,b.

Using azide ions (N$_3^-$; 50 mM NaN$_3$) instead of Br$^-$ ions in N$_2$O-saturated phosphate buffer, oxidizing azide radicals (N$_3^\cdot$) were also generated as in reaction 7 (k = 1.2 × 10^{10} dm^3 mol^{-1} s^{-1}, E^0 (N$_3^\cdot$/ N$_3^-$) = 1.3 V vs. NHE).[14,15]

$$\text{N}_3^- \quad + \quad \cdot\text{OH} \quad \rightarrow \quad \text{N}_3^\cdot \quad + \quad \text{OH}^- \tag{7}$$
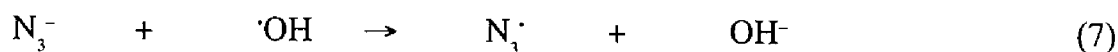
Table 1 shows the results of N$_3^\cdot$-induced oxidation of **1a[meso]** (0.5 mM) in phosphate buffer solutions at pH 4, 7, and 10. The dimer **1a[meso]** split into the monomer **2a** in high yield at each pH, despite the reduction potential of the azide radical being more negative by about 0.25 V than that of Br$_2$ radical anion. While the G-value of the N$_3^\cdot$-induced splitting of **1a[meso]** was reduced to approximately 10% the level of the SO$_4^-$-induced splitting, selectivity of the restoration to **2a** was significantly enhanced (Table 1). A similar difference in oxidizing reactivity between azide radicals and Br$_2$ radical anions was also observed for the reactions with other nucleic acids. It has been thus suggested that azide radicals react by an outer-sphere electron transfer mechanism depending on the reduction potential of a given nucleic acid, whereas Br$_2$ radical anions react by an inner-sphere electron transfer mechanism.[20] Therefore, the splitting of C5–C5'-linked dihydrothymine dimers[1a,b] into **2a,b** by SO$_4$ radical anion or azide radical proceeds via one-electron oxidation (path 1 in Scheme 1) most possibly by an outer-sphere electron transfer mechanism.

Previously, strongly oxidizing OH radicals with a high reduction potential (E^0(·OH/ OH$^-$) = 2.7 V vs. NHE)[15] were shown to restore cyclobutane thymine photodimer to thymine with G-values of 2.0 to 3.1.[5,21] This reaction might proceed by C6- or C6'-hydrogen abstraction rather than direct electron transfer, on analogy of similar ·OH-induced restoration of 5,6-dihydrothymine to thymine involving a hydrogen-abstraction mechanism as in reactions 8–10.[21] For comparison, we further studied the reactivity of **1a,b** toward radiation chemically generated OH radicals.

$$TH_2 \quad + \quad \cdot OH \quad \rightarrow \quad TH\cdot \quad + \quad H_2O \tag{8}$$

$$TH\cdot \quad + \quad \cdot OH \quad \rightarrow \quad TH^+ \quad + \quad OH^- \tag{9}$$

$$TH^+ \quad + \quad OH^- \quad \rightarrow \quad T \quad + \quad H_2O \tag{10}$$

Upon γ-radiolysis (600 Gy) of N_2O-saturated solution in phosphate buffer, **1a,b** (0.5 mM) could not be restored to **2a,b** in contrast to cyclobutane thymine photodimer. This result clearly rules out a hypothetical one-electron oxidation of the C5–C5'-linked dihydrothymine dimers **1a,b** by OH radicals to form the dimer radical cations **4a,b**. Although C5–C5'-linked dihydrothymine dimer 6-yl radicals (**7a,b**) are most likely intermediates derived from C6-hydrogen abstraction by OH radicals (path 6 in Scheme 1), fragmentation of **7a,b** to yield thymines **2a,b** and 5,6-dihydrothymin-5-yl radicals **6a,b** (path 5) should not occur in the OH radical reaction. Concerning a mechanism of the oxidative splitting of **1a,b**, on the other hand, such a reactivity of **7a,b** implies that the dimer radical cations **4a,b** as the probable intermediates could not yield thymines **2a,b**, if deprotonation at the C6 of **4a,b** was predominant (path 4). Thus, it is plausible that the dimer radical cations **4a,b** is liable to undergo C5–C5'-bond splitting into the corresponding 5-yl radical **6a,b** and C5-cation (**5a,b**) (path 2).

Splitting of C5–C5'-Linked Dihydrothymine Dimers by Photoexcited Oxidizing Sensitizer. As demonstrated previously by means of CIDNP,[6] oxidative splitting of cyclobutane pyrimidine photodimers (Pyr<>Pyr) into pyrimidine monomers (Pyr) was effectively induced upon photoexcitation of oxidizing sensitizers such as anthraquinone-2-sulfonate AQS which possesses a reduction potential of –0.39 V vs. NHE.[15] The observation of a substrate and product photo-CIDNP signals led to a one-electron oxidation mechanism of the photodimer splitting by which electron transfer from photodimer Pyr<>Pyr to the excited triplet state of AQS (^{3}AQS*) occurs to produce the photodimer radical cation (Pyr<>Pyr$^{\cdot\cdot}$) and ASQ radical anion (AQS$^-$). The radical cation Pyr<>Pyr$^{\cdot\cdot}$ thus photogenerated may undergo splitting into

pyrimidine and its radical cation, the latter of which is one-electron reduced to pyrimidine by the radical anion AQS⁻.

In this light, the author also examined similar AQS-sensitized photooxidation reactivity of the C5–C5'-linked dihydrothymine dimers 1a,b. Upon photoexcitation of AQS (0.4 mM) in deoxygenated phosphate buffer (5.0 mM, pH 4, 7 and 10) containing 1a,b (1.0 mM), efficient splitting of 1a,b into 2a,b and 3a,b was observed in a similar manner as in the one-electron oxidative splitting by SO_4 radical anions or azide radicals. This photooxidative splitting of 1a,b is likely to proceed via electron transfer from 1a,b to the ³AQS*, as in the case of cyclobutane pyrimidine photodimers, since it was suppressed by the addition of diacetyl (4.0 mM), a typical triplet quencher (E_T = 236 kJ mol⁻¹).[22] In contrast to the splitting by oxidizing radicals in the radiolysis systems, the photosensitized splitting by AQS involved no isomerization of the dimers 1a,b. This suggests that one-electron reduction of the 5-yl radical intermediates 6a,b by the radical anion AQS⁻ may occur more efficiently than radical coupling and disproportionation (paths 7 and 8 in Scheme 1), followed by protonation to yield 3a,b. Therefore, in the AQS-sensitized photoreaction system, the electron transfer from ³AQS* and the back electron transfer from AQS⁻ would lead to a net splitting of the C5–C5'-linked dihydrothymine dimers 1a,b into the corresponding thymines 2a,b and 5,6-dihydrothymines 3a,b in a 1:1 ratio.

Figure 2 shows the time course of the AQS-sensitized photooxidative splitting of 1a,b in phosphate buffer at pH 7. It is evident that 2a,b and 3a,b were produced in almost equivalent yields in the initial stage of photoirradiation, while the yield of 2a,b became considerably higher than that of 3a,b during the prolonged photoirradiation. This behavior suggests concurrent oxidation of 3a,b to produce 2a,b as a secondary reaction in the AQS-sensitized photooxidation system. In a separate experiment, it was confirmed that photoexcitation of AQS (0.2 mM) induced oxidation of 3a (1.0 mM) to yield 2a almost quantitatively in Ar-purged phosphate buffer at pH 7 (Figure 3). Therefore, direct one-electron oxidation of dihydrothymines 3a,b by ³AQS*
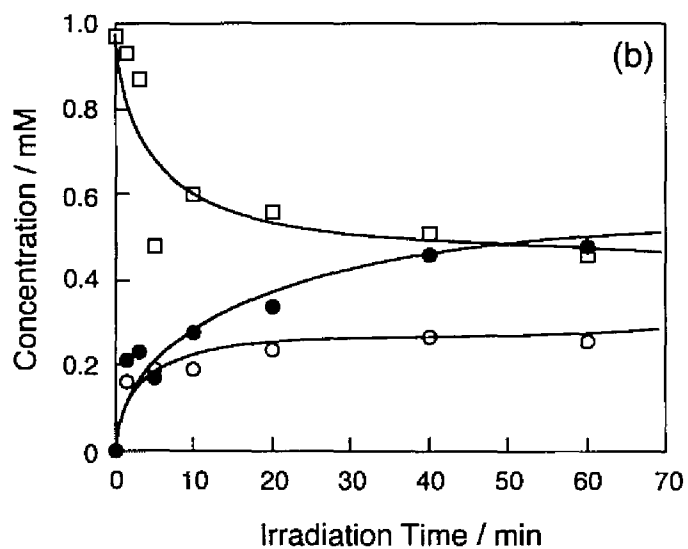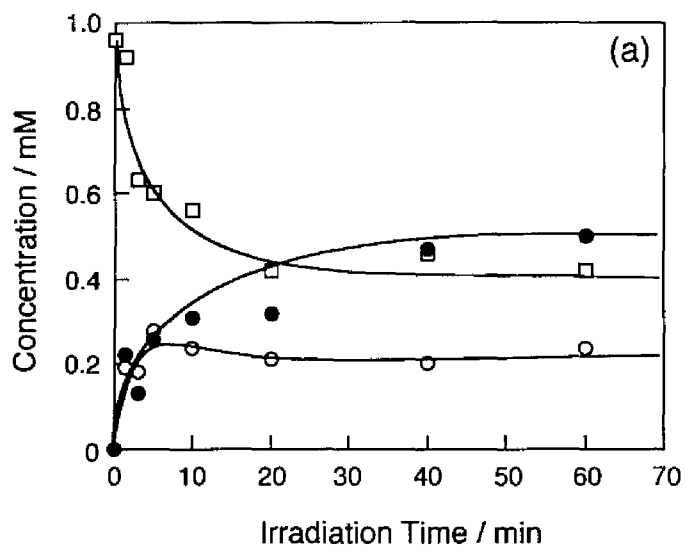
Figure 2. Oxidative splitting of (a) **1a**[*meso*] and (b) **1a**[*rac*] (1.0 mM) in Ar-purged phosphate buffer upon photoexcitation (λ_{ex} > 280 nm) of AQS (0.4 mM): (□) decomposition of **1a**[*meso*]; formation of (●) **2a** and (○) **3a**.
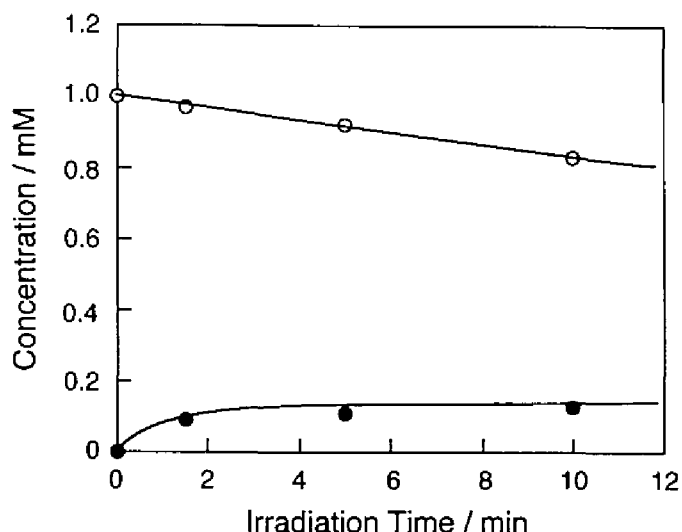
Figure 3. Oxidation of **3a** (1.0 mM) in Ar-purged phosphate buffer upon photoexcitation (λ_{ex} > 280 nm) of AQS (0.2 mM): (O) decomposition of **3a**; (●) formation of **2a**.

accounts for the secondary conversion to the corresponding monomers **2a,b**. According to a semiquinone-semiquinolate equilibrium with pKa = 8.2 (reaction 11) as characterized by the previous flash photolysis study,[23] on the other hand, the semiquinone radicals (AQSH·) are derived from protonation of the semiquinolate ions AQS⁻ at an almost diffusion-controlled rate under neutral conditions.

$$AQS^- \quad + \quad H^+ \quad \rightarrow \quad AQSH· \qquad\qquad (11)$$

An alternative reaction pathway is also possible where the primary photoproduct **3a,b** may undergo hydrogen abstraction by the semiquinone radicals AQSH· to yield **2a,b**. Similar hydrogen abstraction is also involved in the ·OH-induced restoration of **3a,b** to **2a,b** (reactions 8–10).[21]

Table 2 shows the influence of pH on the photosensitized splitting of **1a,b** into

109

Table 2. Oxidative Splitting of **1a,b** (1.0 mM) in Ar-Purged Phosphate Buffer upon Photoexcitation ($\lambda_{ex} > 280$ nm) of AQS (0.4 mM) for 8 min with a High Pressure Hg-Lamp

Substrate	pH	Conversion of	Yield / %	
		1a,b / %	**2a,b**	**3a,b**
1a[*meso*]	4	17	65	42
	7	16	63	44
	10	27	48	52
1a[*rac*]	4	17	47	35
	7	17	53	41
	10	24	58	71
1b[*meso*]	4	20	75	65
	7	18	106	106
	10	15	73	100
1b[*rac*]	4	29	55	34
	7	30	60	67
	10	30	43	60

2a,b and 3a,b as observed in the initial stage of photoirradiation for 8 min. Although the pH dependence was not clear, the decomposition of 1a,b seemed to become more facilitated with increasing pH of aqueous solution, as expected from the semiquinone-semiquinolate equilibrium, as in reaction 11. As observed in the $SO_4{}^-$- and $N_3{}^-$-induced splittings, a trend was also seen in the AQS-sensitized photoreaction that 1b[*meso*] and 1b[*rac*] favor a one-electron oxidative splitting more than 1a[*meso*] and 1a[*rac*] (Tables 1 and 2).

Laser Flash Photolysis. Laser flash photolyses at 355 nm of aqueous solutions of C5–C5'-linked dihydrothymine dimers 1a,b (1.0 mM) and AQS (50 μM) as an oxidizing sensitizer were first attempted to detect transient absorptions originating from oxidative splitting of 1a,b, but were unsuccessful because of overlapping with intense absorption due to AQS⁻ in the wavelength region of 300 to 530 nm $(\varepsilon(AQS^-)_{500} = 6.8 \times 10^3 \text{ dm}^3 \text{ mol}^{-1} \text{ cm}^{-1}; \varepsilon(AQS^-)_{385} = 5.37 \times 10^3 \text{ dm}^3 \text{ mol}^{-1} \text{ cm}^{-1}).$[24] In light of the $SO_4{}^-$-induced oxidation in the radiolysis experiment as above, oxidizing SO_4 radical anions were generated to react with 1a,b by the laser flash photolysis of $S_2O_8{}^{2-}$ in aqueous solution as in reaction 12.[25]

$$S_2O_8{}^{2-} \quad + \quad h\nu \quad \rightarrow \quad SO_4{}^- \qquad (12)$$
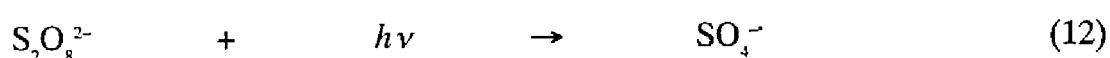
In a control experiment, upon laser flash excitation at 266 nm of peroxodisulfate ion $S_2O_8{}^{2-}$ (50 mM) in deoxygenated aqueous solution, a broad transient absorption band assigned to the SO_4 radical anion at wavelengths of 300 to 550 nm (λ_{max} = 460 nm) was observed as reported previously.[25] Similar 266 nm laser flash photolyses of Ar-purged acidic solution (pH 3.3) of 1a[*meso*] (1.0 mM) in the presence of $K_2S_2O_8$ (50 mM) resulted in the transient absorption spectra as shown in Figure 4. Substantially the same behavior was observed for a solution of 1a[*rac*] (1.0 mM) under similar conditions. The spectrum recorded within 1 μs after the laser flash
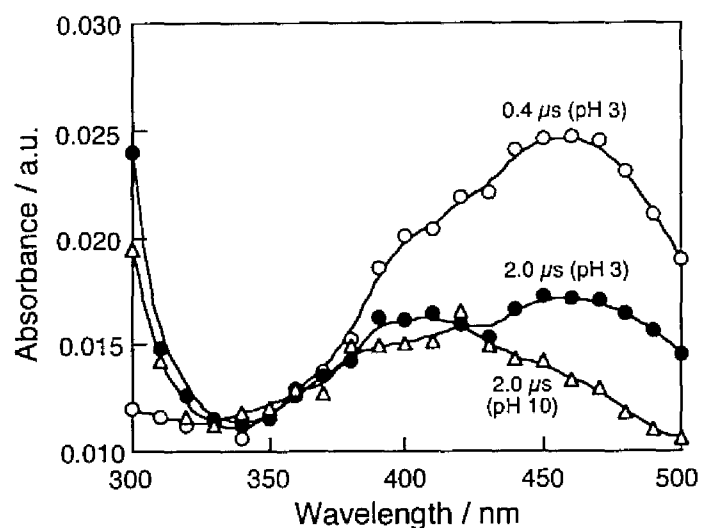
Figure 4. Transient absorption spectra of the intermediates as observed 0.4 and 2.0 μs after the 266-nm laser photolysis of $S_2O_8^{2-}$ (50 mM) in phosphate buffer solution containing (●) 1a[*meso*] and (▲) 1a[*rac*] (1.0 mM) at pH 3.3, and (○) 1a[*meso*] at pH 10.2.

contained an absorption maximum at $\lambda_{max} = 460$ nm ($\varepsilon(SO_4^-)_{455} = 4.6 \times 10^2$ dm^3 mol^{-1} cm^{-1}) characteristic of SO_4 radical anions.[25] The SO_4 radical anions decayed rapidly and thereafter a common absorption maximum at $\lambda_{max} = 400$ nm emerged from both aqueous solutions of 1a[*meso*] and 1a[*rac*], as was evidently observed 2 μs after the laser flash. This transient may be assigned to 1-methyl-5,6-dihydrothymin-5-yl radical **6a** by reference to the previous pulse radiolysis study, in which 5,6-dihydrothymin-5-yl radicals as generated by one-electron reductions of 5-bromo-5,6-dihydrothymine and 5-bromo-5,6-dihydrouracil derivatives by hydrated electrons e_{aq}^- in aqueous solution showed broad absorptions at around 400 nm ($\lambda_{max} = 380$ nm, $\varepsilon_{380} = 1150$ dm^3 mol^{-1} cm^{-1}).[26] When the laser flash photolysis was performed in a basic solution of 1a[*meso*] (1.0 mM) and $K_2S_2O_8$ (50 mM) at pH 10.2, the SO_4 radical anions decayed much more rapidly due to a reaction with OH$^-$ to generate OH radicals ($k = 6.5 \times 10^7$ dm^3 mol^{-1} s^{-1}, reaction 13),[27] which occurs in competition with the one-

electron oxidation of **1a[*meso*]**.

$$SO_4^- + OH^- \rightarrow SO_4^{2-} + \cdot OH \qquad (13)$$

In the present experiments, the dimer radical cations **4a** with a characteristic absorption at wavelengths shorter than 350 nm could not be identified. It follows that the dimer radical cations **4a** would be liable to split into C5-cations **5a** and radicals **6a** on the nanosecond time scale.

Parts a and b of Figures 5 compares the decays of absorbancies due to 1-methyl-5,6-dihydrothymin-5-yl radical **6a** and SO_4^- at 400 and 500 nm, respectively. In the initial stage up to 20 μs after the laser flash, the transient absorbance at 400 nm is likely to involve the overlapped absorption tail of SO_4^-. The contribution of SO_4 radical anions to the absorbance at 400 nm was therefore estimated from the corresponding decay behavior at 500 nm, taking into account the relative molar extinction coefficients ($\varepsilon_{400}(SO_4^-)$ / $\varepsilon_{500}(SO_4^-)$ = 1.1). Thus, the buildup of 1-methyl-5,6-dihydrothymin-5-yl radicals **6a** (λ_{max} = 400 nm) could be obtained by subtracting the contribution of SO_4 radical anions from the apparent absorbance at 400 nm as shown in Figure 5c. The decay of **6a** was of the second-order kinetics (see Figure 6), indicating the occurrence of disproportionation (formation of **2a** and **3a**) and/or recombination (isomerization) as in reaction 14.

$$TH\cdot + TH\cdot \rightarrow TH_2 + T \quad or \quad TH-TH \qquad (14)$$

The second-order rate constants were approximately evaluated as $2k$ = 2.7 × 10⁹ dm³mol⁻¹ s⁻¹ in the splitting of **1a[*meso*]** and 2.2 × 10⁹ dm³ mol⁻¹ s⁻¹ in the splitting of **1a[*rac*]** from the slopes of the reciprocal of absorbance at 400 nm vs. time plots (Figure 6), assuming that the molar extinction coefficient of **6a** is equal to the reported value of the 5,6-dihydrothymin-5-yl radical at 380 nm (ε_{380} = 1150 dm³ mol⁻¹ cm⁻¹).[26]
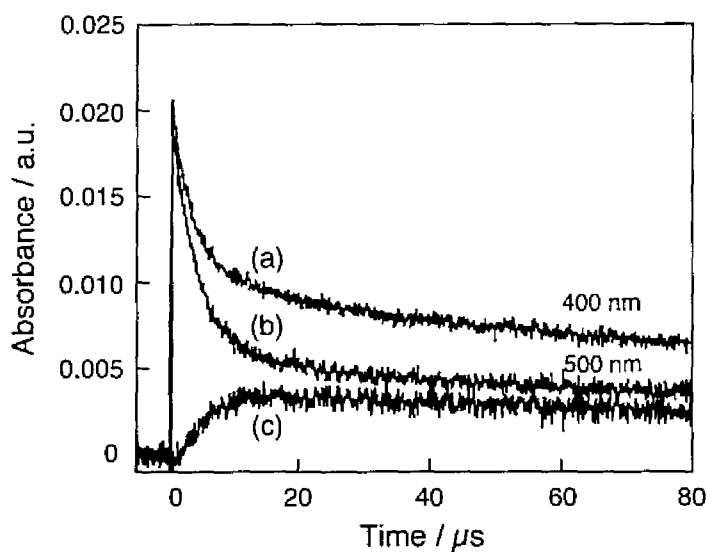
113

Figure 5. Time-courses of the absorbancies at (a) 400 nm and (b) 500 nm in the 266-nm laser photolysis of $S_2O_8^{2-}$ (50 mM) in phosphate buffer solution containing **1a**[*meso*] (1.0 mM). (c) Buildup of the absorbance at 400 nm derived from the decay profile at 400 nm by subtracting a decay component following the kinetics as in the absorbance at 500 nm. Inset shows a plot of 1/OD vs. time for the buildup component at 400 nm.
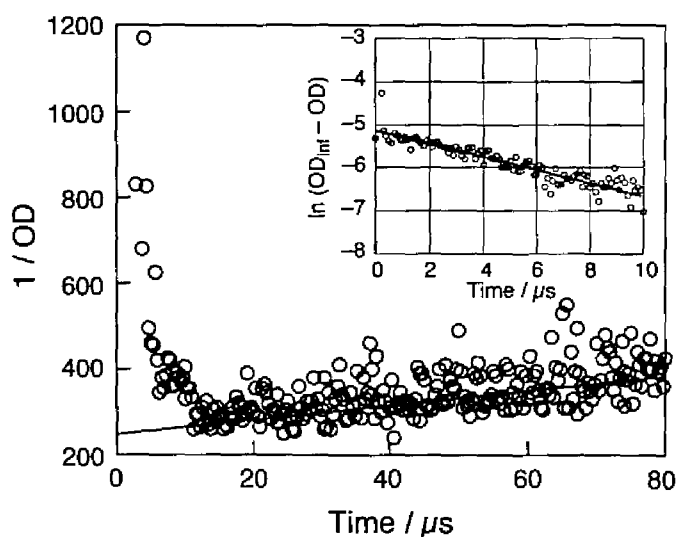

Figure 6. Pseudo-first order kinetics for the buildup component with absorbance at 400 nm in the 266-nm laser photolysis of $S_2O_8^{2-}$ (50 mM) in phosphate buffer solution containing **1a**[*meso*] (1.0 mM). The OD_{inf} corresponds to a plateau value of the absorbance at 400 nm due to the buildup component.

114

The rate constants thus evaluated are in good agreement with the literature value ($2k$ = 2.35 $\times$ 10^9 dm^3 mol^{-1} s^{-1} at pH 6.8) for the 5,6-dihydrothymin-5-yl radical as derived from the pulse radiolysis study on the reaction of 5,6-dihydrothymine with OH radicals.[28]

The SO$_4$ radical anions decayed following the pseudo-first-order kinetics in the presence of 1a[*meso*] or 1a[*rac*], while being of the second-order kinetics in the control photolysis of peroxodisulfate ion S$_2$O$_8^{2-}$ alone. The pseudo-first order decays gave the corresponding rate constants for the oxidation of dimers by the SO$_4$ radical anion as k = 2.4 $\times$ 10^8 dm^3 mol^{-1} s^{-1} (1a[*meso*] = 1.0 mM) and k = 1.5 $\times$ 10^8 dm^3 mol^{-1} s^{-1} (1a[*rac*] = 1.0 mM). In accord with the decay behavior of SO$_4$ radical anions, the buildup of 5-yl radicals 6a to attain its plateau level was represented in terms of a pseudo-first order kinetics (the inset in Figure 6), leading to similar rate constants of k = 1.8 $\times$ 10^8 dm^3 mol^{-1} s^{-1} (1a[*meso*]) and k = 1.0 $\times$ 10^8 dm^3 mol^{-1} s^{-1} (1a[*rac*]). On the other hand, the SO$_4^-$-induced oxidation of 5,6-dihydrothymine (DHT) at varying concentrations of 0.5 to 5.0 mM was determined to show a rate constant of k (DHT + SO$_4^-$) = 8.5 $\times$ 10^7 dm^3 mol^{-1} s^{-1}. These values were at least one-order of magnitude smaller than those of 5,6-unsaturated pyrimidines such as 1-methylthymine (k (2a + SO$_4^-$) = 5.0 $\times$ 10^9 dm^3 mol^{-1} s^{-1}) and 1,3-dimethylthymine (k (2b + SO$_4^-$) = 4.6 $\times$ 10^9 dm^3 mol^{-1} s^{-1}).[29] This is probably attributable to the lower nucleophilicity of 5,6-dihydrothymine compounds including 1a[*meso*] and 1a[*rac*] toward SO$_4$ radical anions.

Oxidative Splitting Mechanism of the C5–C5'-Linked Dihydrothymine Dimers. Scheme 1 illustrates a proposal for a mechanism by which the C5–C5'-linked dihydrothymine dimers 1a,b undergo splitting into thymines 2a,b and 5,6-dihydrothymines 3a,b by oxidizing radicals such as SO$_4^-$ and N$_3^{\cdot}$, but not Br$_2^-$, and by photoexcited oxidizing sensitizers such as [3]AQS*. The failure of the oxidant Br$_2^-$ in reacting toward 1a,b is not surprising in view of the fact that Br$_2^-$ is also unreactive

toward the cyclobutane thymine dimers.[5] The laser flash photolysis study has provided a spectroscopic evidence in support of 5,6-dihydrothymin-5-yl radical intermediates 6a,b involved in the SO_4^--induced oxidative splitting of 1a,b. The C5–C5'-linked dihydrothymine dimer radical cations 4a,b would be the most likely precursor leading to the observed 5-yl radicals 6a,b, although spectroscopic detection of the transients 4a,b was unsuccessful in the laser flash photolysis experiments. A similar mechanistic aspect has been proposed for the oxidative splitting of cyclobutane pyrimidine photodimers in that the radical cations are generated by electron transfer from the photodimers to a photoexcited oxidizing sensitizer.[4a]

Concerning the fate of dihydrothymine dimer radical cations 4a,b, two possible routes to thymines 2a,b and 5,6-dihydrothymin-5-yl radicals 6a,b, involving C5–C5'-bond splitting followed by deprotonation (paths 2 and 3) or vice versa (paths 4 and 5), can be assumed as shown in Scheme 1. The latter route is, however, ruled out from the experimental evidence that OH radicals could not produce 2a,b. Thus, the C5–C5'-linked dihydrothymin dimer 6-yl radicals 7a,b, that are potentially derived from C6-deprotonation of 4a,b (path 4) or C6-hydrogen abstraction from 1a,b by OH radicals (path 6), are unlikely to undergo the C5–C5'-bond splitting into 2a,b and 6a,b (path 5). Alternatively, 4a,b may favor the C5–C5'-bond splitting into the 5-yl radicals 6a,b and C5'-cations 5a,b (path 2). In view of the oxidizing property of 5,6-dihydropyrimidin-5-yl radicals,[17] the C5-cations 5a,b must be so unstable as to be deprotonated at C6 into thymines 2a,b. In relation to the C5–C5'-bond splitting reactivity of 4a,b, it is interesting to note that the cyclobutane photodimer radical cation undergoes a stepwise fragmentation involving sequential cleavage of the C6–C6' and the C5–C5' bonds, as supported by the successful trapping of a single-bond-cleaved intermediate in a model reaction system.[30] Such a preferential C6–C6'-bond splitting of the photodimer radical cations resulting in intramolecular formation of a pair of a dimer C6 radical and a C6' cation seems to be rationalized by the reducing property of 5,6-dihydrothymin-6-yl radicals.[1a] Accordingly, a pair of radical
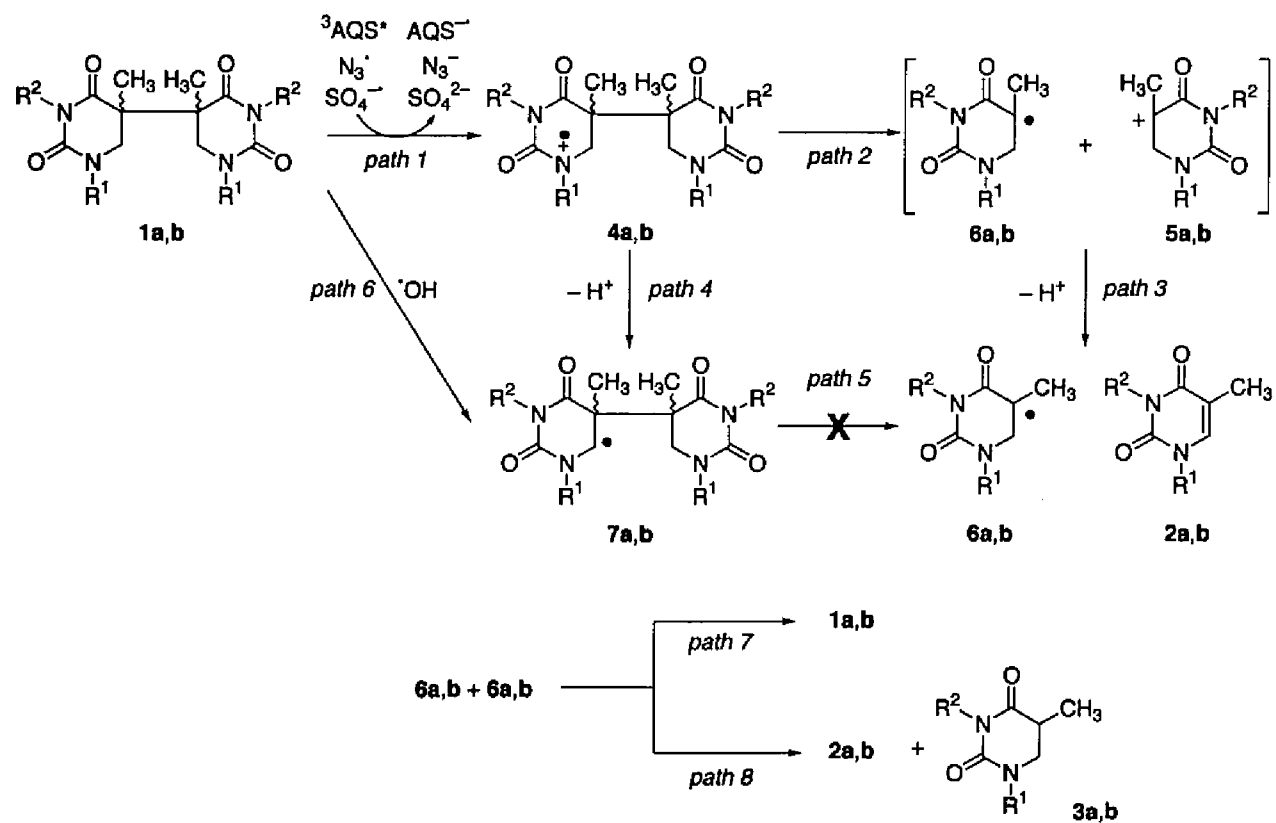
Scheme 1. Oxidative splitting mechanism of the C5–C5'-linked dihydrothymine dimers.

and carbocation pair formed by the C6–C6'-bond splitting of the photodimer radical cation would be energetically more stable than that by the C5–C5'-bond splitting of 4a,b.

The C5–C5'-linked dimers 1a[*meso*] and 1a[*rac*] are of the N3-protonated forms in the pH range of 4 to 10, since their pKa values in aqueous solution are 11.7, as measured by the UV-absorption spectral changes (data not shown). The pH dependence of the $SO_4^{\cdot-}$- and $N_3^{\cdot}$-induced splitting of 1a,b that the restoration to 2a,b becomes more efficient with increasing the pH value (Table 1) can be explained by the more facilitated C6-deprotonation of 5a,b (path 3). On the other hand, base-enhanced C6-deprotonation of 4a,b to form 7a,b is unlikely, because it will reduce the restoration efficiency if occurred.

In accord with the decay of the second-order kinetics as shown in Figure 5, two types of bimolecular reactions of 5,6-dihydrothymin-5-yl radicals 6a,b may proceed competitively in the reaction system. Recombination and disproportionation of 6a,b accounts for the apparent isomerization of the dimers 1a,b (path 7) and formation of 2a,b and 3a,b (path 8), respectively. As a concomitant minor reaction, oxidizing radical 6a,b could one-electron oxidize the C5–C5'-linked dimers 1a,b, thereby resulting in the enhanced G-value for the decomposition of 1a,b (see Table 1; $G(-1a,b) > G(SO_4^-) = 3.3 \times 10^{-7}$ mol J^{-1}).[17]

Conclusion

It was demonstrated that oxidative splitting of the C5–C5'-linked dihydrothymine dimers 1a,b by oxidizing radicals (SO_4^- and $N_3^{\cdot}$) generated in the radiolysis and by photoexcited oxidizing sensitizer (^{3}AQS*) affords thymine monomers 2a,b along with byproducts of 5,6-dihydrothymines 3a,b. As characterized by the laser flash photolysis, 5,6-dihydrothymin-5-yl radicals 6a,b are intermediates

involved in the oxidative splitting. A mechanism involving generation of the C5–C5'-linked dihydrothymine dimer radical cations **4a,b** by electron transfer from **1a,b** to an oxidant has been proposed, by reference to a similar oxidative splitting mechanism of cyclobutane pyrimidine photodimers. While the pyrimidine photodimer radical cation prefers the C6–C6'-bond splitting to the counterpart C5–C5'-bond splitting, the C5–C5'-linked dihydrothymine dimer radical cations **4a,b** may undergo the C5–C5'-bond splitting into the 5,6-dihydrothymin-5-yl radicals **6a,b** and the C5-cations **5a,b**. Because of the oxidizing property, the intermediate radicals **6a,b** can also be a one-electron oxidants toward **1a,b**.

References and Notes

(1)   (a) von Sonntag, C. In *The Chemical Basis of Radiation Biology*; Taylor and Francis: London, 1987. (b) Fuciarelli, A. F.; Zimbrick J. D. In *Radiation Damage in DNA: Structure / Function Relationship at Early Times*; Battelle Press: Columbus, 1995. (c) Bensasson, R. V.; Land, E. J.; Truscott, T. G. In *Excited States and Free Radicals in Biology and Medicine*; Oxford University Press: Oxford, 1993.

(2)   (a) Friedberg, E. C.; Walker, G. C.; Siede, W. In *DNA Repair and Mutagenesis*; ASM Press: Washington, D.C., 1995. (b) David, S. S.; Williams, S. D. *Chem. Rev.* **1998**, *98*, 1221–1261. (c) Wallace, S. S. *Radiat. Res.* **1998**, *150*, Suppl., S60–S79.

(3)   (a) Cadet, J.; Vigny, P. In *Bioorganic Photochemistry: Photochemistry and the Nucleic Acids*; Morrison, H., Ed.; John Wiley & Sons: New York, 1990; pp 1–272. (b) Taylor, J. -S. *Acc. Chem. Res.* **1994**, *27*, 76–82. (c) Görner, H. *J. Photochem. Photobiol. B: Biol.* **1994**, *26*, 117–139. (d) Pfeifer, G. P. *Photochem. Photobiol.* **1997**, *65*, 270–283.

(4)   (a) Begley, T. P. *Acc. Chem. Res.* **1994**, *27*, 394–401. (b) Kim, S. -T.; Sancar, A. *Photochem. Photobiol.* **1993**, *57*, 895–904. (c) Carell, T.; Epple, R. *Eur. J. Org. Chem.* **1998**, 1245–1258.

(5)   Heelis, P. F.; Deeble, D. J.; Kim, S. -T.; Sancar, A. *Int. J. Radiat. Biol.* **1992**, *62*, 137–143.

(6)   (a) Young, T.; Nieman, R.; Rose, S. D. *Photochem. Photobiol.* **1990**, *52*, 661–668. (b) Pouwels, P. J. W.; Hartman, R. F.; Rose, S. D.; Kaptein, R. *Photochem. Photobiol.* **1995**, *61*, 563–574.

(7)   Pouwels, P. J. W.; Hartman, R. F.; Rose, S. D.; Kaptein, R. *Photochem. Photobiol.* **1995**, *61*, 575–583.

(8)   Heelis, P. F.; Hartman, R. F.; Rose, S. D. *J. Photochem. Photobiol. A: Chem.* **1996**, *95*, 89–98.

(9)   (a) Voityuk, A. A.; Michel-Beyerle, M. -E.; Rösch, N. *J. Am. Chem. Soc.* **1996**, *118*, 9750–9758. (b) Voityuk, A. A.; Rösch, N. *J. Phys. Chem. A* **1997**, *101*, 8335–8338.

(10)   Nishimoto, S.; Ide, H.; Nakamichi, K.; Kagiya, T. *J. Am. Chem. Soc.* **1983**, *105*, 6740–6741.

(11)   Ito, T.; Shinohara, H.; Hatta, H.; Nishimoto, S. *J. Org. Chem.* **1999**, *64*, 5100–5108. (Chapter 2)

(12)   (a) Angelov, D.; Berger, M.; Cadet, J.; Getoff, N.; Keskinova, E.; Solar, S. *Radiat. Phys. Chem.* **1991**, *37*, 717–727. (b) Bansal, K. M.; Fessenden, R. W. *Radiat. Res.* **1978**, *75*, 497–507.

(13)   The number of molecules produced or changed per 1 J of radiation energy absorbed by the reaction system.

(14)   Buxton, G. V.; Greenstock, C. L.; Helman, W. P.; Ross, A. B. *J. Phys. Chem. Ref. Data* **1988**, *17*, 513–886.

(15)   Wardman, P. *J. Phys. Chem. Ref. Data* **1989**, *18*, 1637–1755.

(16)   Direct reaction of e_{aq}^- with the substrate was negligible at 5 mM of $K_2S_2O_8$ employed in the present γ-radiolysis study, as confirmed by a separate comparative experiment: the yields of the radiolysis products were virtually invariant, when γ-irradiated in the presence of 10-fold and 40-fold excess amounts (5 and 20 mM) of $K_2S_2O_8$ (see also ref. 29).

(17)   (a) Steenken, S.; Neta, P. *J. Phys. Chem.* **1979**, *83*, 1134–1137. (b) Fujita, S.; Steenken, S. *J. Am. Chem. Soc.* **1981**, *103*, 2540–2545.

(18)   (a) Yeh, S. -R.; Falvey, D. E. *J. Am. Chem. Soc.* **1992**, *114*, 7313–7314. (b) Scannell, M. P.; Prakash, G.; Falvey, D. E. *J. Phys. Chem. A* **1997**, *101*, 4332–4337. (c) Scannell, M. P.; Fenick, D. J.; Yeh, S. -R.; Falvey, D. E. *J. Am. Chem. Soc.* **1997**, *119*, 1971–1977.

(19)   Neta, P.; Huie, R.; Ross, A. B. *J. Phys. Chem. Ref. Data* **1988**, *17*, 1027–1284.

(20)   (a) Steenken, S. In *Topics in Current Chemistry*; Mattay, J., Ed.; Springer-

Verlag: Berlin, 1996; Vol. 177, pp 125-145. (b) Faraggi, M.; Broitman, F.; Trent, J. B.; Klapper, M. H. *J. Phys. Chem.* **1996**, *100*, 14751–14761. (c) Jovanovic, S. V.; Simic, M. G. *J. Phys. Chem.* **1986**, *90*, 974–978.

(21)   Grossweiner, L. I.; Kepka, A. G.; Santus, R.; Vigil, J. A. *Int. J. Radiat. Biol.* **1974**, *25*, 521–523.

(22)   Murov, S. L.; Carmichael, I.; Hug, G. L. *Handbook of Photochemistry*, *2nd ed., Revised and Expanded*; Marcel Dekker: New York, 1993.

(23)   Roy, A.; Aditya, S. *J. Photochem.* **1983**, *22*, 361–367.

(24)   Phillips, G. O.; Worthington, N. W.; McKellar, J. F.; Sharpe, R. R. *J. Chem. Soc. A* **1969**, 767–773.

(25)   (a) Dogliotti, L.; Hayon, E. *J. Phys. Chem.* **1967**, *71*, 2511–2516. (b) Neda, O.; Yamauchi, K.; Masuda, T. *Bull. Chem. Soc. Jpn.* **1985**, *58*, 227–229.

(26)   Deeble, D. J.; Das, S.; von Sonntag, C. *J. Phys. Chem.* **1985**, *89*, 5784–5788.

(27)   Hayon, E.; Treinin, A.; Wilf, J. *J. Am. Chem. Soc.* **1972**, *94*, 47–57.

(28)   Myers, L. S., Jr.; Theard, L. M. *J. Am. Chem. Soc.* **1970**, *92*, 2868–2870.

(29)   Deeble, D. J.; Schuchmann, M. N.; Steenken, S.; von Sonntag, C. *J. Phys. Chem.* **1990**, *94*, 8186–8192.

(30)   Burdi, D.; Begley, T. P. *J. Am. Chem. Soc.* **1991**, *113*, 7768–7770.

Chapter 5

Radiation-Induced and Photosensitized Splitting of C5–C5'-Linked Dihydrothymine Dimers: Conformational Effects on the Reductive Splitting Mechanism

Abstract: Radiation-induced and photosensitized reductive splitting of stereoisomeric C5–C5'-linked dihydrothymine dimers (**1a,b**[*meso*], meso compound of (*5R*, *5'S*)- and (*5S*, *5'R*)-bi-5,6-dihydrothymines; **1a,b**[*rac*], racemic compound of (*5R*, *5'R*)- and (*5S*, *5'S*)-bi-5,6-dihydrothymines) in aqueous solution were studied to compare with the one-electron oxidative splitting mechanism and the photorepair reaction of cyclobutane pyrimidine photodimers. Reacting with radiation-chemically and photochemically generated hydrated electrons or with photoexcited reduced form of flavin adenine dinucleotide (*FADH$^-$), the C5–C5'-linked dihydrothymine dimers **1a,b** produced the corresponding 5,6-dihydrothymine derivatives (**3a,b**) along with the thymine monomers (**2a,b**) in minor yields. Both the product and laser flash photolysis studies indicated that one-electron adducts of the C5–C5'-linked dimers **1a,b** undergo C5–C5'-bond cleavage to generate the 5,6-dihydrothymin-5-yl radicals (**5a,b**) and the 5,6-dihydrothymine C5-anions (**6a,b**) resulting in the formation of **3a,b** by facile protonation at C5. In the reduction by *FADH$^-$, splitting of the 5,6-dihydro-1-methylthymine dimer **1a**[*meso*] into the monomer **2a** was more efficient than that of the racemic isomer **1a**[*rac*]. Conformational analysis by NMR of **1a**[*meso*] and **1a**[*rac*] in solution suggested that **1a**[*meso*] may favor a "closed-shell" conformation and undergo one-electron reduction to form **5a** and **6a**, whereas **1a**[*rac*] may be in a "opened-shell" conformation and undergo successive two-electron reduction by

*FADH⁻ to produce two equivalents of **6a** as a precursor of **3a**.

Introduction

Ionizing radiation and ultraviolet (UV) light are the etiological agents of gene carcinogenesis and mutagenesis that give rise to a variety of DNA-base modifications.[1,2] Pyrimidine cyclobutane photodimers are among the most representative DNA-base lesions, being produced as a consequence of [2 + 2] photocycloaddition at a tandem pyrimidine moiety in the DNA duplex upon exposure to UV light.[2] The base residues thus modified are subjected to an intracellular repair process of photoreactivation by a photoenzyme, DNA photolyase, consisting of a deprotonated reduced flavin adenine dinucleotide (FADH⁻) and an antenna chromophore of methenyltetrahydrofolate (MTHF) or 8-hydroxy-5-deazaflavin (8-HDF). While both radical cation and radical anion of the photodimer undergo facile fragmentation into monomers as confirmed by the model photochemical electron-transfer reactions, the enzymatic photoreactivation may favor a reductive fragmentation.[3] Thus, a likely mechanism of the photoreactivation has been drawn from extensive biochemical and photochemical studies:[3] the antenna chromophore of the photolyase complexed to the photodimer in DNA absorbs light in the 300–500-nm range and transfer the excitation energy to the reduced flavin FADH⁻ moiety, thereby splitting of cyclobutane photodimer being induced via one-electron transfer from the excited state of FADH⁻. Concerted C5–C5' and C6–C6' bond splitting of the resulting cyclobutane photodimer radical anions, followed by electron transfer back to the flavin, reproduces the monomeric pyrimidines. Previous laser flash photolysis and photo-induced CIDNP spectroscopic studies have detected the radical anion intermediates in the reductive splitting reaction, indicating that the splitting of the photodimer radical anion involves a concerted but nonsynchoronous fragmentation of

124

C5–C5' and C6–C6' bonds with a rate constant of the order $1 \times 10^6 \text{ s}^{-1}$.[4,5]

An alternative [2 + 2] photocycloaddition between adjacent pyrimidines is simultaneously induced by UV exposure to result in a similar mutagenic photo-lesion of pyrimidine(6–4)pyrimidone [(6–4)photoadduct]. A photoenzyme (6–4)photolyase that shows a specific repairing ability towards the (6–4)photoadduct has also been identified.[6] As characterized more recently by a sequence analysis of the genes, the (6–4)photolyase has a high degree of structural identity to the DNA photolyase.[6c] These results strongly suggest a similarity of the repair mechanism between the (6–4)photolyase and DNA photolyase, involving a common electron-transfer process from the excited state of the enzyme to the UV-damaged DNA bases.[6c]

As demonstrated in Chapter 2, it was identified that formation of stereoisomeric C5–C5'-linked dihydrothymine dimers, as fractionated into the meso forms of (5R, 5'S)- and (5S, 5'R)-bi-5,6-dihydrothymines (1a,b[meso]) and racemic compounds of (5R, 5'R)- and (5S, 5'S)-bi-5,6-dihydrothymines (1a,b[rac]), in the radiolytic one-electron reduction of thymine derivatives [1-methylthymine (2a) and 1,3-dimethylthymine (2b)] in anoxic aqueous solution.[7] The X-ray crystallography demonstrated that the C5–C5'-linked dihydrothymine dimers are structurally similar to the cyclobutane thymine photodimers. Especially, as in the cis-syn-cyclobutane thymine photodimers, the meso-dimer structure like 1a[meso] seemed to cause insufficient stacking of the pyrimidine rings that will weaken the hydrogen bonds between the dimer and the complementary adenine when formed by chance in a DNA duplex. A remarkable observation with respect to the reactivity was that the C5–C5'-linked dihydrothymine dimers 1a,b undergo oxidative splitting to regenerate the corresponding thymine monomers 2a,b via one-electron transfer from the dimer to radiation chemically or photochemically generated oxidants.[8] Formally this oxidative splitting of 1a,b is a reverse reaction of the reductive dihydrodimerization of 2a,b.

In view of the fact that the splitting of cyclobutane photodimers into monomers occurs in principle by both oxidative and reductive pathways, further attempt has been

made to characterize reductive splitting reactivity of the C5–C5'-linked dihydrothymine dimers **1a,b** under conditions of generating hydrated electrons (e_{aq}^-) or photoexcited state of dihydroflavin FADH⁻. Laser flash photolysis study using *N,N*-dimethylaniline as a reducing photosensitizer has also been conducted to identify the mechanism and evaluate the kinetic parameters involved in the reductive splitting of **1a,b**.
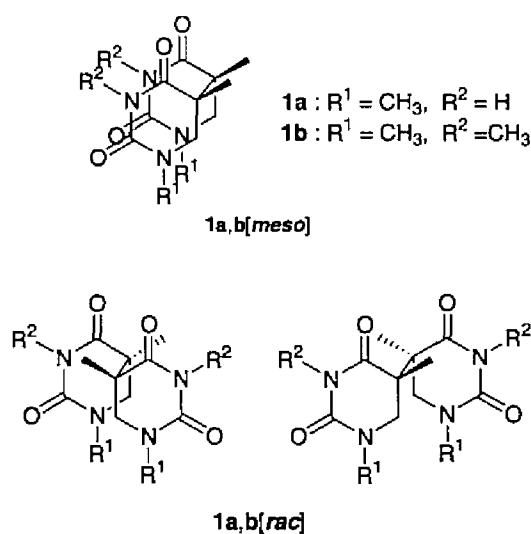

1a : R¹ = CH₃, R² = H
1b : R¹ = CH₃, R² =CH₃

1a,b[*meso*]

1a,b[*rac*]

Chart 1. Structures of the C5–C5'-linked dihydrothymine dimers.

Experimental Section

Materials. 1-Methylthymine (**2a**) and flavin adenine dinucleotide (FAD) disodium salt were used as received from Sigma Chemical. Purified 1,3-dimethylthymine (**2b**) was kindly supplied by Fujii Memorial Research Institute, Ohtsuka pharmaceutical.

126

Ethylenediaminetetraacetic acid (EDTA), N,N-dimethylaniline (DMA), and 2-methyl-2-propanol were purchased from Nacalai Tesque and used without further purification. N,N,N',N'-Tetramethyl-p-phenylenediamine (TMPD), 2'-deoxythymidine, and reagents for high-performance liquid chromatography (HPLC) including solvents, sodium dihydrogenphosphate (NaH_2PO_4) and methanol (HPLC grade) were used as received from Wako Pure Chemical Industries. For fluorescence quenching experiments, tris(2,2'-bipyridyl)ruthenium(II) chloride hexahydrate ($Ru(bpy)_3Cl_2 \cdot 6H_2O$; Aldrich Chemical), dimethylbenzoquinone (Aldrich Chemical), terephthalaldehyde (Kanto Chemical), 1-methylnicotinamide chloride (Tokyo Chemical Industries), 5-nitrouracil (Tokyo Chemical Industries), methylviologene (Nacalai Tesque), anthraquinone-2-sulfonate (Nacalai Tesque), and p-benzoquinone (Nacalai Tesque) were used as obtained commercially. C5–C5'-linked dihydrothymine dimers **1a,b** of 1-methylthymine **2a** and 1,3-dimethylthymine **2b** were synthesized and purified following the methods reported previously.[7] Aqueous solutions for all experiments were prepared using water purified with Corning Mega-Pure System MP-190 (> 16 MΩ cm).

HPLC Analysis. Analytical HPLC was performed with Shimadzu 6A HPLC system equipped with Rheodyne 7725 sample injector. Sample solutions were injected onto a 5 μm C18 reversed-phase column (Wakosil 5C18, ϕ 4.6 mm × 150 mm, Wako). The phosphate buffer solutions (10 mM, pH 3.0) containing various concentrations of methanol (10–25 vol %) were delivered as the mobile phase. The column eluents were monitored by the UV absorbance at 210 nm.

Radiolytic Reduction. Aqueous solutions of C5–C5'-linked dihydrothymine dimers **1a,b** (0.5 mM) containing 2-methyl-2-propanol (50 mM) were buffered at pH 7.0 with phosphate buffer, and then purged with Ar before γ-irradiation. Steady-state γ-irradiation was performed in sealed ampules at room temperature with a ⁶⁰Co γ-ray source (dose rate: 0.75 Gy min⁻¹).

Photosensitized Reduction. Typically, solutions of **1a,b** (0.5 mM) in phosphate

127

buffer containing FAD (0.2 mM) were purged with Ar before photoirradiation. For effective generation of the reduced form of FAD (FADH⁻) in situ, EDTA (20 mM) was added to the solutions. The solutions in sealed Pyrex glass tubes were photoirradiated (λ_{ex} > 280 nm) under magnetic stirring (1000 rpm) at 24 °C with a high-pressure Hg arc (450 W, Eiko-sha 400).
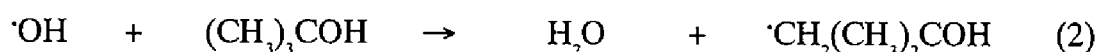
Nanosecond Laser Flash Photolysis. The laser flash photolysis experiments were carried out with a Unisoku TSP-601 flash spectrometer, as described in Chapter 4.[8] Aqueous solutions of **1a,b**[*meso*] and **1a,b**[*rac*] (1.0 mM) at pH 6.7 containing DMA (0.16–0.50 mM) were deaerated by Ar bubbling prior to the laser flash photolysis experiments.

Fluorescence Quenching. Various kinds of quenchers (0.1–4.0 mM) at varying concentrations were dissolved in phosphate buffer (10 mM, pH 7.0) solutions of Ru(bpy)$_3^{2+}$ (10 μM). Each sample solution (2 mL) was purged with Ar for 10 min, sealed in a quartz cell (10 × 10 × 35 mm) with a Teflon cap, and then subjected to the measurement of the fluorescence spectrum which was recorded on a Hitachi F-2000 fluorescence spectrophotometer (slit width: 1.0 nm, λ_{ex} = 450 nm, λ_F = 600 nm).
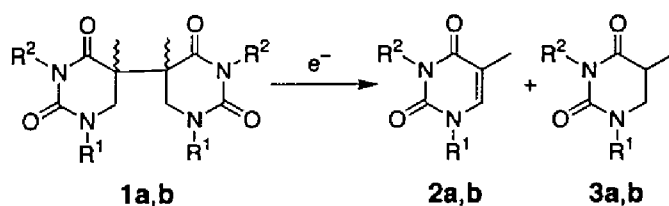
Results

Splitting of C5–C5'-Linked Dihydrothymine Dimers by Hydrated Electrons Generated in the Radiolysis. γ-Radiolyses of deoxygenated solutions of 1-methyl-5,6-dihydrothymine dimers (**1a**[*meso*] and **1a**[*rac*]; 0.5 mM) and 1,3-dimethyl-5,6-dihydrothymine dimers (**1b**[*meso*] and **1b**[*rac*]; 0.5 mM) in phosphate buffer containing 2-methyl-2-propanol (50 mM) were carried out to characterize the reductive splitting reactivity of the C5–C5'-linked dihydrothymine dimers. In the radiolysis of a diluted aqueous solution, water radicals such as oxidizing hydroxyl radicals (·OH), reducing hydrated electrons and reducing hydrogen atoms (·H) are

primarily generated with the G values[9] of $G(\cdot OH) = 2.8 \times 10^{-7}$ mol J^{-1}, $G(e_{aq}^-) = 2.8 \times 10^{-7}$ mol J^{-1}, and $G(\cdot H) = 0.6 \times 10^{-7}$ mol J^{-1} (reaction 1). Under the present conditions, the OH radicals are scavenged by excess amount of 2-methyl-2-propanol into substantially unreactive 2-hydroxy-2-methylpropyl radicals $(\cdot CH_2(CH_3)_2COH)$ as in reaction 2. Consequently, the hydrated electrons e_{aq}^-, $(E(nH_2O/e_{aq}^-)= -2.9$ V vs NHE[10] at pH 7.0) along with smaller amount of the hydrogen atoms $(E(H^+/\cdot H)= -2.4$ V vs NHE[10] at pH 7.0) are involved as the reductants in the reactions of **1a,b**.

$$H_2O \rightarrow \cdot OH, \quad \cdot H, \quad e_{aq}^- \qquad (1)$$

$$\cdot OH + (CH_3)_3COH \rightarrow H_2O + \cdot CH_2(CH_3)_2COH \qquad (2)$$

Analytical HPLC of the γ-irradiated solutions by reference to authentic samples demonstrated that the C5-C5'-linkages of stereoisomeric dimers, **1a,b**[*meso*] and **1a,b** [*rac*], split via one-electron reduction by hydrated electrons to produce the corresponding 5,6-dihydrothymine derivatives (**3a,b**) as the major products along with relatively smaller amounts of thymine monomers **2a,b** (Scheme 1). The one-electron reductive splitting of **1a,b** to **2a,b** and **3a,b** was accompanied to a lesser extent by isomerization from meso dimers **1a,b**[*meso*] to racemic dimers **1a,b**[*rac*] or vice versa. Apart from the distribution of product yields (see Table 1), the apparent reaction characteristics of one-electron reductive splitting are essentially the same as
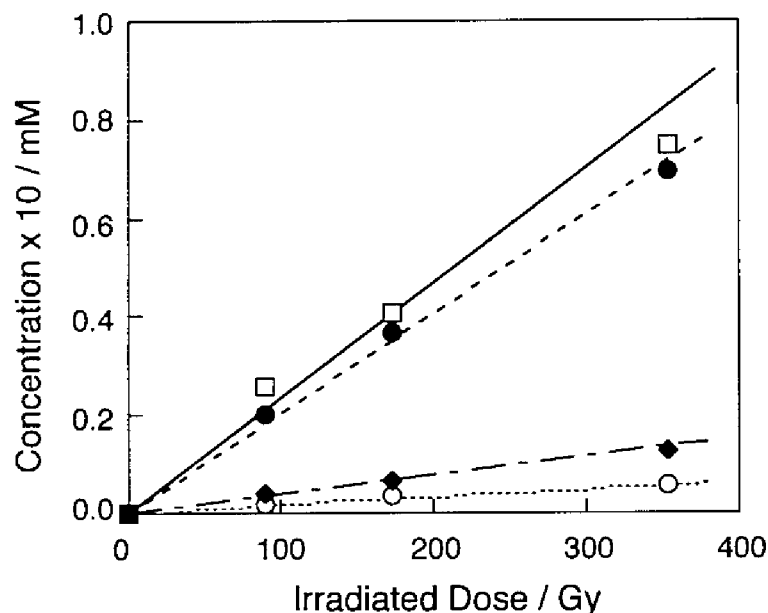

1a,b   **2a,b**   **3a,b**

Scheme 1

Concentration x 10 / mM

1.0

0.8

0.6

0.4

0.2

0.0

0   100   200   300   400

Irradiated Dose / Gy

Figure 1. Reductive splitting of **1a**[*rac*] (0.5 mM) in the *γ*-radiolysis of deoxygenated phosphate buffer containing 2-methyl-2-propanol (50 mM): (□) decomposition of **1a**[*rac*]; formation of (◆) 1-methylthymine **2a**, (●) 5,6-dihydro-1-methylthymine **3a**, and (○) isomeric dimers **1a**[*meso*].

in the one-electron oxidative splitting as described in Chapter 4. Figure 1 shows linear dose-responses of the dimer decomposition and the product formation in the radiolytic reduction, the slopes of which gave the respective G values as listed in Table 1. Comparing with the G value of hydrated electrons $(G(e_{aq}^{-}) = 2.8 \times 10^{-7}$ mol $J^{-1})$ as the substantial species for one-electron reduction, it is apparent that the stereoisomeric 5,6-dihydro-1,3-dimethylthymine dimers **1b** underwent reductive decomposition almost quantitatively $(G(-\mathbf{1b}) = 2.7\sim2.8 \times 10^{-7}$ mol $J^{-1})$, while the stereoisomeric 5,6-dihydro-1-methylthymine dimers **1a** showed somewhat smaller reactivity towards hydrated electrons $(G(-\mathbf{1a}) = 2.2\sim2.3 \times 10^{-7}$ mol $J^{-1})$. In these radiolytic reductions, the major products of 5,6-dihydrothymines **3a,b** and thymines **2a,b** accounted for about 50 % and 15 % of the decomposed dimers, respectively. The

130

Table 1. Reductive Splitting of **1a,b** (0.5 mM) in Deoxygenated Aqueous Solution by Radiation-Chemically Generated Hydrated Electrons

Substrate	G values $\times 10^7$ / mol J^{-1}			
	−1	2	3	isomerization
1a[*meso*]	2.2	0.59 (13 %)[a]	2.1 (48 %)	0.25 (11 %)
1a[*rac*]	2.3	0.36 (8 %)	2.0 (43 %)	0.32 (14 %)
1b[*meso*]	2.7	0.80 (15%)	2.8 (52 %)	0.17 (6 %)
1b[*rac*]	2.9	0.96 (17 %)	2.9 (50 %)	0.31 (11 %)

[a] Selectivities based on G values for decomposition of **1a,b**.

Table 2. Reductive Splitting of **1a,b** (0.5 mM) by Photoexcited Reduced Form of FAD (*FADH⁻) in Phosphate Buffer

Substrate	Additive	Conversion / %	Yield / %		Ratio / %
		−1	2	3	2 / 3
1a[*meso*]	FAD	4	17	34	50
	FAD/EDTA	30	1	79	1
1a[*rac*]	FAD	5	5	72	7
	FAD/EDTA	26	1	75	1
1b[*meso*]	FAD	11	7	97	7
	FAD/EDTA	42	2	86	2
1b[*rac*]	FAD	11	8	93	9
	FAD/EDTA	28	2	91	2

minor isomerization occurred in 6~14 % yields, which is comparable to the isomerization in the previously reported one-electron oxidative splitting.[8]

The above results are rationalized by a mechanism involving the primary intermediates of electron-dimer adducts (**4a,b**) that undergo splitting at the C5–C5' linkages into 5,6-dihydrothymin-5-yl radicals (**5a,b**) and C5-anions (**6a,b**), as outlined in Scheme 2. The formation of the 5-yl radicals **5a,b** is common to both the one-electron reductive and oxidative splittings, while the counterparts in the latter splitting are C5-cations (**7a,b**).[8] It has been established that β-oxoalkyl radicals possess oxidizing property for several aromatic amines; e.g., 6-hydroxy-5,6-dihydrothymin-5-yl radical oxidizes TMPD $[E^0(\text{TMPD}^{+}/\text{TMPD}) = 0.16$ V vs. NHE][11] readily to form 6-hydroxy-5,6-dihydrothymine C5-anion and TMPD radical cation (TMPD^{+}).[12] In accord with such an oxidizing property, the 5,6-dihydrothymin-5-yl radicals **5a,b** could one-electron oxidize 5,6-dihydrothymine dimers **1a,b** to regenerate **5a,b** along with the formation of C5-cations **7a,b** that produce thymines **2a,b** via protonation, as reported recently.[8] Separate experiments with deoxygenated solution of **1a**[*meso*] containing TMPD (0.6 mM) gave only **3a** as a major product, suggesting that the intermediate 5-yl radical is one-electron reduced almost quantitatively by TMPD into C5-anion which undergoes protonation at C5 to form [3a]. Consequently, the restoration of **2a** and the isomerization may be suppressed in the presence of TMPD.
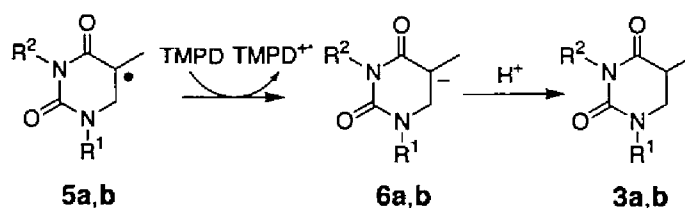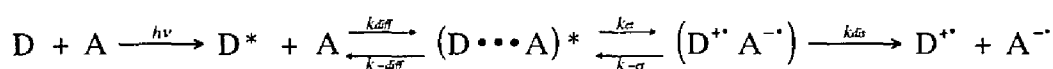

Scheme 2

Splitting of C5–C5'-Linked Dihydrothymine Dimers by Photoexcited Reducing Sensitizer. It has been suggested that in the DNA photorepair process the cyclobutane photodimer flips out of the DNA helix to fit into the "hole" domain of photolyase,[3c-i] and the fully reduced form of FAD cofactor (FADH⁻) can catalyze the splitting reaction. In view of the photorepair reaction, FADH⁻-sensitized photoreductive splitting reaction of the C5–C5'-linked dihydrothymine dimers **1a,b** was performed as a related model reaction. Upon photoexcitation of FAD (0.2 mM) in deoxygenated phosphate buffer containing **1a,b** (0.5 mM) in the presence of EDTA (20 mM), splitting of **1a,b** occurred to afford 5,6-dihydrothymine derivatives **3a,b** in considerably high yield (> 75%) along with the minor yield (< 10%) of monomeric thymines **2a,b**, in which the formation of **3a,b** were more efficient than that in the radiation chemical reductions (Table 2). In the presence of a secondary reductant EDTA that converts FAD into a fully reduced form FADH⁻ *in situ*, hydrogen transfer from EDTA to intermediate 5,6-dihydrothymin-5-yl radicals **5a,b** is possibly involved in the enhanced formation of **3a,b**. To remove the influence of the secondary reaction by EDTA, photoreactivity of the dimers in phosphate buffer was also investigated in the absence of EDTA. In a separate pulse radiolysis study, we confirmed that phosphate buffer is a weak reductant toward several radicals.[13] It is therefore likely that FAD may undergo photoreduction by phosphate buffer even in the absence of EDTA to produce FADH⁻.[14] As shown in Table 2, while the efficiencies for decomposition of **1a,b** were decreased to significant extent, the yields of **2a,b** relative to **3a,b** became higher upon excluding hydrogen-donating EDTA. It is also remarkable that the restoration efficiency of **2a** from **1a**[*meso*] in the absence of EDTA is much greater than those from **1a**[*rac*], **1b**[*meso*], and **1b**[*rac*], and is comparable to those in the reductive γ-radiolysis (see also Table 1).

For comparing the reduction potentials of the four C5–C5'-linked isomeric dimers investigated, fluorescence quenching kinetic study was carried out using tris(2,2'-bipyridyl)ruthenium(II) complex as a fluorescent electron donor. Recently,

the reduction potentials of pyrimidine bases were successfully estimated from the rate constants of electron-transfer fluorescence quenching of several electron donors with varying oxidation potentials.[15] In general, electron transfer from an excited state fluorescent molecule (electron donor D*) to a quencher molecule (electron acceptor A) proceeds as follows: D and A diffuse to encounter at a distance where electron transfer becomes favorable, and thereafter an ion-pair state (D$^{+\cdot}$ A$^{-\cdot}$) forms to undergo dissociation into free radical ions D$^{+\cdot}$ and A$^{-\cdot}$.

$$D + A \xrightarrow{h\nu} D^* + A \underset{k_{-diff}}{\overset{k_{diff}}{\rightleftharpoons}} (D\cdots A)^* \underset{k_{-et}}{\overset{k_{et}}{\rightleftharpoons}} (D^{+\cdot}A^{-\cdot}) \xrightarrow{k_{dis}} D^{+\cdot} + A^{-\cdot}$$

Upon 450-nm excitation of Ru(bpy)$_3^{2+}$ (10 μM; E^*_{ox} = –1.29 V[11,16]) in aqueous solution, the characteristic fluorescence was observed with a maximum wavelength of 600 nm. The fluorescence quenching rate constants (k_q) of [Ru(bpy)$_3^{2+}$]* by a series of electron accepting quenchers (see Table 3) were determined by a Stern-Volmer analysis.[17] Figure 2 shows a plot of k_q against the reduction potentials of quenchers, in which the Rehm-Weller relationship (equations 3–6)[18] was fitted to the experimental data.

$$k_q = \frac{k_{diff}}{1 + \frac{k_{-diff}}{k_a K_{diff}}\left(\exp\left(\frac{\Delta G_{et}^{\ddagger}}{RT}\right)\right)} \tag{3}$$

$$\Delta G_{et}^{\ddagger} = \left[\left(\frac{\Delta G_{et}}{2}\right)^2 + \left(\frac{\lambda}{4}\right)^2\right]^{\frac{1}{2}} + \frac{\Delta G_{et}}{2} \tag{4}$$

$$\Delta G_{et} = 96.5\left(E^*_{ox} - E_{red} - \frac{q^2}{r\varepsilon}\right) \tag{5}$$

$$\frac{k_{-diff}}{k_{diff}} = \frac{1}{K_{eq}} \tag{6}$$

Table 3. Ru(bpy)$_3^{2+}$ Fluorescence Quenching Rate Constants and Reduction Potential (vs. SCE) of Various Quenchers in Aqueous Solution

Quencher	E_{red} / V	k_q / 10^9 dm^3 mol^{-1} s^{-1}
p-Benzoquinone	−0.16 [a]	6.32
Dimethylbenzoquinone	−0.32 [a]	4.56
Nitrofurantoin	−0.50 [a]	11.4
3,5-Dinitrobenzoic acid	−0.58 [a]	7.16
Anthraquinone-2-sulfonate	−0.63 [a]	6.73
Methylviologene	−0.69 [a]	5.13
5-Nitrouracil	−0.77 [a]	4.58
1-Methylnicotinamide	−1.01 [b]	0.323
Terephthaldialdehyde	−1.04 [b]	1.40
1,4-Dimethylpyridinium	−1.39 [b]	0.0379

[a] Reference 10. [b] Reference 19. The reduction potentials vs NHE are converted to the values vs SCE.
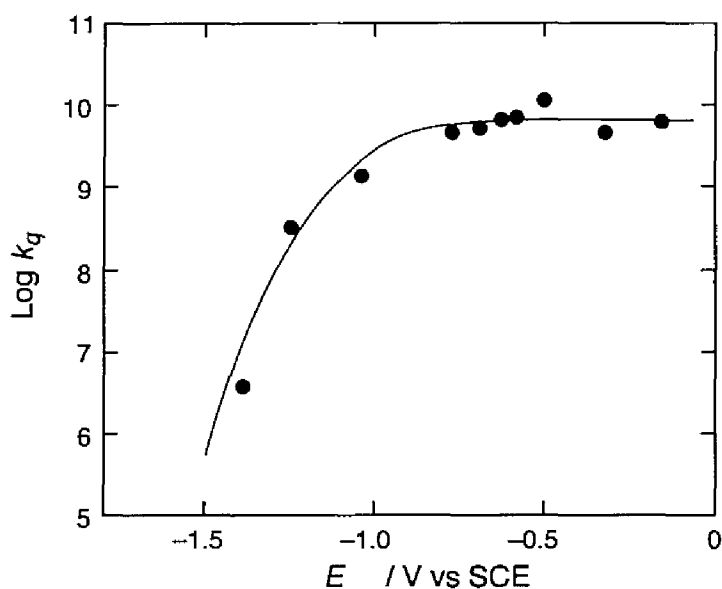
Figure 2. Rehm-Weller plot of the fluorescence quenching rate constant (k_q) in aqueous solution as a function of the reduction potential (E_{red}) of quencher. The solid curve is obtained from a best fit of experimental data to the Rehm-Weller empirical expression (see equation 3-7).
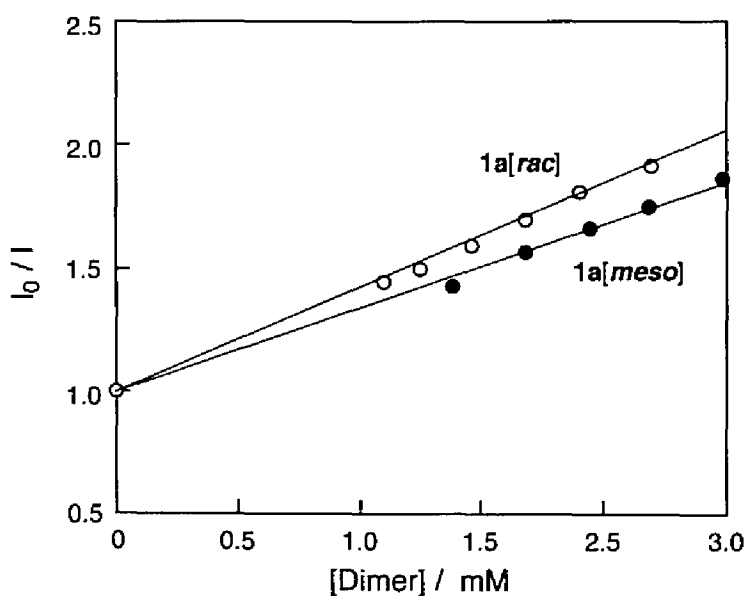
Figure 3. Stern-Volmer plots of the fluorescence quenching of $*Ru(bpy)_3^{2+}$ by (●) 1a[*meso*] and (○) 1a[*rac*]. Relative intensity (I_0/I) of the emission at 600 nm was measured in the presence of 10 μM $Ru(bpy)_3^{2+}$ in deoxygenated phosphate buffer solution (10 mM, pH 7).

where λ refers to solvent reorganization energy, $-q^2/r\varepsilon$ is the coulomb energy of the incipient ion pair formed after electron transfer, and k_a ($= \kappa_{el}\nu_n$) is the preexponential term of the expression for the rate constant of electron transfer.

It is evident in Figure 2 that k_q approaches the diffusion control limit ($k_{diff} = 6.5 \times 10^9$ dm^3 mol^{-1} s^{-1} in aqueous solution) as the reduction potential becomes increasingly positive (Figure 2). The best fit of the Rehm-Weller relationship in Figure 2 was obtained with kinetics parameters of $k_a K_{eq} = 5.0 \times 10^{12}$ dm^3 mol^{-1} s^{-1} and $\lambda = 117$ kJ mol^{-1}. The rate constants of quenching by 1a,b[*meso*] and 1a,b[*rac*] were also determined by a Stern-Volmer analysis (Figure 3), from which the corresponding redox potentials were estimated based on the best fitted Rehm-Weller relationship. Thus, almost the same k_q values for isomers of 1a (k_q(1a[*meso*]) = 5.48×10^8 dm^3 mol^{-1} s^{-1}, k_q(1a[*rac*]) = 6.66×10^8 dm^3 mol^{-1} s^{-1}) and 1b (k_q(1b[*meso*]) = 2.50×10^8 dm^3 mol^{-1} s^{-1}, k_q(1a[*rac*]) = 2.58×10^8 dm^3 mol^{-1} s^{-1}) were obtained, respectively, leading to the reduction potentials of E_{red}(1a) ≈ -1.15 and E_{red}(1b) ≈ -1.25 V vs SCE independent of isomeric structures. These E_{red} values are slightly positive compared to those of thymine ($E_{red} = -1.34$ V vs SCE) and thymidine ($E_{red} = -1.33$ V) in aqueous solution.[19] It follows that the difference in restoration efficiency between the isomeric dimers can not be explained in terms of the reduction potentials.

Laser Flash Photolysis Study. Laser flash photolyses with the forth harmonic at 266 nm of aqueous solutions of the stereoisomeric dimers 1a,b (1.0 mM) containing *N,N*-dimethylaniline (DMA; 0.5 mM) as a reducing sensitizer were attempted to detect transient absorptions originating from the splitting reaction. Previous laser flash photolysis study has shown that DMA possessing an excited-state oxidation potential of −3.3 V is a good electron donor for splitting of the cyclobutane photodimers by a single electron-transfer mechanism.[4] In this study, upon laser photolysis of DMA in deoxygenated aqueous solution, hydrated electrons and radical cations of DMA (DMA⁺⁻) were generated with the characteristic transient absorptions at $\lambda_{max} = 460$ and

650 nm, respectively.[20,21] Therefore, the hydrated electron generated by the direct photoionization of DMA (reactions 7 and 8) may be responsible for reductive splitting of the C5–C5'-linked dimers, rather than the photoexcited DMA (DMA*).

$$\text{DMA} \quad + \quad h\nu \quad \rightarrow \quad \text{DMA}^{\cdot+} \quad + \quad e_{aq}^{-} \qquad (7)$$

$$\text{T–T} \quad + \quad e_{aq}^{-} \quad \rightarrow \quad \text{T–T}^{\cdot-} \qquad (8)$$
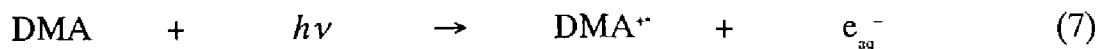
Transient absorption spectra of DMA$^{\cdot+}$ (λ_{max} = 460 nm) and hydrated electron (λ_{max} = 650 nm) were detected immediately after the laser flash photolysis of deoxygenated aqueous solutions of 1a,b and DMA. As shown in Figure 4, the absorption at 650 nm due to hydrated electrons decayed following pseudo-first order kinetics (k = 2.6 ~ 4.4 × 10^9 dm^3 mol^{-1} s^{-1}, [1a,b] = 1.0 mM), possibly as a consequence of the diffusion-controlled reaction with 1a,b (Table 4). Previous pulse radiolysis and laser flash photolysis studies have demonstrated that N-substituted 5,6-dihydrothymin-5-yl radicals 5a,b show broad absorption spectra at around 400 nm (5a: λ_{max} = 400 nm;[8] 5b: λ_{max} = 430 nm[22]), but such transient absorption spectra of 5a,b

Table 4. Rate Constants for One-Electron Reductions of 1a,b and 5a,b with Hydrated Electrons (e_{aq}^{-}) and DMA, Respectively

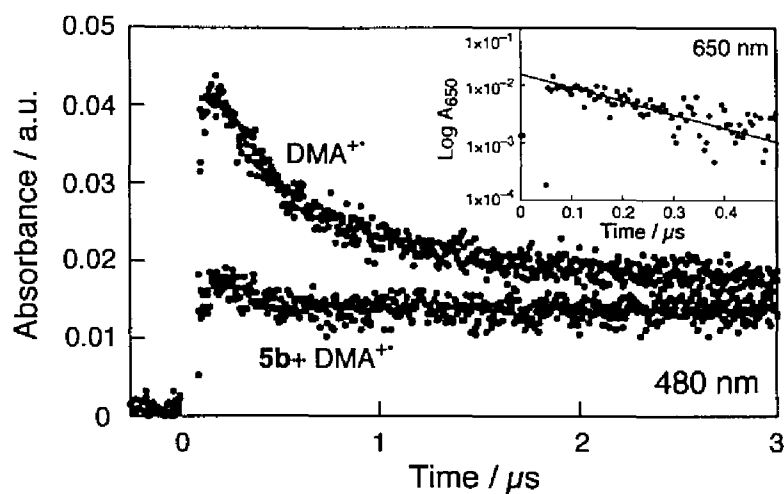| Substrate	e_{aq}^{-} + 1	DMA + 5
1a[meso]	4.4 × 10^9	3.1 × 10^9
1a[rac]	3.7 × 10^9	4.8 × 10^9
1b[meso]	2.6 × 10^9	7.1 × 10^9
1b[rac]	3.0 × 10^9	6.7 × 10^9

(header: k / dm^3 mol^{-1} s^{-1})

Figure 4. Time courses of the absorbancies at 460 nm in the 266 nm laser photolysis of DMA (0.5 mM) in phosphate buffer containing **1b**[*rac*] (1.0 mM): in the (O) presence and (●) absence of **1b**[*rac*]. Inset: Kinetic plot of the absorption at 650 nm due to e_{aq}^- in the presence of **1b**[*rac*].
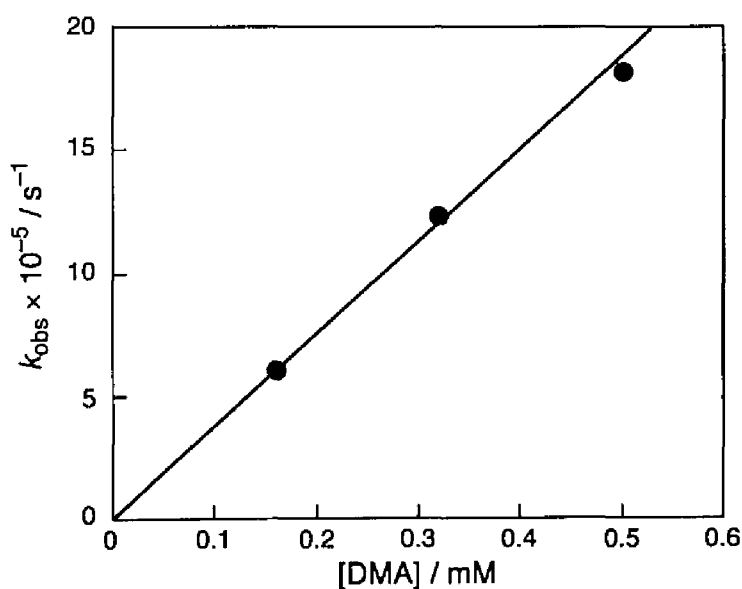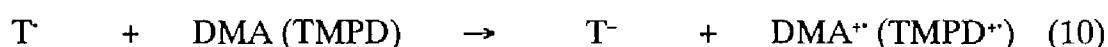

Figure 5. Dependence of k_{obs} of differential absorption growth at 460 nm on the concentration of DMA.

139

were not observed in this study. Alternatively, a slow buildup component of the transient absorption of DMA⁺˙ was observed about 5 μs after the laser flash excitation, concomitant with a first-order decay profile for DMA⁺˙ generated by photoionization (Figure 4). It is therefore most likely that the oxidizing 5-yl radicals **5a,b**, which should be generated by the C5–C5' bond splitting of the primary intermediate radical anions of **1a,b** (reaction 9), are spontaneously reduced by DMA to form the corresponding C5-anions and DMA⁺˙ (reaction 10), as in the reaction of **5a,b** with TMPD (Scheme 3).[12]

$$\text{T--T}^{\cdot-} \quad\longrightarrow\quad \text{T}^- + \text{T}^{\cdot} \qquad (9)$$

$$\text{T}^{\cdot} + \text{DMA (TMPD)} \quad\longrightarrow\quad \text{T}^- + \text{DMA}^{+\cdot} \text{(TMPD}^{+\cdot}) \quad (10)$$

In accord with the secondary one-electron oxidation of DMA in the ground state, the slow buildup component of DMA⁺˙ could be obtained by subtracting the contribution from the decay of primarily photogenerated DMA⁺˙, as occurred within 5 μs after the laser flash, from the apparent overall absorption at 460 nm in the presence of the dimers. Thus, the slow buildup of DMA⁺˙ was of the pseudo-first order kinetics, and the corresponding formal rate constant was in proportion to the concentration of DMA (Figure 5). The slope of the linear plot in Figure 5 gives the intrinsic rate
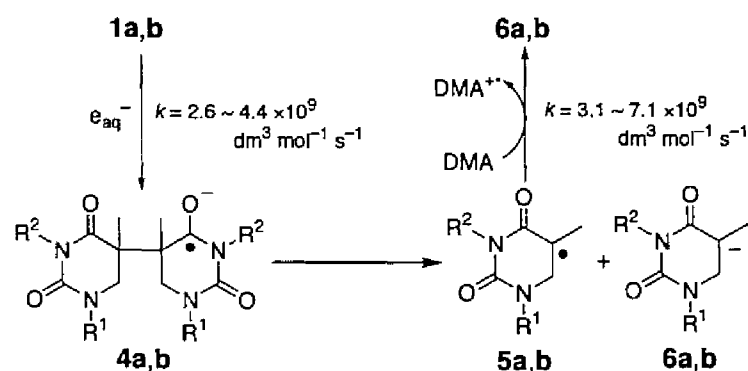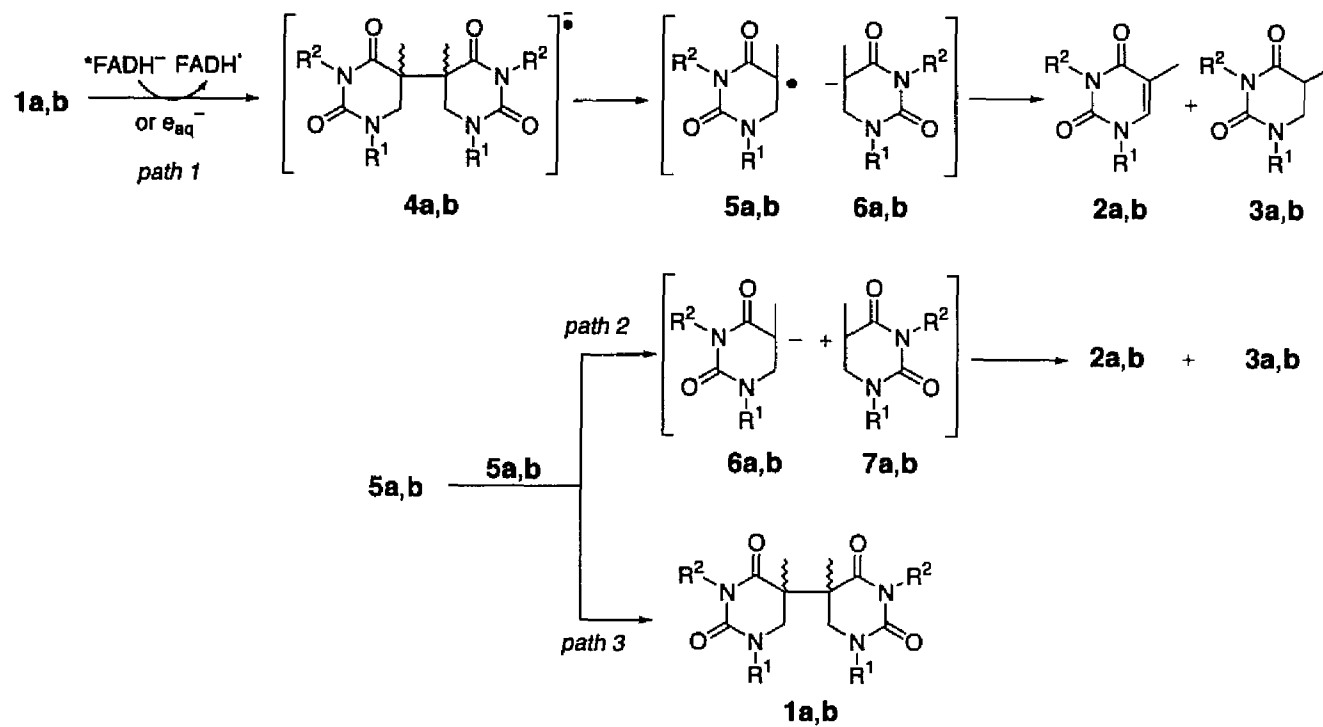

Scheme 3

constants for reaction 10, as listed in Table 4. The rate constants thus evaluated are almost in a diffusion-controlled rate limit, and are in good accordance with the literature value for the one-electron oxidation of TMPD by 6-hydroxythymin-5-yl radical (k = 1.3 × 10^9 dm^3 mol^{-1} s^{-1}) as derived from pulse radiolysis.[12]

Discussion

Reductive Splitting Mechanism of C5–C5'-Linked Dihydrothymine Dimers. In the light of the proposed mechanisms for the photo-repair of cyclobutane pyrimidine dimers[3] and the oxidative splitting of the C5–C5'-linked dihydrothymine dimers,[8] possible pathways for the reductive splitting of C5–C5'-linked dihydrothymine dimers are proposed as illustrated in Schemes 4 and 5. Under the present experimental conditions of photochemical and radiation-chemical generation of hydrated electrons, the splitting is likely to be initiated by one-electron reduction of the C5–C5'-linked dimers into the dimer radical anions **4a,b**, although direct observation of the corresponding transient absorption spectra was unsuccessful in the present nanosecond laser flash photolysis. In view of the earlier results that the formation of radical anion intermediate of cyclobutane pyrimidine photodimer (Pyr<>Pyr⁻) could not be confirmed clearly by nano- and pico-second laser flash photolysis, such radical anion intermediates **4a,b** may have much shorter lifetimes.[4,23] Subsequent C5–C5'-bond cleavage of **4a,b** produces the C5-anions (**6a,b**) and the 5,6-dihydrothymin-5-yl radicals **5a,b**, as confirmed by the redox reaction with reducing aromatic amines (DMA and TMPD). The isomerization of C5–C5'-linked dimers supports the formation of **5a,b** (Scheme 4, path 3). Concomitant formation of **2a,b** in the absence of aromatic amines suggests that disproportionation of **5a,b** leading to a pair of C5-anion **6a,b** and C5-cation (**7a,b**) is involved in the reductive splitting pathway (Scheme 4, path 2), which is a common reaction with the oxidative splitting

141

Scheme 4. Reductive splitting mechanism of the C5–C5'-linked dihydrothymine dimers.

mechanism.[8]

Flavin-Photosensitized Splitting of C5–C5'-Linked Dihydrothymine Dimers.

Because of the existence of multiple protonation-reduction states of the flavin chromophore, the photoreactivation mechanism of photodimers has not been fully understood. The most likely mechanism involves initiation by exoergic one-electron transfer from the excited state of FADH$^-$ in DNA photolyase to the photodimers (ΔG_{et} = -125 ± 30 kJ mol^{-1})[24] with rate constants of $k_{et} = 5.5$~6.5×10^9 s^{-1}.[25] The Rehm-Weller analysis on the flavin-photosensitized splitting of C5–C5'-linked dimers gave reasonable reduction potentials $E_{red} = -1.15$~1.25 V, which are slightly more positive than those of the monomers **2a,b**. Taking into account the reduction (E(FADH$^{\cdot}$ / FADH$^-$) = -0.364 V at pH 7.0),[26] and the excitation energy (E_{00}(*FADH$^-$ / FADH$^-$) = 2.58 V)[27] of FADH$^-$, the free energy for the electron transfer from *FADH$^-$ to the dimers **1a,b** is calculated from equation 5 as $\Delta G_{et} = -79.4$ kJ mol^{-1}, which shows exothermicity of the reaction.

A remarkably high efficiency of thymine restoration in the photoreduction of **1a[meso]** by *FADH$^-$, comparing with those of the other dimers (**1a[rac]**, **1b[meso]**, and **1b[rac]**), could not be explained by the difference in the initial electron transfer efficiency. As a possibility, this feature may be related to the X-ray crystal structures of **1a[meso]** that is distinct from those of **1a[rac]**, **1b[meso]**, and **1b[rac]**.[7b] For better understanding, the frame structures of **1a[meso]** and **1a[rac]** are illustrated in Figure 6.[7b] In a crystal, **1a[meso]** has a stacked conformation by which the two pyrimidine rings face to each other, while the pyrimidine rings of **1a[rac]** are separated to reduce the mutual overlapping. In view of these structures, **1a[rac]** may allow successive two-electron reduction by FADH$^-$ (Scheme 5, path 4), whereas **1a[meso]** would favor one-electron reduction, rather than two-electron reduction, because of generating an electrostatic repulsion between the one-electron reduced dihydropyrimidine rings. The intermediates (**4'a,b**) derived from successive two-electron reduction are expected
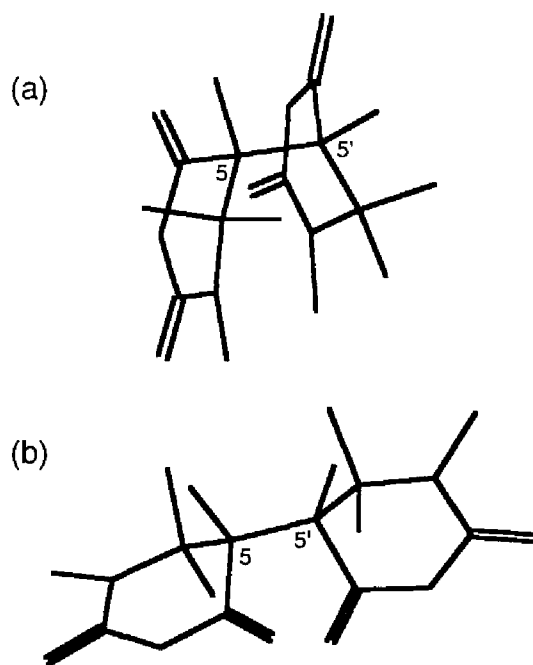
Figure 6. Frame structures of (a) 1a[*meso*] and (b) 1a[*rac*] obtained by X-ray crystallography. (See also Chapter 2.)

to afford two equivalents of C5-anions **6a,b**, thus resulting in exclusive formation of **3a,b** by protonation at C5. To characterize the conformation of **1a,b** in solution, NMR spectra were measured in dimethyl sulfoxide-d_6 at room temperature (Figure 7). In accord with the results of X-ray crystallography, the NOE difference spectra between H6 protons and N1-methyl protons of the two pyrimidine rings increased about 16 % for **1a**[*meso*] and 6 % for **1a**[*rac*], respectively. This result suggests that **1a**[*meso*] exhibits a "closed-shell" conformation in solution in contrast to the "open – shell" conformation of **1a**[*rac*]. Furthermore, the NOE difference spectra for **1b**[*meso*] and **1b**[*rac*] in solution increased to much lesser extent and there was no substantial difference between these stereoisomers (data not shown), although the dihydropyrimidine rings of **1b**[*meso*] and **1b**[*rac*] are stacked in a similar manner as those of **1a**[*meso*] in the crystal.[7b] Hence, due to the conformational preference in solution that may relieve the intramolecular electrostatic repulsion between the
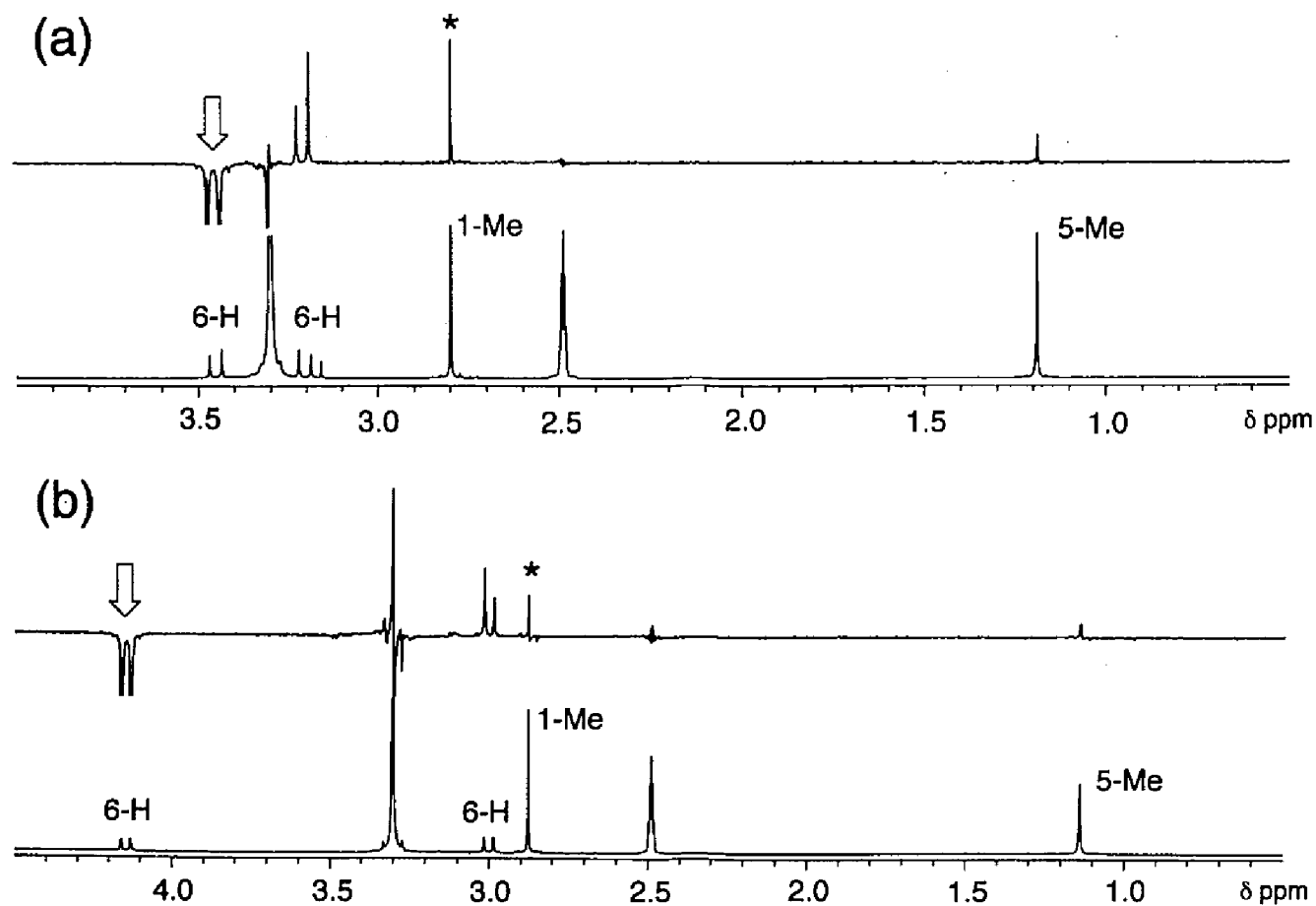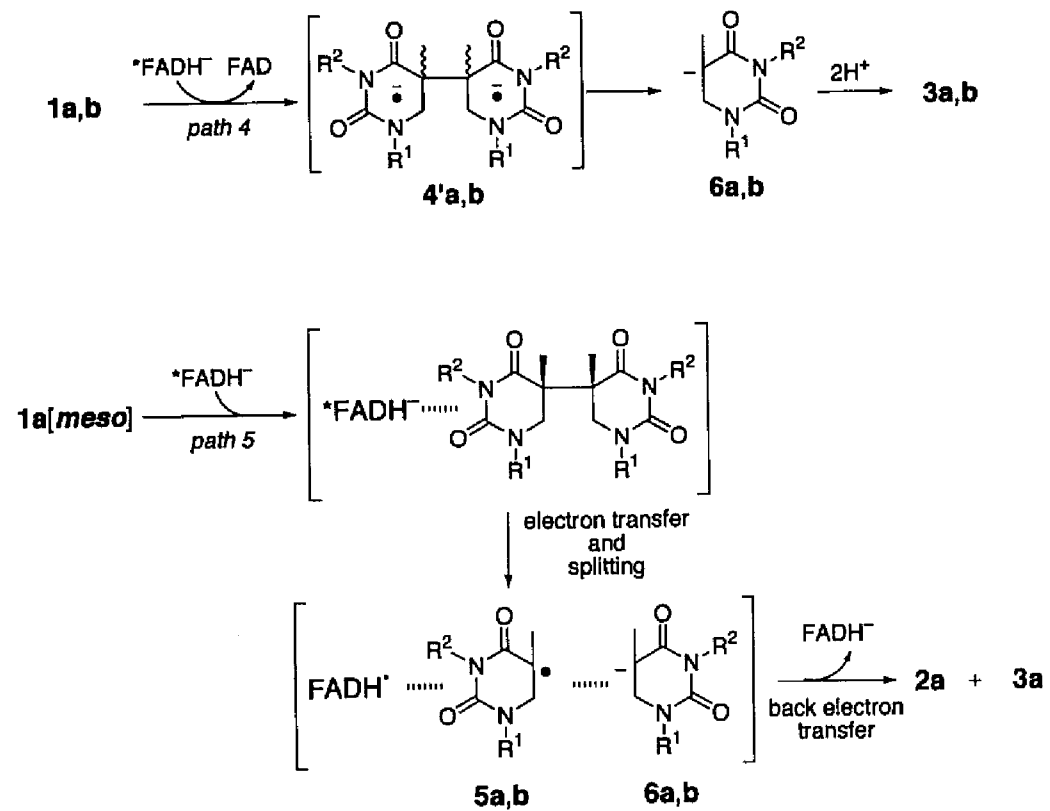
Figure 7. 400 MHz ^{1}H NMR spectra (lower trace) and NOE difference spectra (upper trace) of (a) **1a**[*meso*] and (b) **1a**[*rac*] in dimethyl sulfoxide-d_6 at 303 K. Arrows show irradiated H6 peaks.

Scheme 5

pyrimidine-electron adducts when formed, **1b**[*meso*] and **1b**[*rac*] could undergo successive two-electron reduction similar to **1a**[*rac*]. In this context, previous EPR spectroscopic studies have demonstrated that the radical anion of *trans-syn*-1,3-dimethyluracil dimer, of which pyrimidine rings are likely to be separated to each other, **2a** is relatively long-lived in contrast to the radical anions of the stacked conformations of *cis-syn*-thymine and uracil dimers that are unstable to split into monomer anions spontaneously.[28]

Another possibility is that the "closed-shell" conformation of **1a**[*meso*] may produce a relatively stable complex state with *FADH$^-$, thereby the 5-yl radical intermediate **5a** formed undergoing readily back electron transfer (BET) (path 5 in Scheme 5). However, such a back electron transfer reaction is less likely in the present case because of the oxidizing properties of pyrimidine 5-yl radicals. This is clearly in contrast to the photoinduced splitting mechanism of photodimers by which thymine monomers are regenerated by BET from the monomer radical anion to the FAD chromophore.

Finally, the reductive splittings of **1b**[*meso*] and **1b**[*rac*] seem to be slightly more effective than those of **1a**[*meso*] and **1a**[*rac*] (see Table 1), although the reduction potentials of **1a** are more positive than those of **1b**. It is likely that *N*-methyl substitution may increase a strain in the dimers to enhance the exothermicity of the splitting reaction. In fact, the enthalpy for splitting of uracil and thymine cyclobutane photodimers tended to become more negative by the methyl-substitution.[29] Accordingly, the radical anion of the C5–C5'-linked dimers of 1,3-dimethylthymine **1b** would be unstable to undergo the C5–C5'-bond cleavage somewhat readily.

147

Conclusion

It was demonstrated that reductive splitting of C5–C5'-linked dihydrothymine dimers **1a,b** by hydrated electrons and the photoexcited reduced form of flavin (*FADH⁻) affords the 5,6-dihydrothymine derivatives **3a,b** along with the corresponding thymine monomers **2a,b**. The efficiency for the reductive restoration into **2a,b** was significantly lower than those in the previously reported oxidative splitting reaction. According to the proposed reductive splitting mechanism, electron-adducts of the dimers undergo the C5–C5'-bond cleavage to produce the 5,6-dihydrothymin-5-yl radicals **5a,b** and the C5-anions **6a,b**. Disproportionation of **5a,b** is the most likely reaction pathway for regeneration of the monomers **2a,b**. The relatively high efficiency of restoration into **2a** in the photoreduction of **1a**[*meso*] by *FADH⁻ suggested that the stacked pyrimidine rings of **1a**[*meso*] does not favor a successive two-electrons reduction as in the other dimers (**1a**[*rac*], **1b**[*meso*], and **1b**[*rac*]) with a common conformation of separated pyrimidine rings. This is in accord with the conformational studies by NOESY and X-ray crystallography.

148

References and Notes

(1)   For reviews, see: (a) von Sonntag, C. *The Chemical Basis of Radiation Biology*; Taylor and Francis: London, 1987. (b) Fuciarelli, A. F.; Zimbrick J. D. *Radiation Damage in DNA: Structure / Function Relationship at Early Times*; Battele Press: Columbus, 1995. (c) Kuwabara, M. *Radiat. Phys. Chem.* **1991**, *37*, 691–704. (d) Steenken, S. *Free Rad. Res. Comms.* **1992**, *16*, 349–379.

(2)   (a) Cadet, J.; Vigny, P. In *Bioorganic Photochemistry: Photochemistry and the Nucleic Acids*; Morrison, H., Ed.; John Wiley & Sons: New York, 1990; pp 1–272. (b) Taylor, J. –S. *Acc. Chem. Res.* **1994**, *27*, 76–82. (c) Görner, H. *J. Photochem. Photobiol. B: Biol.* **1994**, *26*, 117–139. (d) Pfeifer, G. P. *Photochem. Photobiol.* **1997**, *65*, 270–283.

(3)   (a) Begley, T. P. *Acc. Chem. Res.* **1994**, *27*, 394–401. (b) Kim, S. –T.; Sancar, A. *Photochem. Photobiol.* **1993**, *57*, 895–904. (c) Carell, T.; Epple, R. *Eur. J. Org. Chem.* **1998**, 1245–1258. (d) Burdi, D.; Begley, T. P. *J. Am. Chem. Soc.* **1991**, *113*, 7768–7770. (e) Park, H. –W.; Kim, S. –T.; Sancar, A.; Deisenhofer, J. *Science* **1995**, *268*, 1866–1872. (f) Tamada, T.; Kitadokoro, K.; Higuchi, Y.; Inaka, K.; Tasui, A.; de Ruiter, P. E.; Eker, P. M.; Miki, K. *Nature Struct. Biol.* **1997**, *11*, 887–891. (g) vande Berg, B. J.; Sancar, G. B. *J. Biol. Chem.* **1998**, *273*, 20276–20284. (h) Ramaiah, D.; Kan, Y.; Koch, T.; Ørum, H.; Schuster G. B. *Proc. Natl. Acad. Sci. U.S.A.* **1998**, *95*, 12902–12905. (i) Butenandt, J.; Burgdort, L. T.; Carell, T. *Angew. Chem. Int. Ed.* **1999**, *38*, 7708–7011.

(4)   Yeh, S. –R.; Falvey, D. E. *J. Am. Chem. Soc.* **1991**, *113*, 8557–8558.

(5)   Pouwels, P. J. W.; Hartman, R. F.; Rose, S. D.; Kaptein, R. *Photochem. Photobiol.* **1995**, *61*, 575–583.

(6)   (a) Todo, T.; Takemori, H.; Ryo, H.; Ihara, M.; Matsunaga, T.; Nikaido, O.; Sato, K.; Nomura, T. *Nature* **1993**, *361*, 371–374. (b) Kim, J. –K.; Patel, D.;

Choi, B. –S. *Photochem. Photobiol.* **1995**, *62*, 44–50. (c) Todo, T.; Ryo, H.; Yamamoto, K.; Toh, H.; Inui, T.; Ayaki, H.; Nomura, T.; Ikenaga, M. *Science* **1996**, *272*, 109–112.

(7) (a) Nishimoto, S.; Ide, H.; Nakamichi, K.; Kagiya, T. *J. Am. Chem. Soc.* **1983**, *105*, 6740–6741. (b) Ito, T.; Shinohara, H.; Hatta, H.; Nishimoto, S. *J. Org. Chem.* **1999**, *64*, 5100–5108. (Chapter 2)

(8) Ito, T.; Shinohara, H.; Hatta, H.; Fujita, S.; Nishimoto, S. *J. Phys. Chem. A.* **1999**, *103*, 8413–8420. (Chapter 4)

(9) The number of molecules produced or changed per 1 J of radiation energy absorbed by the reaction system.

(10) Wardman, P. *J. Phys. Chem. Ref. Data* **1989**, *18*, 1637–1755.

(11) Kavarnos, G. J.; Turro, N. J. *Chem. Rev.* **1986**, *86*, 401–449.

(12) (a) Steenken, S.; Neta, P. *J. Phys. Chem.* **1979**, *83*, 1134–1137. (b) Fujita, S.; Steenken, S. *J. Am. Chem. Soc.* **1981**, *103*, 2540–2545.

(13) In the course of steady-state γ-radiolysis and pulse radiolysis studies on the behavior of deprotonated adenosine C8 radicals (Ado(–H)$^\cdot$) in phosphate buffer, it was suggested that phosphate ions enhance one-electron reduction of Ado(–H)$^\cdot$ with a rate constant $k = 10^3 \sim 10^4$ dm^3 mol^{-1} s^{-1}. (Nishimoto, S.; Kuno, S.; Fujita, S. unpublished results.)

(14) In the absence of EDTA, **3a,b** are major products (see Table 2) whereas oxidative splitting of **1a,b** by anthraquinone-2-sulfonate (AQS) sensitization afford almost equivalent amounts of **2a,b** and **3a,b**. (ref. 8). This indicates the reduction process is predominant in the present case. In addition, photoreduction of FADH$^-$ by pyrimidine photodimer has not been observed. (Heelis, P. F.; Payne, G.; Sancar, A. *Biochemistry* **1987**, *26*, 4634–4640.)

(15) (a) Yeh, S. –R.; Falvey, D. E. *J. Am. Chem. Soc.* **1992**, *114*, 7313–7314. (b) Scannell, M. P.; Prakash, G.; Falvey, D. E. *J. Phys. Chem. A* **1997**, *101*, 4332–4337. (c) Scannell, M. P.; Fenick, D. J.; Yeh, S. –R.; Falvey, D. E. *J.*

150

Am. Chem. Soc. **1997**, *119*, 1971–1977.

(16) Excited-state oxidation potential E^*_{ox} was calculated using $E^*_{ox} = E_{ox} - E_{00}$ with the oxidation potential of $Ru(bpy)_3^{2+}$ (E_{ox}) and zero excitation energy (E_{00}) evaluated from λ_{0-0} (= 530 nm) in aqueous solution.

(17) The dynamic quenching rate constants k_q were determined by the Stern-Volmer equation: $I_0/I = 1 + k_q\tau_0[Q]$ where I_0 and I are the intensity of the fluorescence at 600 nm when excited at 450 nm in the absence and presence of a quencher, respectively. The lifetime τ_0 of $*Ru(bpy)_3^{2+}$ in the absence of a quencher is known to be 0.62 μs (Kalyanasundaram, K. *Coord. Chem. Rev.* **1982**, *46*, 159–244.).

(18) Rehm, D.; Weller, A. *Isr. J. Chem.* **1970**, *8*, 259–271.

(19) Steenken, S.; Telo, J. P.; Novais, H. M.; Candeias, L. P. *J. Am. Chem. Soc.* **1992**, *114*, 4701–4709.

(20) Habersbergerová, A.; Janovsk'y, I.; Tepl'y, J. *Radiation Res. Rev.* **1968**, *1*, 109–181.

(21) Land, E. J.; Porter, G. *Trans Faraday Soc.* **1963**, *59*, 2027–2037.

(22) Deeble, D. J.; Das, S.; von Sonntag, C. *J. Phys. Chem.* **1985**, *89*, 5784–5788.

(23) (a) Okamura, T.; Sancar, A.; Heelis, P. F.; Begley, T. P.; Hirata, Y.; Mataga, N. *J. Am. Chem. Soc.* **1991**, *113*, 3143–3145. (b) Kim, S. –T.; Volk, M.; Rousseau, G.; Heelis, P. F.; Sancar, A.; Michel-Beyerle, M. –E. *J. Am. Chem. Soc.* **1994**, *116*, 3115–3116.

(24) (a) Heelis, P. F.; Kim, S. –T.; Okamura, T.; Sancar, A. *J. Photochem. Photobiol. B: Biol.* **1993**, *17*, 219–228. (b) Heelis, P. F.; Deeble, D. J.; Kim, S. –T.; Sancar, A. *Int. J. Radiat. Biol.* **1992**, *62*, 137–143.

(25) (a) Kim, S. –T.; Heelis, P. F.; Okamura, T.; Hirata, Y.; Mataga, N.; Sancar, A. *Biochemistry* **1991**, *30*, 11262–11270. (b) Kim, S. –T.; Sancar, A.; Essenmacher, C.; Babcock, G. T. *J. Am. Chem. Soc.* **1992**, *114*, 4442–4443.

(26) Anderson, R. F. *Biochem. Biophys. Acta* **1983**, *722*, 158–162.

(27)   Ramsey, A. J.; Jorns, M. S. *Biochemistry* **1992**, *31*, 8437–8441.

(28)   Pezeshk, A.; Podmore, I. D.; Heelis, P. F.; Symons, M. C. R. *J. Phys. Chem.* **1996**, *100*, 19714–19718.

(29)   Heelis, P. F.; Hartman, R. F.; Rose, S. D. *J. Photochem. Photobiol. A: Chem.* **1996**, *95*, 89–98.

General Conclusions

In Chapter 1, the addition reactivity of carbon dioxide radical anion (CO_2^{-}) toward N1-substituted thymine derivatives in aqueous solution was investigated to compare with their one-electron reducing reactivity. One-electron reduction of thymine derivatives produced 5,6-dihydrothymines and stereoisomeric C5–C5'-linked dihydrothymine dimers, in which 5,6-dihydrothymin-5-yl radicals are the key intermediates. Nucleophilic addition of CO_2 radical anion to N-methylthymines occurred preferentially at C6 position to form 6-carboxy-5,6-dihydrothymin-5-yl radicals, thereby yielding 5,6-dihydrothymine-6-carboxylic acid. Similar carboxylation by CO_2 radical anions was also observed for thymine dinucleotide (TpT). Based on the G-values of the major products, the partition ratio between one-electron reduction and nucleophilic addition of CO_2 radical anion in the reaction with N-substituted thymines was approximately estimated as 0.8 : 0.2. The X-ray crystallographic analysis demonstrated that 5,6-dihydro-1-methylthymine-6-carboxylic acid (1,5-dimethyl-DHO) involved in the carboxylated products is structurally similar to dihydroorotate, which is a well known intermediate in the de novo pyrimidine biosynthesis.

Chapter 2 demonstrated the formation of stereoisomeric C5–C5'-linked dihydrothymine dimers by radiolytic one-electron reduction of N-substituted thymines including thymidine in the hydrated electron (e_{aq}^{-}) and CO_2 radical anion (CO_2^{-}) in anoxic aqueous solution. The dimers (5R, 5'S)-, (5S, 5'R)-, (5R, 5'R)- and (5S, 5'S)-bi-5,6-dihydrothymines had a structural similarity to the cyclobutane pyrimidine photodimers. X-Ray crystal structures indicated that two pyrimidine rings of the stereoisomeric dimers, except the racemic compound of (5R, 5'R)- and (5S, 5'S)-C5–C5'-linked 1-methylthymine dimers, overlap with each other to considerable extents, as in the cis-syn-cyclobutane photodimers. It was predictable that the

C5–C5'-linked dihydrothymine dimers may cause some distortion within a DNA duplex if they were incorporated. The pH-dependence of the reactivities was in accord with a mechanism of the C5–C5'-linked dimerization by which electron adducts of thymine derivatives are irreversibly protonated at C6 position and the resulting 5,6-dihydrothymin-5-yl radicals undergo bimolecular coupling.

In Chapter 3, photophysical characteristics of stereoisomers of N-substituted C5–C5'-linked dihydrothymine dimers have been investigated in protic and aprotic solvents by UV-absorption, and steady-state and time-resolved fluorescence spectroscopies. Among the C5–C5'-linked dihydrothymine dimers, meso dimer of 1-methylthymine in phosphate buffer (pH < 10) at 293 K showed a weak absorption at around 270–350 nm and a fluorescence emission in the range of 300–550 nm (Φ_F ~0.1). Racemic compound of the C5–C5'-linked 1-methylthymine dimer, meso and racemic compounds of the C5–C5'-linked 1,3-dimethylthymine dimers were non-fluorescent in phosphate buffer. The unusual fluorescence spectrum with a long lifetime (τ_F^{ave} = 1.76 ns) of the 1-methylthymine meso-dimer as well as the red-shifted UV-absorption in aqueous solution were presumably derived from the formation of an excimer that favors a "closed-shell" conformation in the ground state and the excited singlet state. In a basic solution (pH > pKa = 11.7), the fluorescence quantum yield of 1-methylthymine meso-dimer decreased due to deprotonation into a dimer dianion structure that may favor an "open — shell" conformation as induced by electric repulsion between the deprotonated pyrimidine rings. A semi-empirical calculation for the meso dimer predicted that the excimer fluorescence and the corresponding UV-absorption might be assigned to a rather forbidden $^1(n,\pi^*)$ transition.

Chapter 4 demonstrated oxidative splitting of the C5–C5'-linked dihydrothymine dimers into thymine monomers and 5,6-dihydrothymines by the oxidizing radicals (SO_4^- and $N_3^{\cdot}$) generated in the radiolysis and photoexcited oxidizing sensitizer ($^3AQS^*$). As characterized by the laser flash photolysis using SO_4^- as oxidants, 5,6-dihydrothymin-5-yl radicals are possible intermediates involved

154

in the oxidative splitting. A mechanism involving generation of the C5–C5'-linked dihydrothymine dimer radical cations through the electron transfer from the C5–C5'-linked dimers to an oxidant has been proposed, which is similar to an oxidative splitting mechanism of cyclobutane pyrimidine photodimers. While the pyrimidine photodimer radical cation prefers the C6–C6'-bond splitting to the counterpart C5–C5'-bond splitting, the C5–C5'-linked dihydrothymine dimer radical cations may undergo the C5–C5'-bond splitting into the 5,6-dihydrothymin-5-yl radicals and the C5-cations. Because of that oxidizing property, the intermediate 5-yl radicals can also be a one-electron oxidant towards the dimers.

Chapter 5 demonstrated that reductive splitting of C5–C5'-linked dihydrothymine dimers by hydrated electrons and photoexcited reduced form of flavin (*FADH$^-$) affords the 5,6-dihydrothymine derivatives along with the corresponding thymine monomers. The efficiency of the reductive restoration into thymines was significantly lower than that of oxidative splitting reaction. According to a reductive splitting mechanism proposed, electron-adducts of the dimers undergo the C5–C5'-bond cleavage to produce the 5,6-dihydrothymin-5-yl radicals and the C5-anions. Disproportionation of 5,6-dihydrothymin-5-yl radicals is the most possible reaction pathway for regeneration of the monomers. The relatively high efficiency of restoration into 1-methylthymine in the photoreduction of the corresponding meso-dimer by *FADH$^-$ suggested that the meso-dimer of 1-methylthymine in a "closed-shell" conformation does not favor a successive two-electrons reduction due to their electrostatic repulsion, whereas the separated dihydrothymine rings of the other dimers (racemic-dimer of 1-methylthymine, and meso- and racemic-dimers of 1,3-dimethylthymine) may favor. This is in accord with the conformational studies by NOESY and X-ray crystallography as well as UV-absorption and fluorescence spectroscopies as described in Chapter 3.

List of Publications

Chapter 1

Thymine Carboxylation: Nucleophilic Addition of Carbon Dioxide Radical Anion

Takeo Ito, Hiroshi Hatta, Sei-ichi Nishimoto

Int. J. Radiat. Biol. **2000**, *in press*.

Chapter 2

Stereoisomeric C5–C5'-Linked Dihydrothymine Dimers Produced by Radiolytic One-Electron Reduction of Thymine Derivatives in Anoxic Aqueous Solution: Structural Characteristics in Reference to Cyclobutane Photodimers

Takeo Ito, Hideki Shinohara, Hiroshi Hatta, Sei-ichi Nishimoto

J. Org. Chem. **1999**, *64*, 5100–5108.

Chapter 3

Conformational Effects on Photophysical Characteristics of C5–C5'-Linked Dihydrothymine Dimers in Solution

Takeo Ito, Hideki Shinohara, Sei-ichi Nishimoto

J. Phys. Chem. A, *submitted*.

Chapter 4

Radiation-Induced and Photosensitized Splitting of C5–C5'-Linked Dihydrothymine Dimers: Product and Laser Flash Photolysis Studies on Oxidative Splitting Mechanism

Takeo Ito, Hideki Shinohara, Hiroshi Hatta, Shin-ichi Fujita, Sei-ichi Nishimoto

J. Phys. Chem. A **1999**, *103*, 8413–8420.

Chapter 5

Radiation-Induced and Photosensitized Splitting of C5–C5'-Linked Dihydrothymine Dimers. Part II. Conformational Effects on the Reductive Splitting Mechanism

Takeo Ito, Hideki Shinohara, Hiroshi Hatta, Shin-ichi Fujita, Sei-ichi Nishimoto

J. Phys. Chem. A **2000**, *in press*.

Acknowledgements